Nanoscale Metal Particles

➢ Metals also have unusual properties on the ~1–100-nm length scale.

➢ Fundamentally, this is because the *mean free path of an electron in metal at room temperature is typically about 1–100 nm*.

➢ So, when the particle size of metal is ~100 nm or less, one might expect unusual effects because the "sea of electrons" encounters a "shore" (the surface of the particle).

➢ Both *physical and chemical properties of metallic nanoparticles may be different from the properties of the bulk materials*.

✓ Gold particles less than 20 nm in diameter melt at a far lower temperature than bulk gold, for instance, and when the particles are between 2 and 3 nm in diameter, gold is no longer a "noble," unreactive metal; in this size range, it becomes chemically reactive.

✓ At nanoscale dimensions, silver has properties analogous to those of gold in its beautiful colors, although it is more reactive than gold.

➢ Nanoscale metal particles have been the subject of intense research over the past 20 years, especially because of their unusual *optical, magnetic, and catalytic properties*.

➢ The synthesis of metal nanocrystals in various shapes has become increasingly sophisticated and rational, like the synthesis of semiconductor nanocrystals described above. By controlling the separate phases of nucleation and growth, and by using ligands that cap specific crystal faces during growth, it is possible to make metal nanocrystals of uniform size in a variety of interesting and useful shapes including cubes, truncated cubes, octahedra, triangular prisms, and high aspect ratio rods.

➢ By exploiting *displacement reactions* that replace one metal with another, complex hollow shapes such as nanocages (as shown on the right) can be made starting with other shapes. In this case, solid silver nanocubes are transformed to gold nanocages.
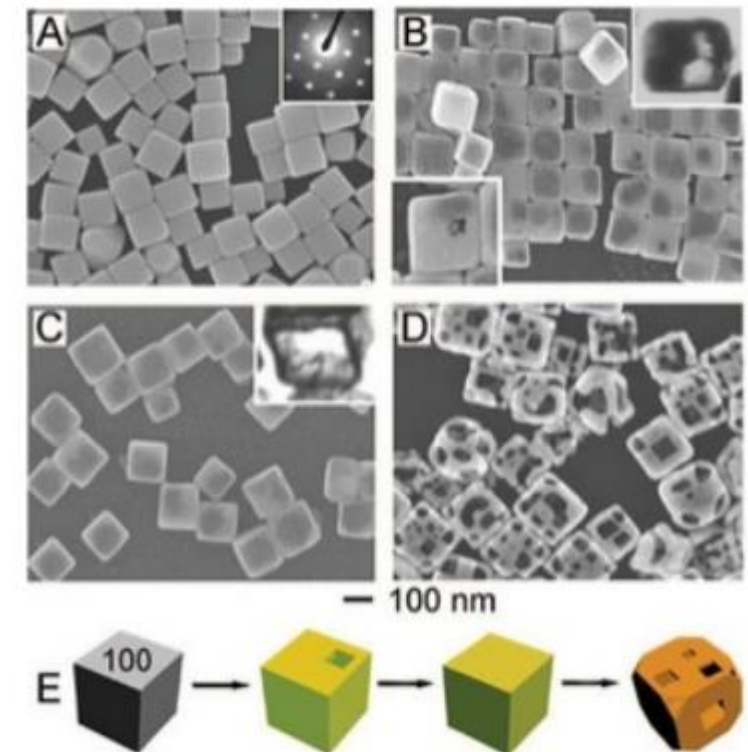
Nanoscale Metal Particles: Optical Properties

Currently, research laboratories around the world are showing great interest in taking advantage of the unusual optical properties of metal nanoparticles *for applications in biomedical imaging and chemical detection*.

➢ The optical properties of metallic nanoparticles of Ag, Au, etc. ***arise from a complex electrodynamic effect that is strongly influenced by the surrounding dielectric medium***. We shall discuss this here.

➢ ***Light impinging*** on metallic particles causes ***optical excitation of their electrons***. The ***principal type of optical excitation that occurs is the collective oscillation of electrons*** in the valence band of the metal.

➢ Such coherent oscillations occur at the interface of a metal with a dielectric medium and are called **surface plasmons**.

➢ *Quantized coherent oscillations of free electrons at the surface of the metal nanoparticles (and dielectric interface) are called the **Surface Plasmons (SPs)**. At a certain frequency* of the incident light there is a ***resonance*** at which there is *a maximum **absorption** or **scattering** of energy from the incident light wave and a peak is observed* in the absorption/scattering spectra. This peak is called the **"*surface plasmon resonance* (SPR)"** peak.

Metals on the Nanoscale: Optical Properties

➢ In metal nanoparticles (that are much smaller than the wavelength of light,) the **surface plasmons are *localized*** and plasmon excitation occurs with high intensity. *The SPR in nanoscale particles is known as* **Localized Surface Plasmon Resonance (LSPR).**

✓ ***Plasmonic Nanoparticles:*** *The nanoparticles that show* ***LSPR.***

➢ The peak intensity of the ***surface plasmon absorption for gold and silver occurs in the visible region of the electromagnetic spectrum***, and so these ***metallic nanoparticles are useful as pigments***.

Figure 1.12 Monodispersed **gold nanoparticles** of different sizes (2–200 nm) in water.

Note the different colors due to different light interactions, which are dominated by particle size. (Courtesy of Ted Pella, Inc., available on the

2nm   5nm   50nm   100nm   200nm

World Wide Web at http://www.tedpella.com/gold_html/goldsols.htm.)

Metals on the Nanoscale: Optical Properties

❖ The characteristics (viz., **spectral** *bandwidth, peak height, and the peak wavelength* of *plasmon absorption depend on the* **nanoparticle's** *chemical* *composition*, *size*, *geometrical shape*, *surface charge*, *surface-adsorbed species*, *interparticle interactions*, and *the dielectric property* *of the surrounding environment*.
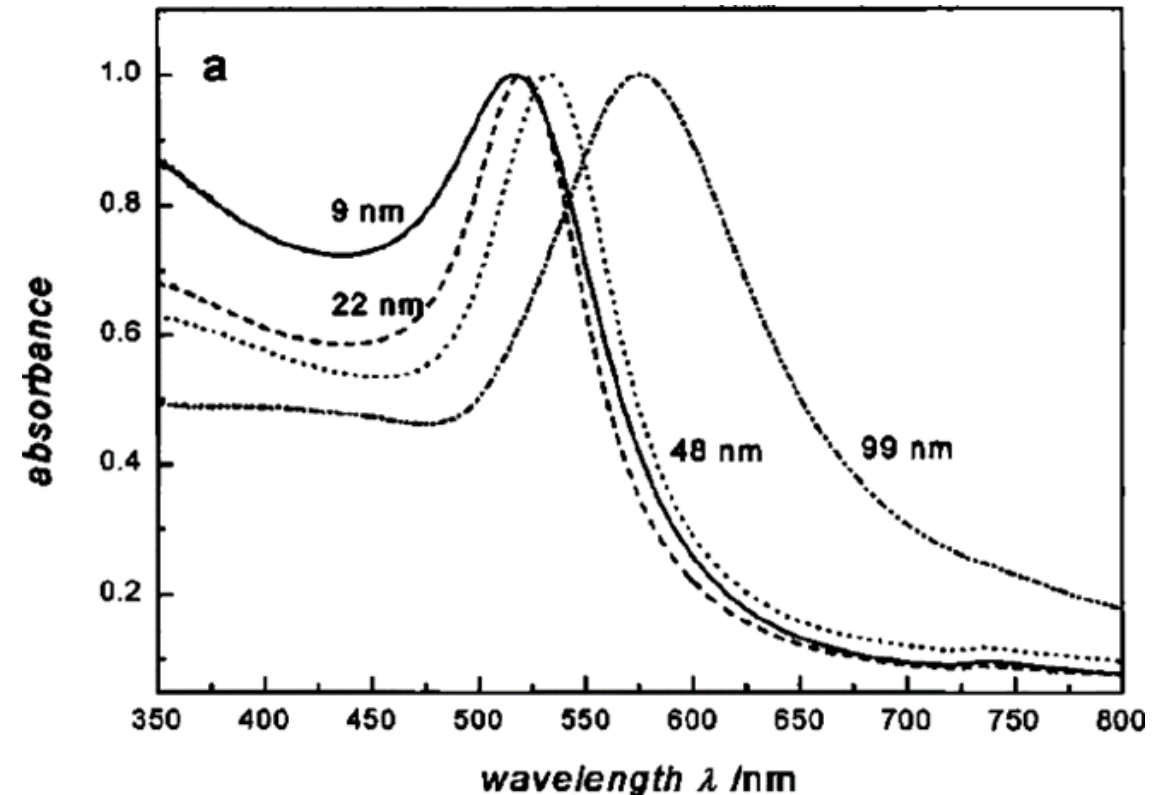
Gold nanoparticle's size effect

Fig. 5.4. Experimental extinction spectra of gold nanoparticles of *diameters 9, 22, 48 and 99 nm*. (reprinted with permission from American Chemical Society).

Metals on the Nanoscale: Shape-Dependent Optical Properties

Dark-Field Light-scattering Images from Gold Nanoparticles of Different Shapes

Insets: TEM of the nanoparticles

(a) 23-nm-diameter spheres : Green.
(b) 70-nm-diameter spheres: Yellow.
(c) Hexagonal : Yellow.
(d) Cubic : Orange-red.
(e) Rods (aspect ratio= 4.4) : Pale green.
(f) Rods (aspect ratio= 16): Dark yellow.
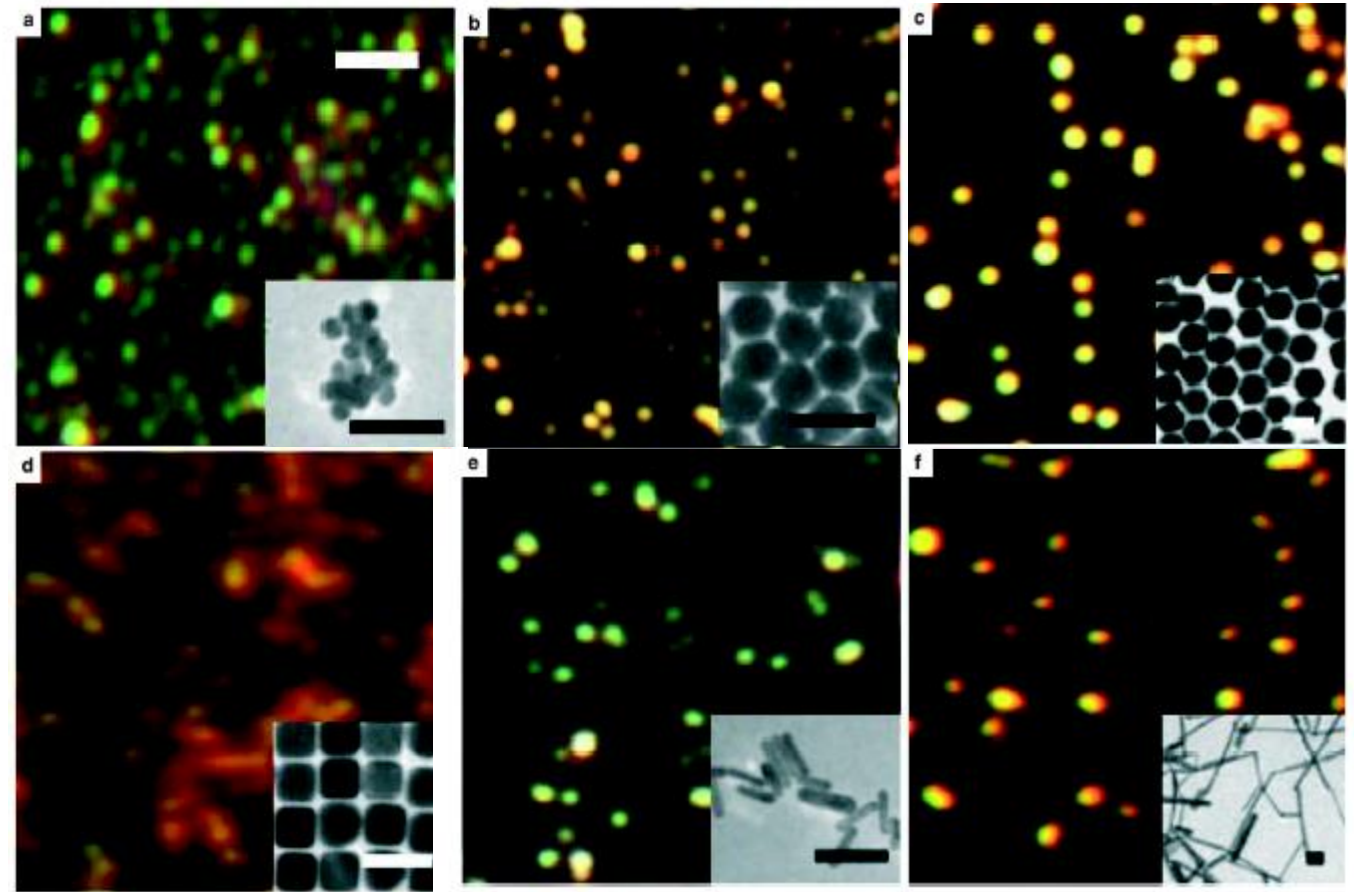
Scale bars : 2 μm in light scattering images and 100 nm in TEM images.

➢ Gold nanoparticles are common examples of metallic nanoparticles and *have found practical applications as biological and chemical sensors*, '**smart bombs**' for *cancer therapy*, and *optical switching* and *fluorescent display* materials. Many of these applications are possible owing to the development of techniques to bind photoresponsive chromophores to the surface of the nanoparticles.

➢ **Gold nanoparticles can be tagged with biomolecules** that afford delivery to specific cells and have found applications as immunoprobes for the early detection of disease.

➢ Metallic nanoparticles and metallic nanoshells are used as **dielectric sensors** because their optical properties change when they come into contact with different dielectric materials.

✓ In particular, *biological sensing* is of interest because biological analytes can bind to the surface of the nanoparticle, *causing a detectable shift* in the plasmon absorption band.

➢ Nanomaterials have also been used as key electron-transfer agents in a new generation of solar materials that couples photoresponsive π-conjugated, polyaromatic molecules to gold nanoparticle surfaces. Chromophore-functionalized gold nanoparticles afford unique device architectures and flexibility in design as these hybrid materials can be coupled covalently to conductive glass substrates that serve as electrodes, so leading to improved charge transport and photoefficiencies.

Optical Properties: Metal Nanoparticles

➤ The optical characteristics of nanosized metals are based on different principles than that of nanosized semiconductors.

➤ We have seen the quantum size confinement effects in semiconductor QDs for ~10 nm size QDs. Quantum confinement effects can be seen in metallic nanoparticles if their size is extremely small.

➤ Due to the **small Fermi wavelength of electrons in metals**, quantum confinement effects for **metallic spheres** become significant for radius values **far below 10 nm**: *perhaps* on the scale of *1 – 2 nm or less*.

➤ However, *for larger than this size*, the optical properties of nanosized metals are mainly determined by the phenomenon of **surface plasmon resonance** which is caused by the ***oscillations of the free electron gas in a metal***.

➤ Plasmon resonances are collective modes of oscillation of the electron gas in the metal. ***This is a classical***, rather than quantum, ***effect***. However, the ***particle size does play roles*** here.

➤ The interesting optical properties of nanocrystalline Au, Ag, Cu, and a number of other metals, derive from the **collective oscillation of their valence electrons**, a phenomenon known as **surface plasmon resonance**.

➤ Remember that in these metals, the electron mean free path is long (about 100 times larger than the size of the atoms), so the valence electrons feel only the average positive charge of the atomic cores as they zoom around the crystal.

➤ *Light impinging on the metal acts as an oscillating electric field, pushing and pulling on the valence electrons at the characteristic frequency of the light wave*. The situation is very much like a pendulum or a weight on a spring. The electrons, pushed away from their equilibrium positions, **feel a restoring force that is proportional to their displacement**. Their motion can be described by **Hooke's Law**: $F = kx$, where the spring constant k determines the "stiffness" of the spring.
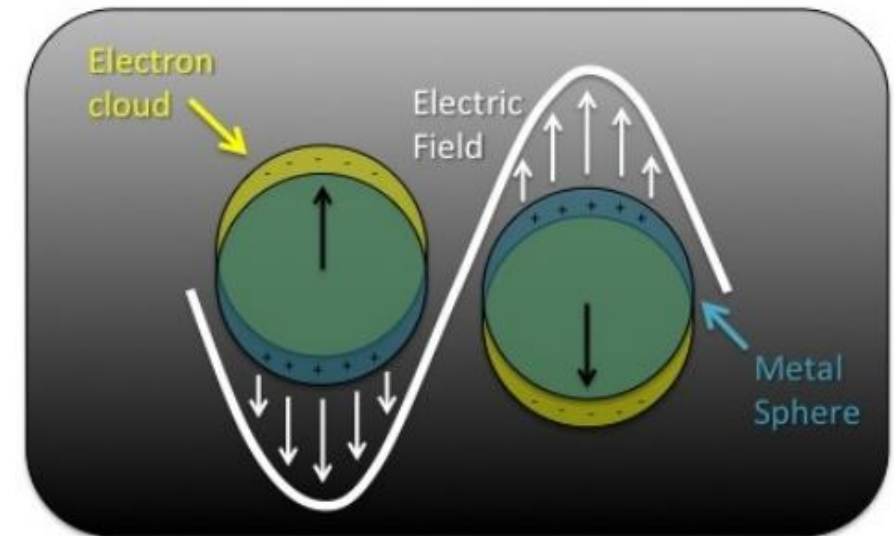
- In the case of the plasmon resonance, k is proportional to the **number density of valence electrons** n, and the square of the electronic charge e: $k = ne^2/\varepsilon_0$.

- The resonant frequency of the plasma oscillation is given by: $\omega_p = (k/m)^{1/2} = (ne^2/m_e\varepsilon_0)^{1/2}$

  where m is the electron mass. Here $\omega_p^2 = \dfrac{ne^2}{m\epsilon_0}$ is known as the volume plasma frequency. It is the natural frequency of oscillation of a collection of electrons for a given system.

- **At very high frequencies (ω) of measurement, the relationship between the refractive index and plasma frequency can be** approximated by

$$\tilde{n}^2 = 1 - \frac{ne^2}{m\epsilon_0\omega^2} = 1 - \left(\frac{\omega_p}{\omega}\right)^2 \qquad \text{(Eq. 5.4)}$$

- where ñ is the complex refractive index function (ñ = n + iκ; the real part is usually the refractive index, n, and the imaginary part is called the extinction coefficient, κ).

- For **most metals, the plasmon resonance is in the ultraviolet** part of the spectrum, but for a **few metals like Au, Ag, and Cu it is in the visible range**.

- For metal particles that are much smaller than the wavelength of light, this effect is called the **localized surface plasmon resonance, or LSPR**.

Simplest theory to describe ε is the Drude–Lorentz–Sommerfeld theory that has been developed. According to this theory, electrons, near conduction band edge, contribute to "n", hence to ε. The *square of the refractive index function is the dielectric constant $\tilde{n}^2 = \varepsilon$.*

In general, dielectric constant of the material is complex in nature ($\varepsilon = \varepsilon_1 + i\varepsilon_2$) and for most of the materials, the dielectric property is independent of the strength of the electric field, but it *depends on the frequency of the external alternating electric field incident on the materials*. (**The real part of the dielectric is related to polarization** and anomalous dispersion, while **the imaginary part is associated with dissipation of energy into the medium**. In a simple forced damped oscillator, the real component describes the phase lag between the driving and response frequency (slowing down of light in a material, described by the refractive index) and the imaginary component is the damping factor (loss of energy or absorption of light, described by the absorption co-efficient in the Lambert Beer law, although in a real material the absorption is of course quantized)… its imaginary part reflecting loss of energy of the propagating light in matter).

*The large imaginary part leads to **rapid attenuation of the wave** in the metal. The metal absorbs the radiation in this range*. This is the case for $\omega \leq 10^{12}$ Hz for copper, for example.

➢ There are **three important consequences of the LSPR effect**:

- Near the plasmon resonance frequency, *metal nanocrystals absorb and scatter light very strongly*. This makes them *brightly visible, and the strong light absorption can be exploited for light-induced local heating*. These properties are being applied in medical diagnostics and therapy, e.g., for detection and photothermal destruction of cancer cells. By adjusting the size and shape of the gold nanoparticles, which are more stable than Ag and Cu in biological media, the plasmon frequency can be tuned to the tissue-transparent near-IR region of the spectrum between 700 and 900 nm. Small quantities of plasmonic Ag and Au particles also make brightly colored and strongly scattering pigments.

- The plasmon frequency is *sensitive to the refractive index of the particle's surroundings*, i.e., its chemical environment. This makes metal nanoparticles of special interest for *sensing and biosensing applications*.

- The *local electric field of the incoming light wave is greatly enhanced at the particle surface*. This gives rise to *huge enhancement factors in optical processes such as Raman scattering and fluorescence*. Thus, certain analytical spectroscopic techniques are greatly enhanced by LSPR.

- The LSPR of the nanoparticles boosts the Raman signal intensity dramatically for molecules of interest near the surface of the nanoparticle. In order to maximize this effect, a nanoparticle should be selected with its resonant wavelength falling in the middle of the incident and scattered wavelengths.
- The overall intensity enhancement of SERS can be as large as a factor of 10^6, with the surface plasmon resonance responsible for roughly four orders of magnitude of this signal increase. The other two orders of magnitude have been attributed to chemical enhancement mechanisms arising charge interactions between the metal particle and the adsorbate or from resonances in the adsorbate alone, as discussed above.

❖ Why is SERS Useful for Studying Surface Chemistry?

- Traditionally, SERS uses nanoparticles made of conductive materials, such as gold, to learn more about a particular molecule. However, of interest in many growing fields that incorporate nanotechnology is the structure and functionalization of a nanoparticle stabilized by some surfactant or capping agent. In this case, SERS can provide valuable information regarding the stability and surface structure of the nanoparticle. Another use of nanoparticles in SERS is to provide information about a ligand's structure and the nature of ligand binding. In many applications it is important to know whether a molecule is bound to the surface of the nanoparticle or simply electrostatically interacting with it.

❑ **Theory of light scattering and absorption by metal nanoparticles**

➢ The valence electrons in metal nanoparticles oscillate in the electric field of a light wave. While the nature of these oscillations is somewhat complex in metal particles that are non-spherical, the theory for spherical particles is relatively simple and in fact was worked out over 100 years ago by German physicist Gustav Mie.

➢ Mie considered the interaction of a spherical particle with a uniform electric field, E, oscillating at angular frequency ω (= $2\pi f$).

➢ This is a good approximation when the particle diameter is much smaller than the wavelength of light, as shown on the right below.
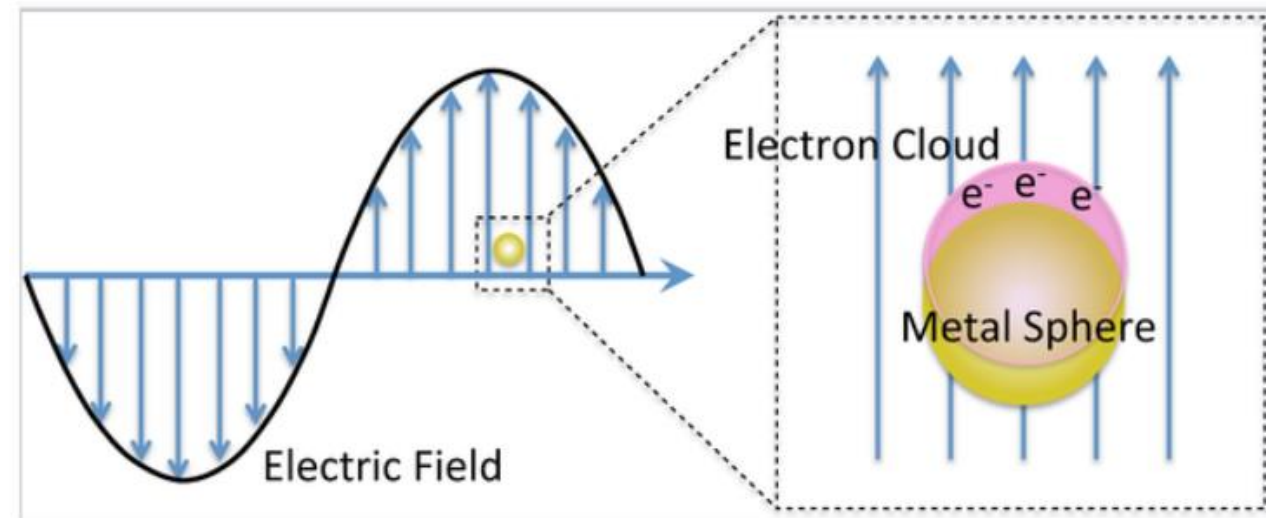
➢ The particle is embedded in a uniform, *insulating material* (e.g. a solvent) that has a dielectric constant ε_{diel}. For insulators, ε_{diel} is a *positive real number.*

➢ The dielectric constant ε of a metal is actually a complex number: $\varepsilon = \varepsilon' + i\varepsilon''$

➢ Here the real part, ***ε', is related to the refraction of light***, and the ***imaginary part, ε'', is related to light absorption***. Both ε' and ε'' are dependent on the frequency of the light.

➢ For metals ***near the plasmon resonance frequency, ε' is typically a negative number***.

➢ The ***cross-section for absorption*** of the light wave by the particle is:

$$\sigma_{absorption} = \frac{9\omega}{c}\epsilon_{diel}^{\frac{3}{2}}V\frac{\epsilon''_{metal}}{(\epsilon'_{metal} + 2\epsilon_{diel})^2 + (\epsilon''_{metal})^2} \qquad (11.6.5)$$

➢ and the ***cross-section for scattering*** is:

$$\sigma_{scattering} = \frac{3}{2\pi}(\frac{\omega^4}{c})\epsilon_{diel}^2 V^2 \frac{(\epsilon'_{metal} - \epsilon_{diel})^2 + (\epsilon''_{metal})^2}{(\epsilon'_{metal} + 2\epsilon_{diel})^2 + (\epsilon''_{metal})^2} \qquad (11.6.6)$$

➢ The sum of these two is the cross-section for extinction:

$$\sigma_{extinction} = \sigma_{absorption} + \sigma_{scattering} \qquad (11.6.7)$$

❖ **Resonance Condition**

➤ These **cross-sections become large** when the **(ε' + 2ε)** term in the denominator becomes **small**.

$$\epsilon'_{metal} \simeq -2\epsilon_{diel} \qquad (11.6.8)$$

➤ This occurs when:

➤ This is known as the **resonance condition**.

➤ For 15 nm diameter gold nanoparticles in water, this happens at about 580 nm, resulting in the characteristic wine-red color of colloidal gold solutions.

➤ Changing the solution environment (e.g., by adsorbing a molecule onto the gold surface) changes ε_{diel} and thus alters the color slightly.

❖ Note that the spherical nanoparticle is distinctly smaller than the incident wavelength (*2R<<λ*), so that **only dipole oscillations have to be accounted for** and higher terms (quadrupole oscillations, etc.) can be neglected.

❖ A curious feature of the above Equation (11.6.5) is that there is no absorption if ε''_{metal} = 0, but there is also no absorption if ε''_{metal} = ∞ (*in both the cases the right-most term fraction in above Eq. becomes zero*).

- We know that a beam of light incident on a surface can undergo reflection, absorption and transmission to different extents depending on *the material and the wavelength of the light.*

- Metal nanoparticles show light *absorption, scattering, and strong to weak light emission or fluorescence.*

- It is important to note that the **cross-section for scattering is proportional to the square of the volume of the particle, V²**, whereas the absorption is proportional to V.

- This means that very **small gold particles (< 5 nm) are strongly absorbing** but not strongly scattering.

- It was found that for NPs with *d* ~20 nm the absorption process dominates, that is, C_{sca}~0, such that $\sigma_{ext} \approx \sigma_{abs}$.

- Larger particles *(>30 nm) scatter* light very strongly.

- Depending on the application, therefore, we choose larger or smaller particles.

- Further, metal nanoparticles cause surface(field)-enhanced Raman scattering (SERS) and surface(field)-enhanced fluorescence spectroscopy.

OPTICAL EXTINCTION OF NANOPARTICLES: *Surface Plasmon*

In bulk metals the light is totally reflected in the visible region and most metals therefore present a shiny (silvery) appearance.

Two exceptions are gold and copper which have distinct colors due to some absorption in the visible range due to inter-band transitions from the filled d bands to the sp conduction band. Only the complimentary part of the light is visible and so these metals appear colored.

On the other hand, the metal powders are dark brown or black. Their large surface area causes the light to be nearly fully absorbed due to repeated reflections.

However, if the particle size is reduced to nm range, true colors appear again, notably for gold and silver.

What is the physical basis of the optical extinction of metal nanoparticles?

The **physical basis of the optical extinction of metal nanoparticles** is follows.

If an obstacle, which could be a single electron, an atom or molecule, a solid or liquid particle, is illuminated by an electromagnetic wave, electric charges in the obstacle are set into oscillatory motion by the electric field of the incident wave.

Accelerated electric charges radiate electromagnetic energy in all directions; it is this secondary radiation that is called the radiation *scattered* by the obstacle.

In addition to reradiating electromagnetic energy, the excited elementary charges may *transform part of the incident electromagnetic energy into other forms* (thermal energy, for example), a process called **absorption**.

Scattering and absorption are not mutually independent processes.

Fig. 6.18 Light extinction by a nanoparticle. After encountering a nanoparticle, incident light with an intensity I_0 is reduced to an intensity I and the amount of light extinguished is given by the extinction efficiency Q_{ext}.

The lost light is either absorbed by the particle or converted to scattered light. The absorbed light is converted to heat and can be used for hyperthermia while the scattered light can be used to detect the location of the particle.
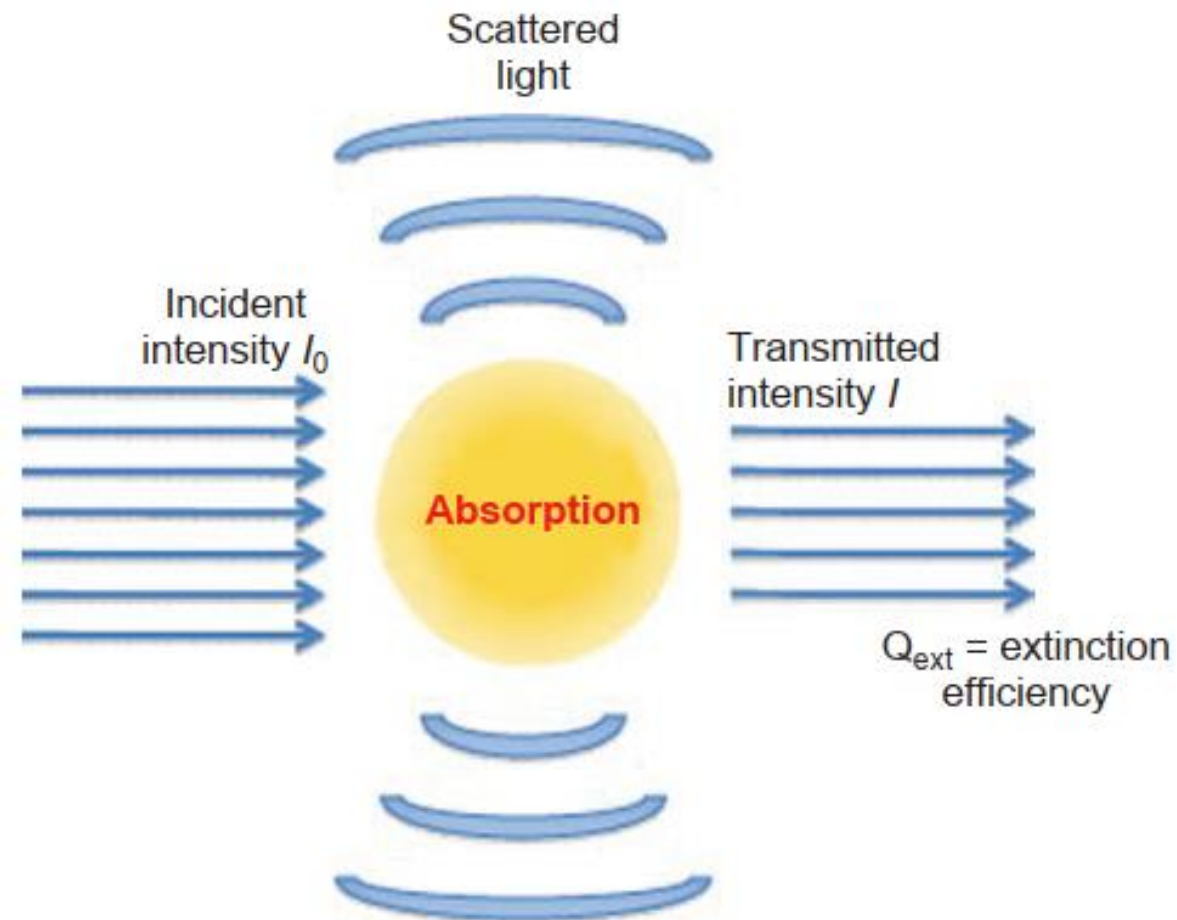
Metals can be considered as confined plasma of positive ions (consisting of nuclei and core electrons which are fixed) and conduction electrons (free and mobile).
In neutral case, the positive charge cloud of ions and negative charge cloud of electrons overlap with each other.
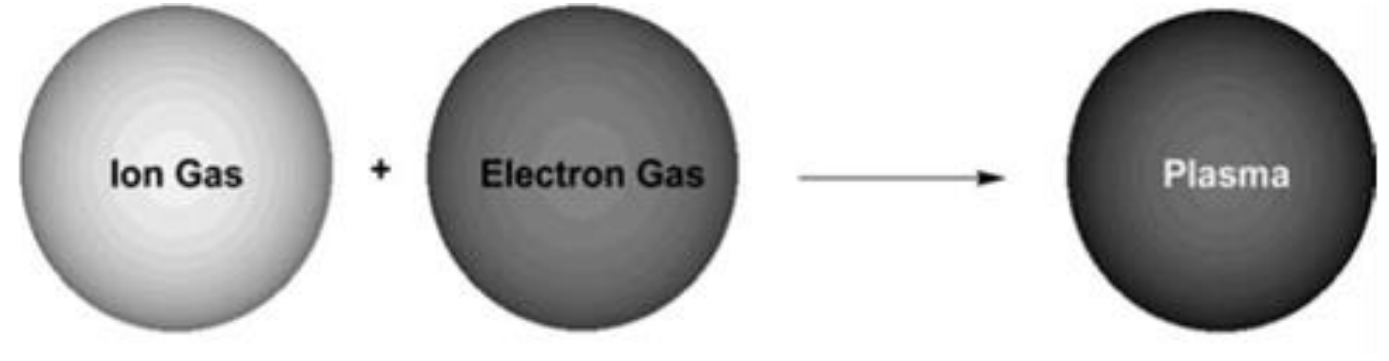

By some external disturbance, i.e. irradiation by electrons or electromagnetic radiation, the charge cloud is disturbed, and electrons are moved away from the equilibrium position.
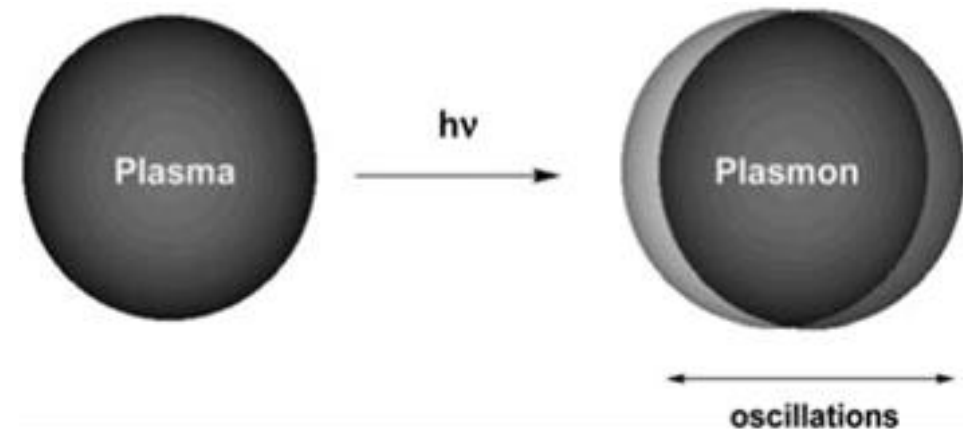
For example, when an electromagnetic radiation interacts with a metal, **the periodic electric field component of the electromagnetic radiation** causes a collective oscillation of the conductance electrons relative to the lattice of positive ions.

The electric field displaces the electrons to create uncompensated charges at the nanoparticle surface (Fig. 16.1).

Scheme 16.1 In a metal, the plasma is created by the combination of a (positive) ion gas and an electron gas. The plasma is then disturbed by the absorption of a photon. The resulting electrodynamic force is causing an oscillation, which is known as plasmon.
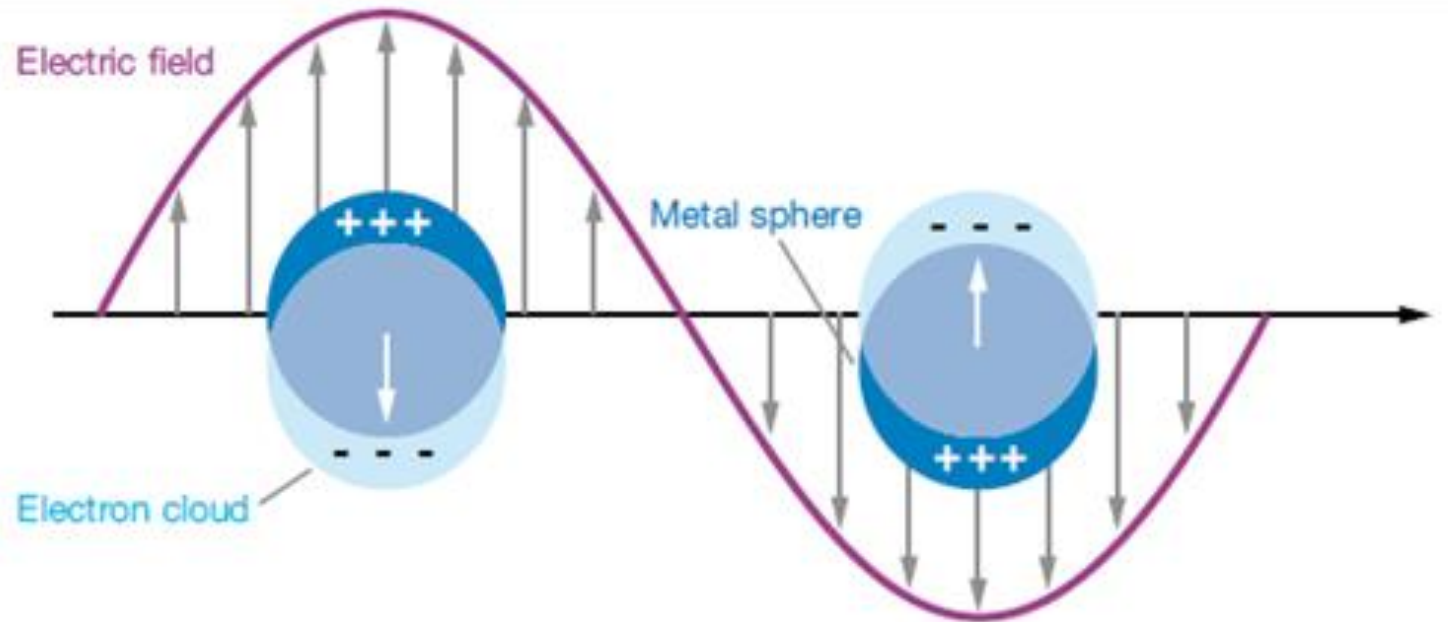
If the density of electrons in one region increases, they repel each other and tend to return to their original equilibrium position.

As electrons move towards their original positions, they pick up kinetic energy and instead of coming to rest in equilibrium configuration, they overshoot.

They oscillate back and forth.

The collective oscillations of conduction electrons in metals are called *plasmons*.

When the particle size is much smaller than the wavelength of light, a dipole is created due to the accumulation of the electrons at one end and the depletion of electrons at the other end. This dipole creates a restoring force for the electron cloud.

Since the *penetration depth of an electromagnetic wave striking the metal surface is limited* (<50 nm for Ag and Au), only *plasmons caused by surface electrons are significant* and are commonly referred to as *surface plasmons*.

At a certain frequency of the incident light there is a *resonance* at which there is *a maximum absorption or scattering of energy from the incident light wave and a peak is observed* in the absorption/scattering spectra. This peak is called the **"surface plasmon resonance (SPR)" peak**.

The electrons in the nanoparticles made of metals couple with an external electromagnetic field to create a *localized* plasmon. This *plasmon cannot propagate* since the nanoparticle is much smaller than the wavelength of the light, however they will have a characteristic resonance frequency that causes absorption of the light at particular frequencies. This is plasmon absorbance is therefore termed as the "*localized surface plasmon resonance* (**LSPR**)"

This LSPR leads to **the buildup of polarization charges on the nanoparticle surface**. A homogeneous field builds up in the interior of the nanoparticle, *while a dipolar field is produced at the exterior, resulting in strong light absorption/scattering, the appearance of intense SPR bands, and the enhancement of the nearfield in the immediate vicinity of the nanoparticles.*

➢ The spectroscopic responses of **larger metallic nanoparticles** are different due to the excitation of higher-order modes such as quadrupoles and retardation and skin-depth effects. For larger particles, the oscillations of electrons become less coherent and higher modes of plasma oscillation (e.g. quadrupolar and multipolar) appear.

➢ When the particle size is much larger than the mean free path of the electrons ($L\sim10\text{-}20$ nm for gold), electrons can be significantly accelerated within the metal between collisions leading to scattering losses. Due to these factors **the surface plasmon peak** *broadens and additional peaks appear* **as the particle size is increased**.

➢ *Note that very small nanoparticles (<1–2 nm) do not display this LSPR phenomenon, as their electrons exist in discrete energy levels, and bulk metal has a continuous absorbance in the ultraviolet (UV)/visible/infrared (IR) regions without any resonance*. By reducing the size of the particles further below the mean free path, critical scale is attained when dimensions become comparable to the Fermi wavelength of metals, $\lambda_F <1$–2 nm. *Electrons in these subnanometric-sized particles* *do not have a continuous DOS**, which is necessary to support the plasmon and the SPR disappears*.

…………………………………………………..

Plasmonic Nanoparticles: *The nanoparticles that show optical properties, known as* **LSPR**.

Plasmon: *Quantized coherent oscillations of free electrons*

Surface Plasmon Resonance (SPR): *Quantized coherent oscillations of free electrons at the surface (at the metal and dielectric interface). SPR is also known as* **Localized Surface Plasmon Resonance (LSPR).**

…………………………………………………..

The ***bandwidth, peak height, and peak wavelength all depend*** *on the nanoparticle chemical composition, size, and geometrical shape, surface charge, surface-adsorbed species, interparticle interactions, and the dielectric property of the surrounding environment.*

➤ The *position of the plasmon absorption band* and *its intensity* are sensitive to the size and shape of nanoparticles (spheres, rods, ellipsoids, disks, triangular plates, cubes) as well as to the *dielectric characteristics of the surrounding material*, that is, **metallic nanoparticles can be considered as "tunable" inorganic chromophores.**

➤ Cu, Ag, and Au NPs, with their s-valence electron nearly free, are highly polarizable showing sharp plasmon resonances in the visible region, (LSPR(Au) = 520 nm, LSPR(Ag) = 400 nm, and LSPR(Cu) = 560-570 nm).

➤ The LSPR induces a strong absorption of the incident light. Gold, silver and copper nanoparticles show strong LSPR absorption in the visible region.

➤ This LSPR absorption is responsible for the appearance of colors in the sols of these metals as only the part of the visible light complimentary to the absorption wavelength reaches the eye.

➤ This LSPR leads to **the buildup of polarization charges on the nanoparticle surface**. A *homogeneous field builds up in the interior of the nanoparticle*, **while a dipolar field is produced at the exterior, ……resulting** in strong *light absorption/scattering*, **the appearance of intense SPR bands,** and ***the enhancement of the near field in the immediate vicinity* of the nanoparticles**.

➤ The *bandwidth*, *peak height*, *and* *peak wavelength* all **depend** *on the nanoparticle's*

   ✓ **chemical composition**,

   ✓ *size*,

   ✓ **geometrical shape**,

   ✓ **surface charge**,

   ✓ **interparticle interactions**,

   ✓ **surface-adsorbed species**, *and*

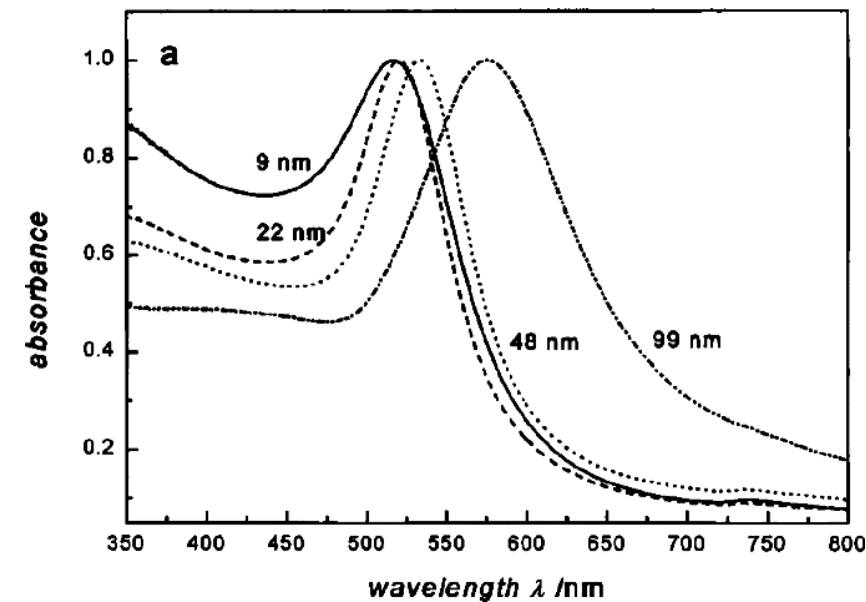   ✓ **the** *dielectric* **property of the** *surrounding environment*.

Fig. 5.4. Experimental extinction spectra of gold nanoparticles of diameters 9, 22, 48 and 99 nm.

Figure 2. Tunability of plasmon resonance in colloidal solutions. A series of ***colloidal silver nanoparticle solutions*** show a variety of colors due to the different sizes and shapes of the nanoparticles within each solution. Photograph courtesy of Keiko Munechika, Ginger Lab.

Figure 1.12 Monodispersed *gold nanoparticles of different sizes* (2–200 nm) in water.

Note the different colors due to different light interactions, which are dominated by particle size. (Courtesy of Ted Pella, Inc., available on the

World Wide Web at http://www.tedpella.com/gold_html/goldsols.htm.)

➤ Nanoparticles of **other metals** **such as platinum, palladium, and iron** do **not show such resonance**. This is because in these metals the resonance is suppressed due to mechanisms such as ***strong conduction electron relaxation*** or ***radiation damping due to scattering***.

➤ In fact, **many metal sols appear yellow or brown in color**. The reason for this is that the ***plasma frequencies of most metals lie in the UV, and the color of the nanoparticle colloid is due to the tail of the surface plasmon band***: being broad, *it tends to produce a yellow color*. Upon aggregation or growth, the band tends to broaden and deepen, so that the color changes slowly to a deeper brown.

➤ *(Do you know why the **yellowish tinge** observed in white dresses made of cellulose? We use products like Ujala or Robin Blue to make it look white!)*

❑ *Size Effect on LSPR*

➢ As mentioned earlier, nanoparticles (NPs) can **absorb** and **scatter** energy, and depending on their size and shape, *one mechanism can dominate over the other*.

➢ To understand the range of the ***different processes as a function of size***, the ***absorption and scattering phenomena were studied*** for spherical NPs using the Mie exact solution (Figs. 5.2 & 6.20).

➢ The spectra (Fig. 5.2b for Ag nanoparticles) show that at about 320 nm all the efficiencies have a local minimum that corresponds to the wavelength at which the **Ag** dielectric function, both real and imaginary parts, almost vanishes. Therefore, this feature of the spectra is inherent to the material properties and *independent of the particle geometry*.

✓ ***Below 320 nm, the absorption of light is mainly due to the inter-band electronic transitions***; therefore, *this feature of the spectra is also independent of the shape*.

❑ *Size Effect on LSPR* (contd.)

✓ It was found that for NPs with d ~20 nm the absorption process dominates, that is, σ_{sca}~0, such that $\sigma_{ext} \approx \sigma_{abs}$.

✓ For such small NPs, the absorption efficiencies show **a single peak always located at the same** wavelength ($\lambda \approx 355$ nm), **but the intensity increases linearly with the sphere size**.

✓ However, **as d increases, light scattering becomes important rapidly and dominates** the response of NPs with d ~100 nm.

➢ Note that the importance of light absorption over scattering depends not only on the NP's size, but also on its shape, composition, and environment.

➢ *The LSPR absorption peaks for small particles (5 nm < diameter < 20 nm) of gold and silver are localized **near** 530 nm and 415 nm respectively.*
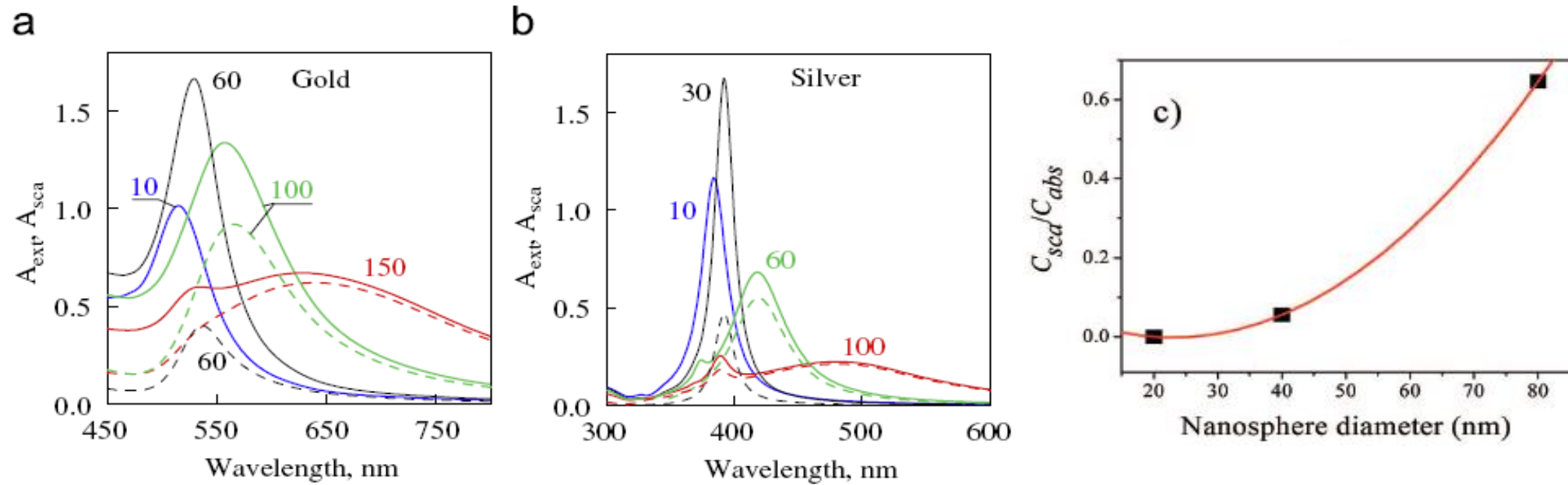
Fig. 5.2. Extinction (solid lines) and scattering (dashed lines) spectra of gold (a) and silver (b) spheres in water. Numbers near curves correspond to the particle diameter. (c) *Increase in the plasmon scattering to absorption ratio by increase in particle volume in gold nanospheres*. *Note that for small particles the extinction is mainly due to the absorption*; scattering (dashed lines) appear for larger particles.

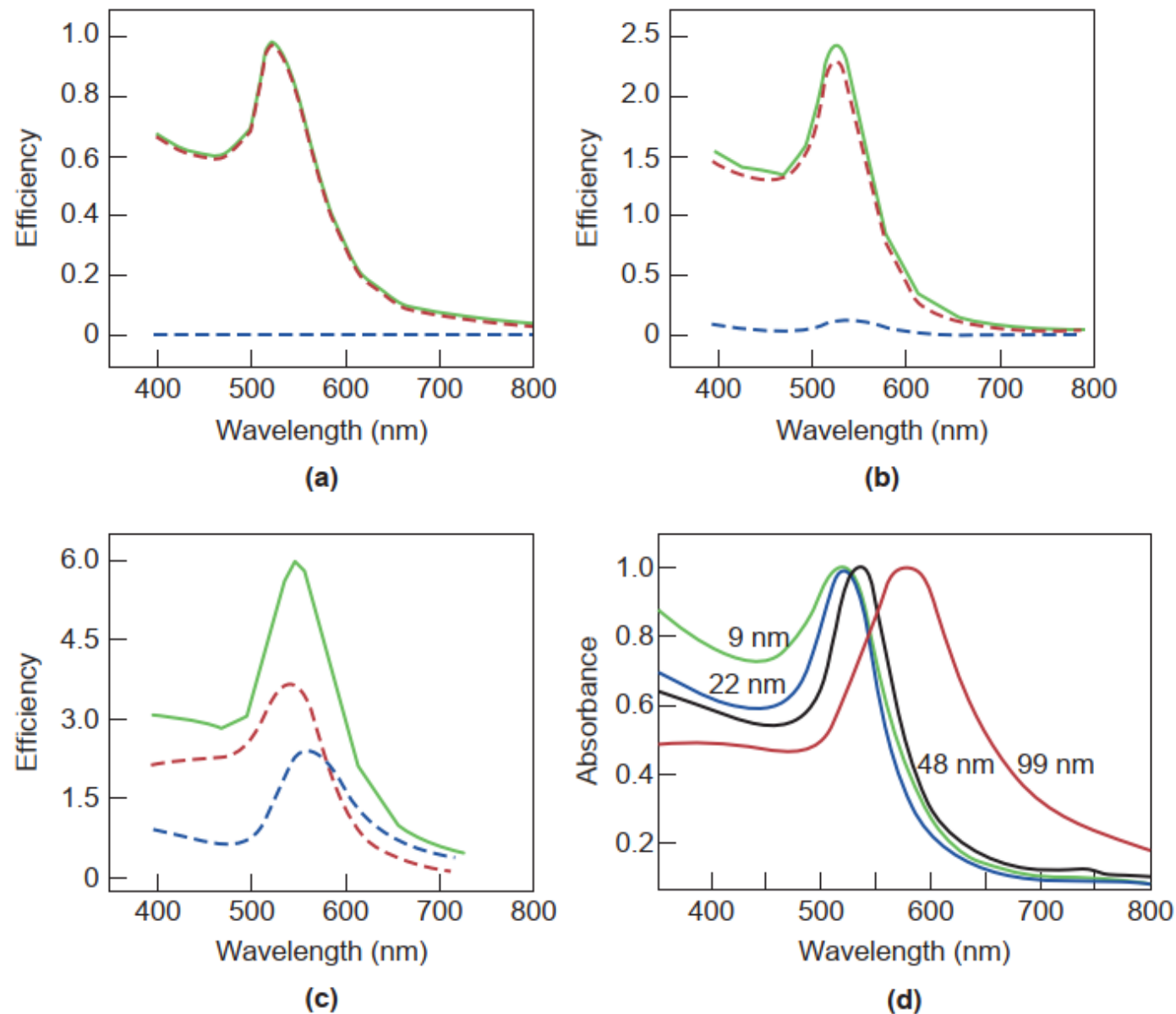(N.G. Khlebtsov, L.A. Dykman, Journal of Quantitative Spectroscopy & Radiative Transfer (2010) 111, 1–35.)

Fig. 6.20 **Extinction vs. size for Au nanoparticles**. Calculations of the absorption (red dashed curves), scattering (blue dashed curves) and extinction efficiency, Q_{ext}, (green solid curves) as a function of the wavelength of the incident light for Au nanospheres of diameter (a) 20 nm, (b) 40 nm, and (c) 80 nm. (d) Measured extinction spectra of Au nanoparticle suspensions of different diameters varying from 9-99 nm.

*Note that up to a **diameter** of ~50 nm the position of the peak is independent of particle size.*

❑ *Size Effect on LSPR* *(contd.)*

➢ Equation (5.6) shows that the extinction cross section varies as R^3. As the number density decreases as R^3 *for a **given amount*** of the colloidal material, *the absorption coefficient is independent of the particle size in the dipolar approximation* (which itself is valid when the particle size is small, $R << \lambda$).

➢ *The extinction coefficient is found to be size-independent in the size range between approximately 5 nm and 30 nm.*

➢ *Above 30 nm, the quadrupole and the multipole terms* in the Mie summation become significant while….

➢ *below 5 nm, the collision of the electrons with the surface of the particle becomes more important as the particle size becomes smaller than the electron mean free path. The electrons are scattered at the metal surface in an elastic and completely random way, inducing a fast loss of the plasmonic oscillation coherence. **The smaller the metal sphere, the faster the coherence loss and the bigger the band broadening** (Fig. 5.6.).*

❑ *Size Effect on LSPR* (contd.)

➢ *The spectroscopic responses of* **larger metallic nanoparticles** *are different due to the excitation of* **higher-order modes such as quadrupoles** *and retardation and skin-depth effects*. For larger particles, the oscillations of electrons become *less coherent*, and higher modes of plasma oscillation (e.g., quadrupolar and multipolar) appear.

✓ When the particle size is much larger than the mean free path of the electrons (L~10-20 nm for gold), electrons can be significantly accelerated within the metal between collisions leading to scattering losses. Due to these factors, **the surface plasmon peak broadens and additional peaks appear as the particle size is increased**.

➢ When the particle size decreases, the *increased rate of electron surface collision changes the dielectric constant of the metal such that* the SPR **band is largely damped** and **broadened**. This phenomenon is called **intrinsic size effect**. *This usually happens for particle sizes below about 5 nm.*

➢ The effect is shown schematically in Fig. 5.6 which shows plots of the extinction coefficient vs. energy (inversely related to wavelength) of the incident light for particle sizes smaller than the mean free path.
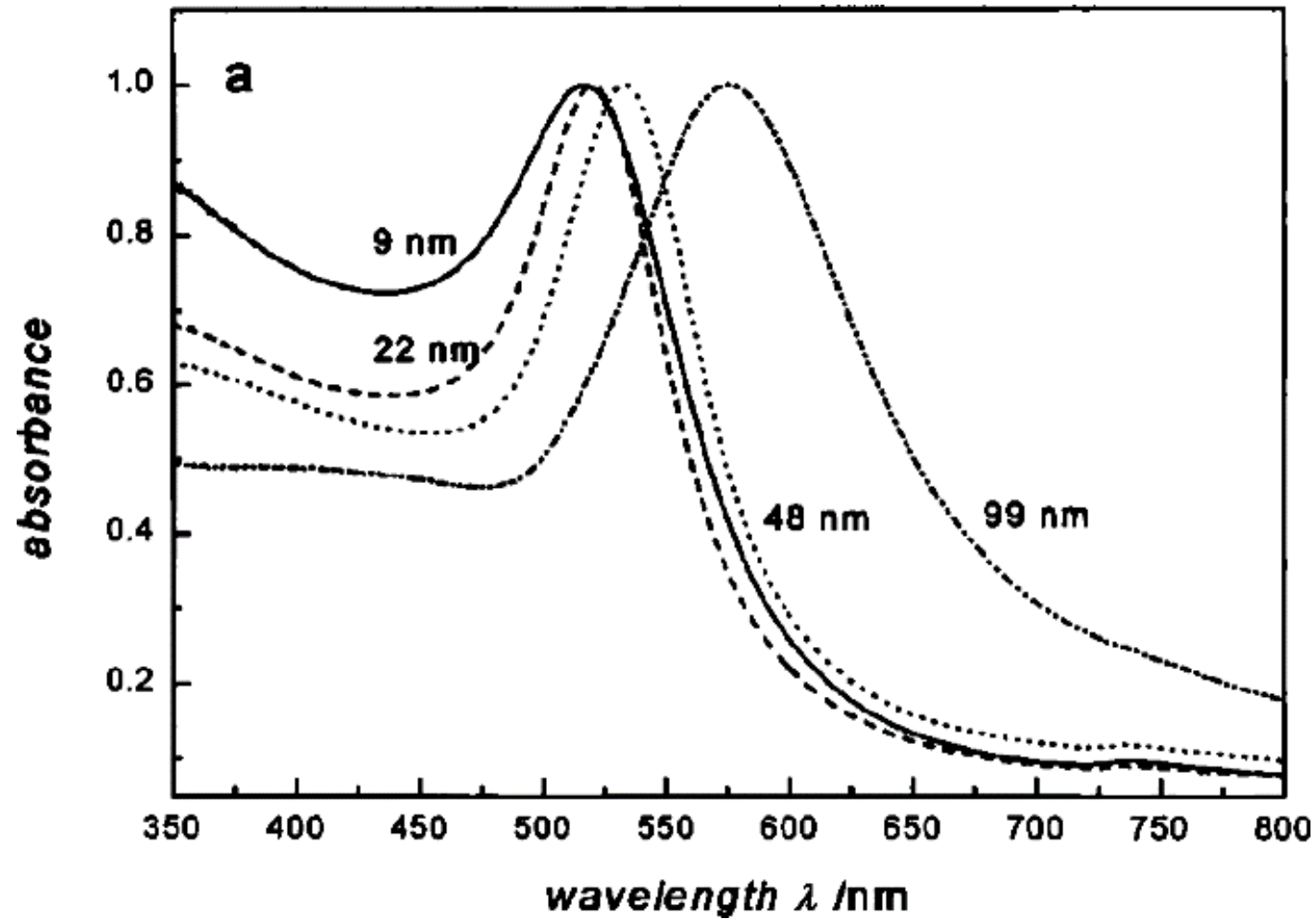
Fig. 5.4. Experimental extinction spectra of gold nanoparticles of diameters 9, 22, 48 and 99 nm. *The shift in the peak occurs due to the contributions from quadrupolar higher resonances as well as due to the contribution of the scattering* (reprinted with permission from American Chemical Society).
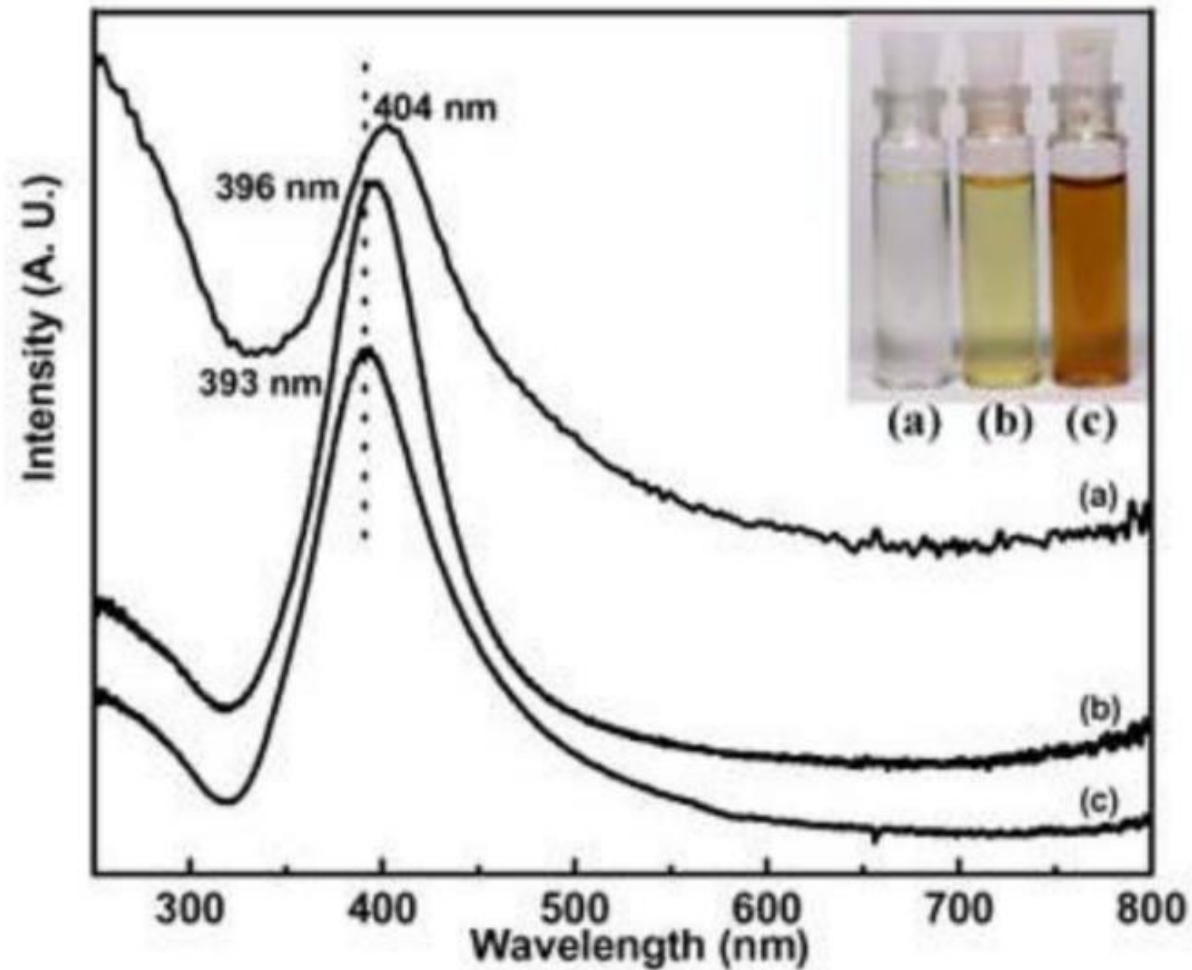
Figure 7. UV-Vis absorption spectra of nanosized silver particles. (Inset) Different colors arising from different sizes. *The shift in the peak occurs due to the contributions from quadrupolar higher resonances as well as due to the contribution of the scattering.*
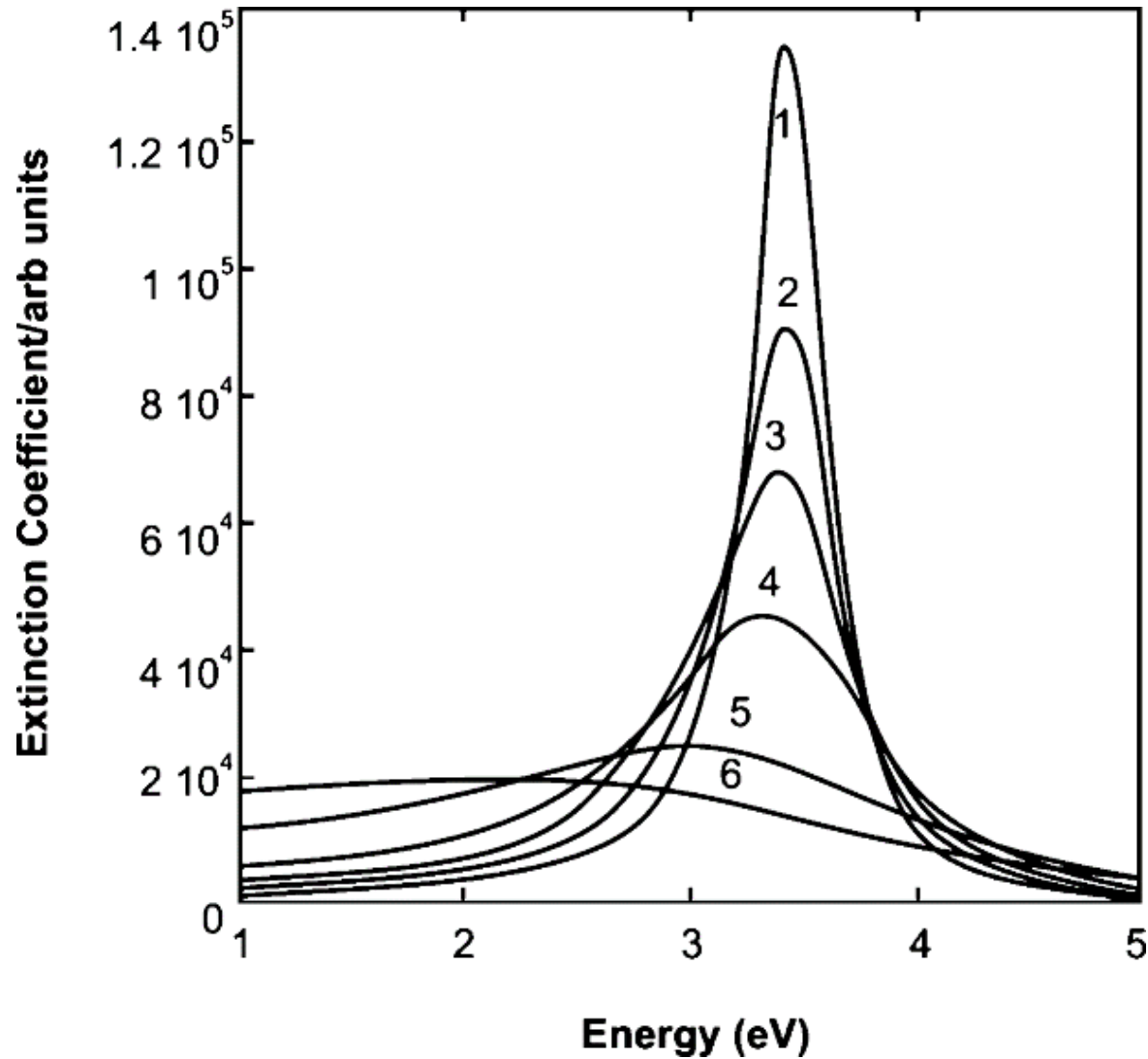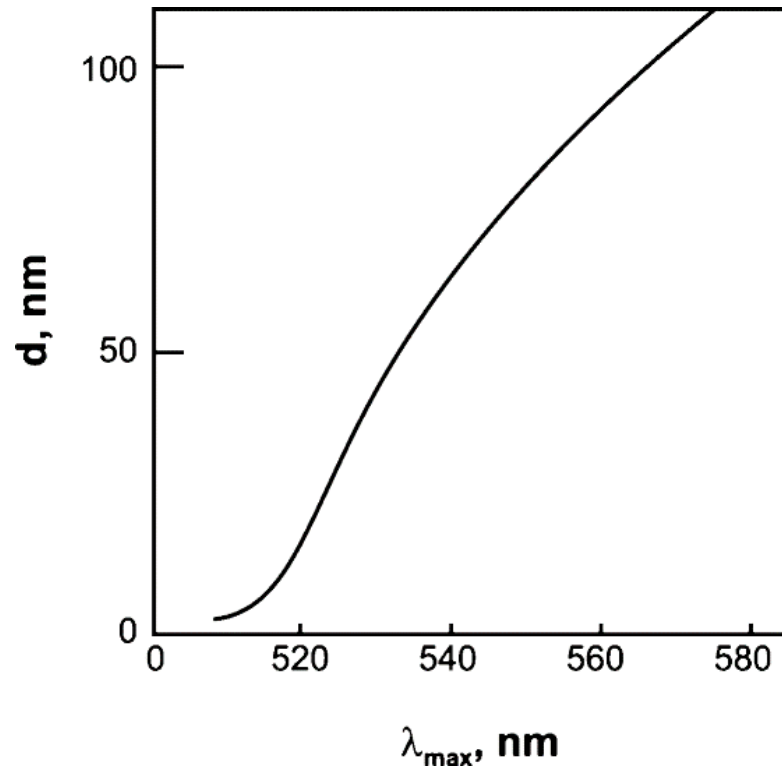
Fig. 5.6. Effect of decreasing the particle size below the mean free path of the electrons in the bulk metal (i.e. usually below 5 nm); the particle size is decreasing from 1 to 6.

(reproduced with permission of John Wiley & Sons, Inc. copyright (2001)).

➢ *Note that **very small** nanoparticles (<~2 nm) do not display this LSPR phenomenon, as their electrons exist in discrete energy levels, and bulk metal has a continuous absorbance in the ultraviolet (UV)/visible/infrared (IR) regions without any resonance.*

➢ ***By reducing the size of the particles further below the mean free path**, critical scale is attained **when dimensions become comparable to the Fermi wavelength of metals**, λ_F ~1–2 nm. **Electrons** in these **subnanometric-sized** particles **do not have a continuous DOS, which is necessary to support the plasmon and therefore SPR disappears.***

➢ The shift in the position of the peak in the extinction coefficient with particle size for the case of gold as determined experimentally by the various researchers has been combined into a single plot by Khlebtsov and Dykman (Fig. 5.5). The plot can be used as a calibration curve to determine the particle size from the absorption spectra.

For insulators and semiconductors, the Mie peak is close to the position of the bulk absorption bands, and the immediate effect of decreasing particle size is much smaller.

Fig.5.5. Shift in the experimentally determined extinction peak position with particle diameter for gold spheres in water.

❑ *Particle shape dependence of LSPR*

➢ A limit of the Mie model resided in the description of elongated or spheroidal NPs (e.g., nanorods, elliptic NPs, etc.).

➢ As noted above, *the surface plasmon peak shows a shift with a change in the particle size*. A ***much more drastic effect on the surface plasmon absorption can be observed when NP shape changes***.

➢ Indeed, for ***anisotropic metal NPs, electrons can oscillate to a different amplitude along the three axes of the nano-object***. Such *different oscillations result in a splitting of the plasmon band into two or more bands*.

✓ For instance, the plasmon absorption of Au nanorods (NRs) splits into two bands corresponding to the oscillation of free electrons along and perpendicular to the long axis of the rods: longitudinal and transverse modes, respectively. The transverse mode shows a resonance at about 520 nm, which is coincident with the plasmon band of spherical particles, while the resonance of the longitudinal mode is red-shifted and strongly depends on the NR *aspect ratio R (defined as the length of the rod divided by its width,* i.e., *a/b* in Fig. 7.3).
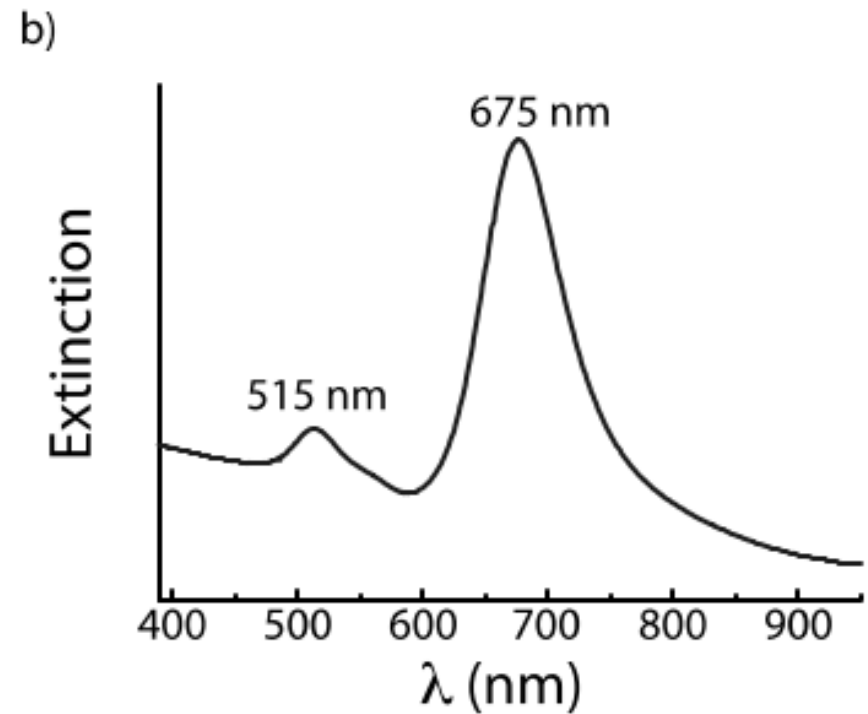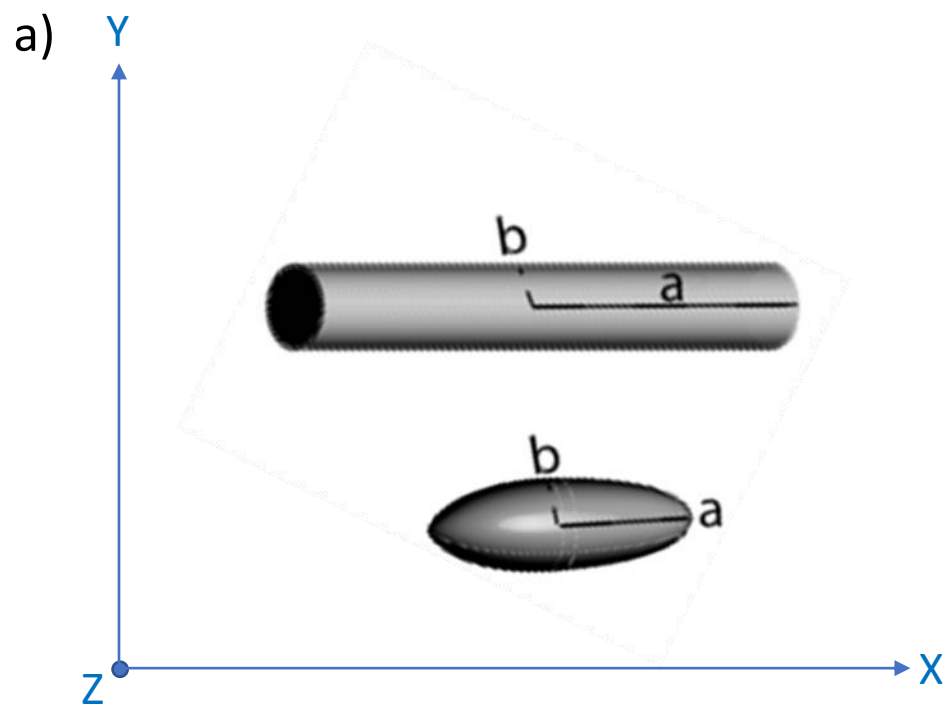
Figure 7.3 (a) Spheroidal metal NP and nanorod with respective axis: ***a is the principal axis*** and ***b is the axis perpendicular to the principal one***. (b) Extinction spectrum of Au nanorods with ***aspect ratio (a/b)*** of about 2.5. The lower energy longitudinal mode is due to the electron cloud oscillation along the spheroid principal axis (along a-axis, x-direction), while the high energy transverse one is referred to the electron oscillations perpendicular to the principal axis (along b-axis, y-direction).

➢ At the end, the energy separation between the two bands increases with the increase in R. The Gans model well describes the LSPR behavior of these systems.

➢ The simplest form of a nonspherical shape is a *spheroid*. For spheroids, a classical quasistatic approach serves well to describe the spectral position, width, and strength of the dipolar plasmon resonance.

➢ Based on classical approaches, *for a metal nanoparticle sufficiently small compared to the wavelength of light* λ, there **is a resonance condition associated with each axis j of a spheroid**:

➢ $$\varepsilon = \varepsilon_m \left(1 - \frac{1}{L_j} \right)$$

where ε is the complex wavelength-dependent dielectric function of the metal, L_j is the *geometrical depolarization factor along the axis j*, and ε_m is the dielectric function of the surrounding medium.

- $L_1 = L_2 = L_3 = 1/3$ for *spherical* particles.

- For *prolate spheroidal* particles ($L_1 = L_2 < L_3$), the dipole resonance *splits into two* absorption bands —*longitudinal* and *transverse modes* —where the induced dipole oscillates *along* *and* *perpendicular* to the *long axis* of the spheroid, respectively.

- The *longitudinal resonance band shifts towards longer wavelengths (red-shift)* and *increases in absorption cross-section* as *the aspect ratio of the spheroid increases*, whereas *the transverse resonance band remains near the wavelengths of the spherical particle absorption band*.

- This example of the simplest nonspherical shape demonstrates that *nonspherical nanoparticles will exhibit multiple optical extinction bands due to their anisotropy.*
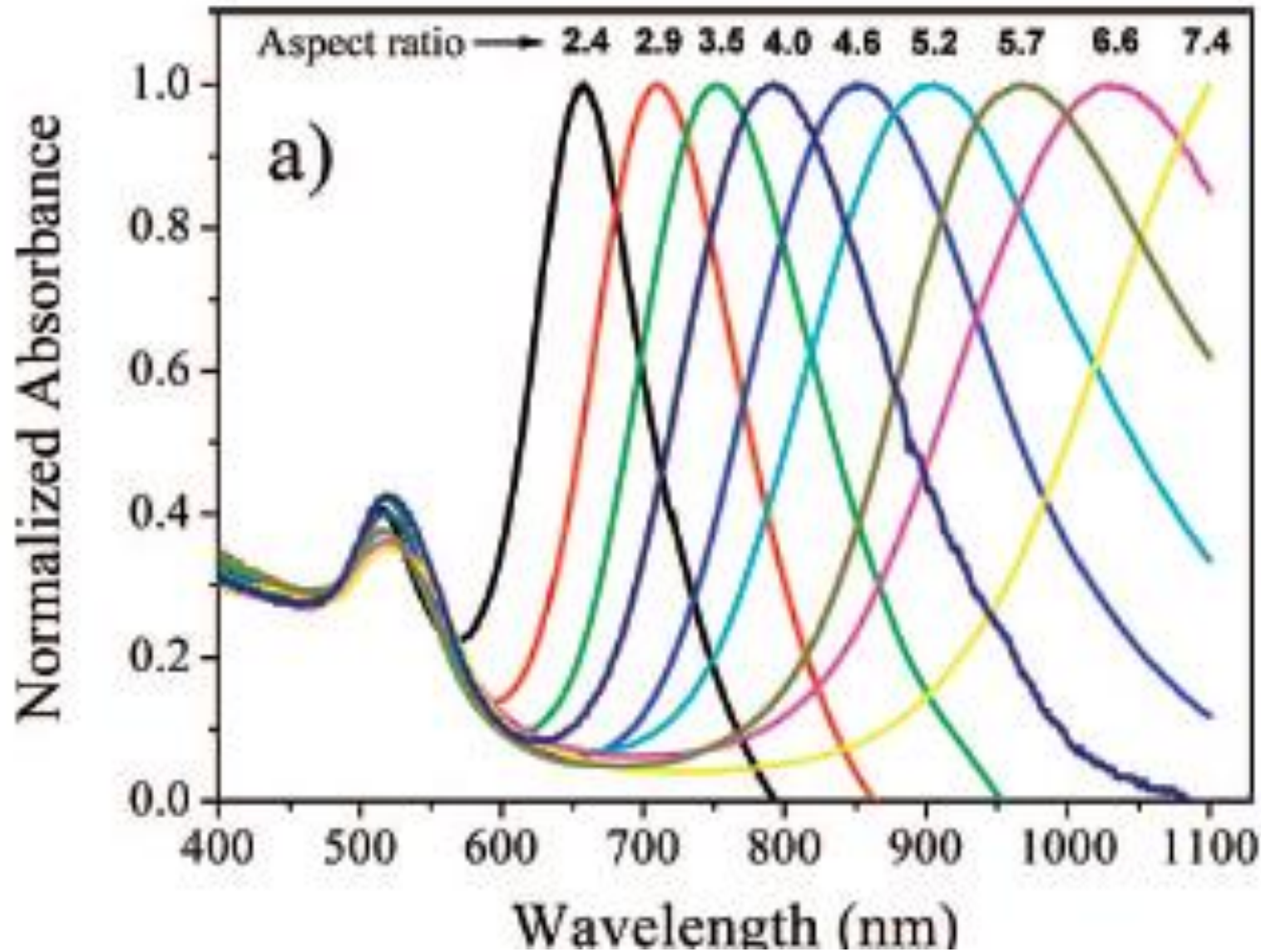
Fig. 5.7. Extinction coefficient of gold nanorods with different aspect ratios (Length/Width); the transverse band at about 520 nm remains nearly unchanged while there is a large shift towards longer wavelengths in the longitudinal mode as the aspect ratio increases. (Reprinted with permission from Elsevier. Copyright (2010)).
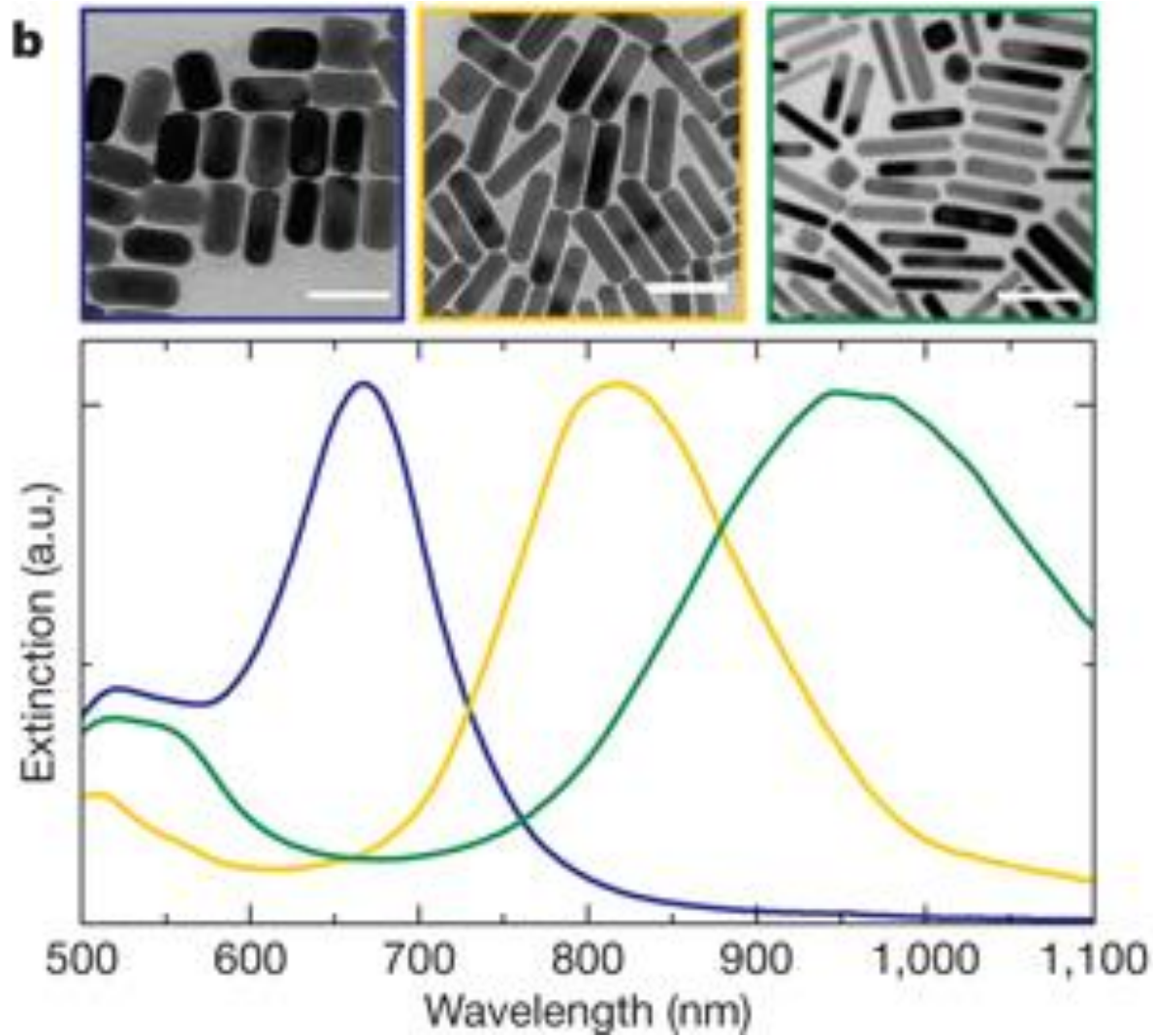
Exptl.: Gold nanorods of different aspect ratios and corresponding extinction spectra.

(P Zijlstra *et al. Nature* **459**, 410-413 (2009))

Fig. 3.8 Absorption efficiency of (a) silver and (b) gold nanorods in air at various *aspect ratios*.
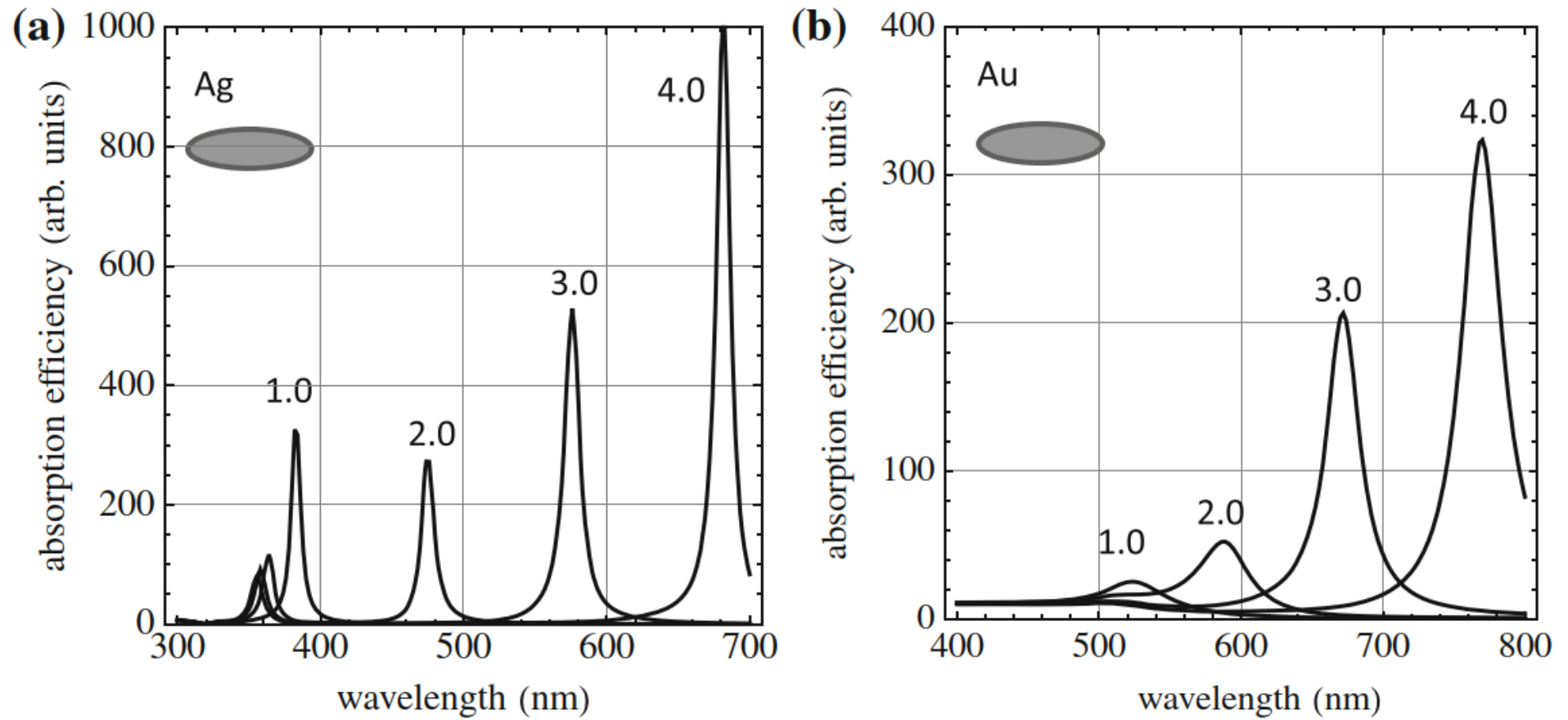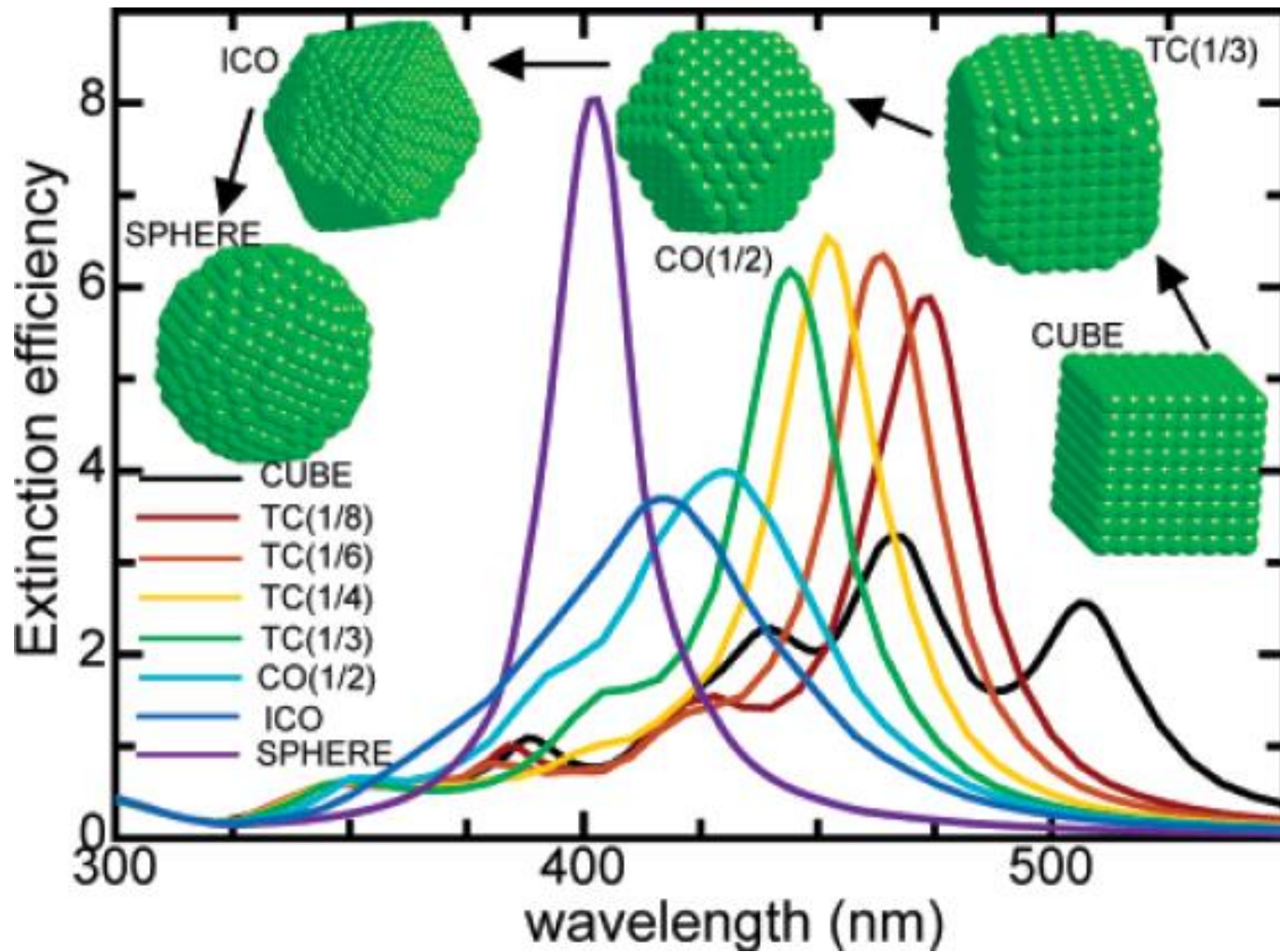
Figure 5. Extinction efficiencies as a function of the wavelength of the incident light of a silver cube, different truncated cubes, and a spherical nanoparticle.

TC= truncated cube; CO=cuboctahedron; ICO=icosahedron.

The nanosphere shows just one SPR signal, whereas the nanocube, due to several distinct symmetries for dipole resonance, shows more peaks. In addition, *the position of the **most intense peak** for the nanocube is **red-shifted** compared with that of the sphere. Such a shift is caused by the accumulation of surface charges at the corners of the nanocube and is observed, in general, for any NP with sharp corners.* In these systems, *the increased charge separation reduces the restoring force for electron oscillation, which in turn results in a shift of the resonance peak to lower energy.*

❑ *Particle aggregation or Proximity effects on LSPR*

➢ The Mie model works well only for spherical nanoparticles (NPs) in solution, or solid-state matrix, with low concentration where NPs mutual interactions can be neglected.

➢ ***Increasing the NP concentration*** *or* ***by some other mechanisms***, when *two metal nanoparticles are brought in proximity to each other*, the inter-particle distance becomes smaller (till aggregation), the near-field on one nanoparticle is influenced by its neighbors. Thus, the electric field E felt by each particle is the sum of the incident light field E_0 and the *near-field E_{nf} of the neighboring particle*.

  ➢ $E = E_0 + E_{nf}$

➢ As a *result of this near-field interaction, plasmon oscillations of the two nanoparticles become coupled.* This ***plasmon coupling*** *modulates the LSPR frequency of the coupled-nanoparticle system*. This phenomenon is well described by the Maxwell–Garnett theory.

➢ As a result of LSP coupling, ***hybridized modes*** are formed, and *the LSPR redshifts*.

➢ For instance, in spherical gold nanoparticles, assembly or aggregation into a close-packed structure results in a strong red-shift of the LSPR wavelength from the LSPR maximum of ~520 nm of an isolated colloidal nanoparticle. ***The redshift is a manifestation of the favorable coupling of the plasmon oscillations of the proximal nanoparticles***, i.e., *a lower energy (or frequency) is required to drive the coupled plasmon oscillation modes of the assembly.*
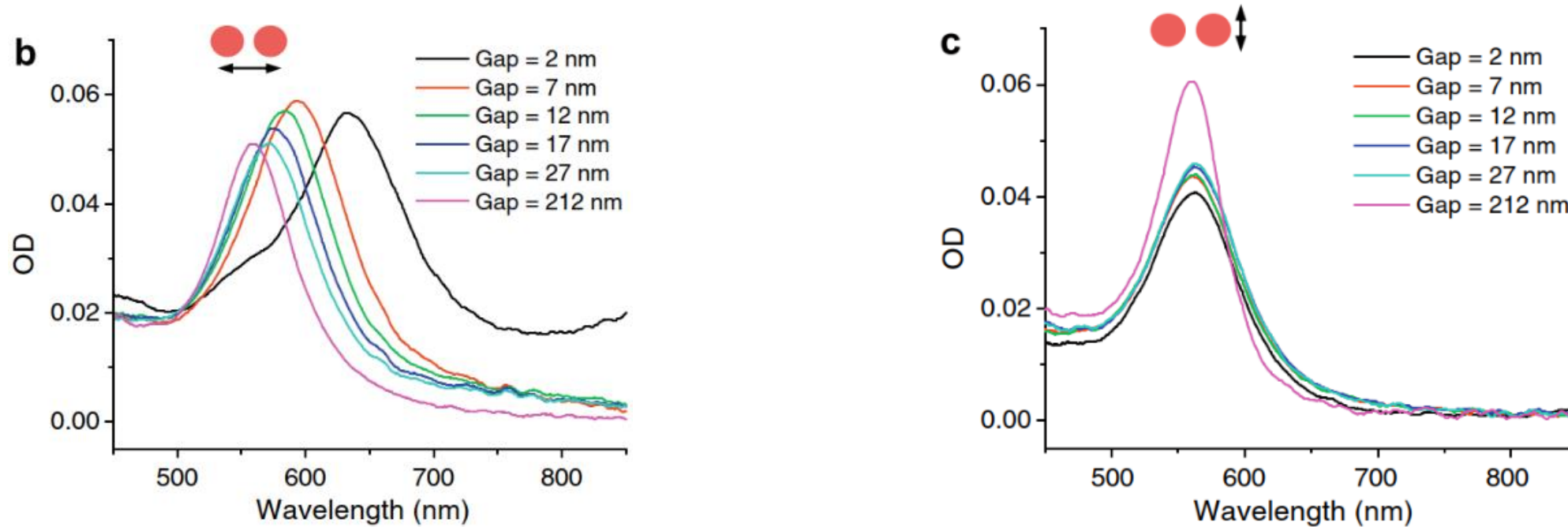

Fig. 2. Extinction spectra show that the LSPR of the nanoparticle pair (b) red-shifts with decreasing gap for polarization along the inter-particle axis and (c) blue-shifts very slightly with decreasing gap for polarization orthogonal to the inter-particle axis. Reprinted with permission. (***OD = Optical Density = Absorbance***)
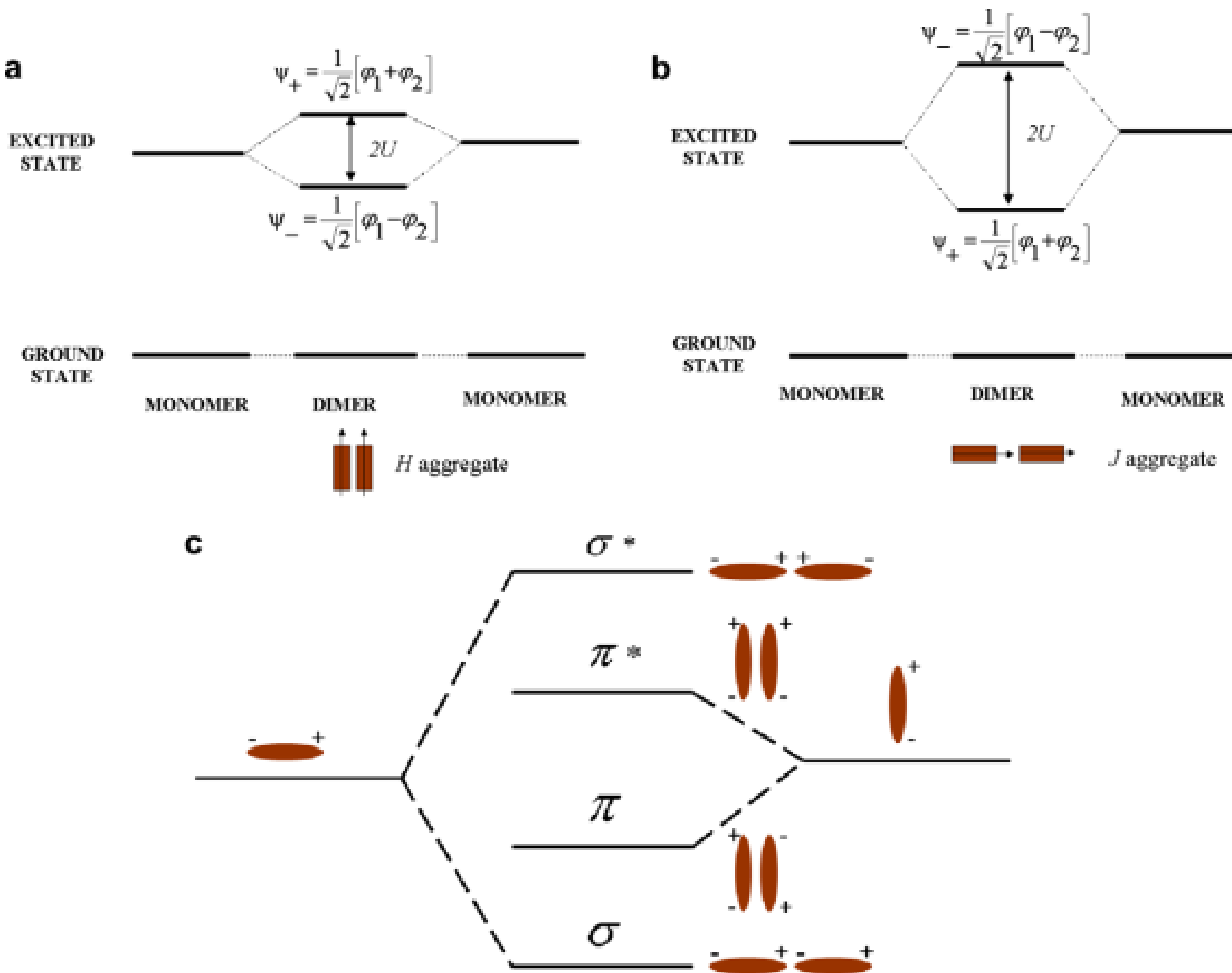
Fig. 4. The energy level splitting resulting from the dipolar coupling of chromophores in a dimer, showing symmetric (ψ+) and anti-symmetric coupling (ψ-) of excitons for (a) *H-aggregate* geometry or *side-by-side* dimer and (b) *J-aggregate* geometry or *end-to-end* dimer.

(c) Analogy of *plasmon coupling in nanorod dimers to hybridization of molecular orbitals.* The end-to-end coupling of the nanorod long-axis LSPR is similar to the formation of a bonding σ and anti-bonding σ* mode. The side-by-side coupling of the nanorod long-axis LSPR is similar to the formation of a bonding π and anti-bonding π* mode. **Note that** the **σ*-like and π-like plasmon modes are optically dark** due to their zero net dipole moment. Reprinted with permission.

Proximity Effect: Application: *Gold nanoparticle probes for the detection of nucleic acid targets*.

➢ Mirkin and coworkers (North-Western University) were the first to **employ this assembly-induced shift** for the **sensing of trace amounts** **of sequence-specific DNA strands**.

➢ The gold nanospheres were functionalized in a programmed scheme such that the presence of a DNA strand with the right DNA sequence would trigger via DNA hybridization the assembly of the gold nanoparticles.

➢ The resulting shift of the plasmon resonance absorption spectrum of the colloidal solution becomes useful for the highly sensitive optical detection of the target sequence.

➢ DNA-AuNPs can be assembled into different structures by designing linker DNA with a *complementary sequence*.

➢ For example, AuNPs modified with either DNA *A* or DNA *B* can be assembled in solution by the addition of a third DNA sequence A'B' which is complementary to *A* and *B*, respectively.

➢ ***The assembly process is marked by a dramatic*** red***-to-***blue *** color change and a dampening and red shifting of the surface plasmon*** (Fig. 12.1).

➢ Like DNA duplex formation, the ***DNA-AuNP assembly process is reversible***.

➢ By denaturing the interconnecting DNA duplexes within the AuNP assembly, the DNA-AuNPs ***can be redispersed, and a return of the red color is observed***.

➢ This "melting" process can be induced by an ***increase in the temperature*** or a ***decrease in salt concentration***.

➢ Note that *the aggregation of (noble) metal nanoparticles (disregarding whether they are ligand-stabilized or not), leads to pronounced changes of their absorption spectra due to plasmonic interaction*. This shift is ideal for the design of optical biosensors.

❖ **Effect of the surrounding media on LSPR**

❖ *Resonance Condition for Spherical Nanoparticles*

➤ Extinction would be maximum when $\varepsilon'_{metal} + 2\varepsilon_{diel} = 0$, which gives rise to a **surface plasmon resonance (SPR) band (maximum extinction cross-section for a given wavelength, when** ε''_{metal} **is small).**

➤ Note the wavelength dependence of the metal dielectric function. Since the dielectric constant of a metal depends on the wavelength of light (ω), the extinction coefficient is a function of the wavelength of light and has a peak.

➤ The resonance peak (LSPR) occurs where a maximum absorption occurs at resonance frequency at which C_{ext} is maximum. This occurs when at $\varepsilon'_{metal} = -2\varepsilon_{diel}$ in the denominator of Eq. 11.5.6.

➤ For a few metal nanoparticles like gold, silver, etc., this condition gives a resonance condition in air, water, etc. in the visible wavelength.

➤ *This dependence of the wavelength of the LSPR peak on the dielectric constants of the surrounding media can used to sense the changes occurring in vicinity of the particles.*

- ➢ *Note: the medium dielectric constant, $\varepsilon_m = n_m^2$ where n_m is the medium refractive index*.
- ➢ Figure 5.7 *illustrates the dependence of the wavelength of the LSPR peak on the dielectric constants* (hence on the *refractive index*) *of the surrounding media for two different metals*.

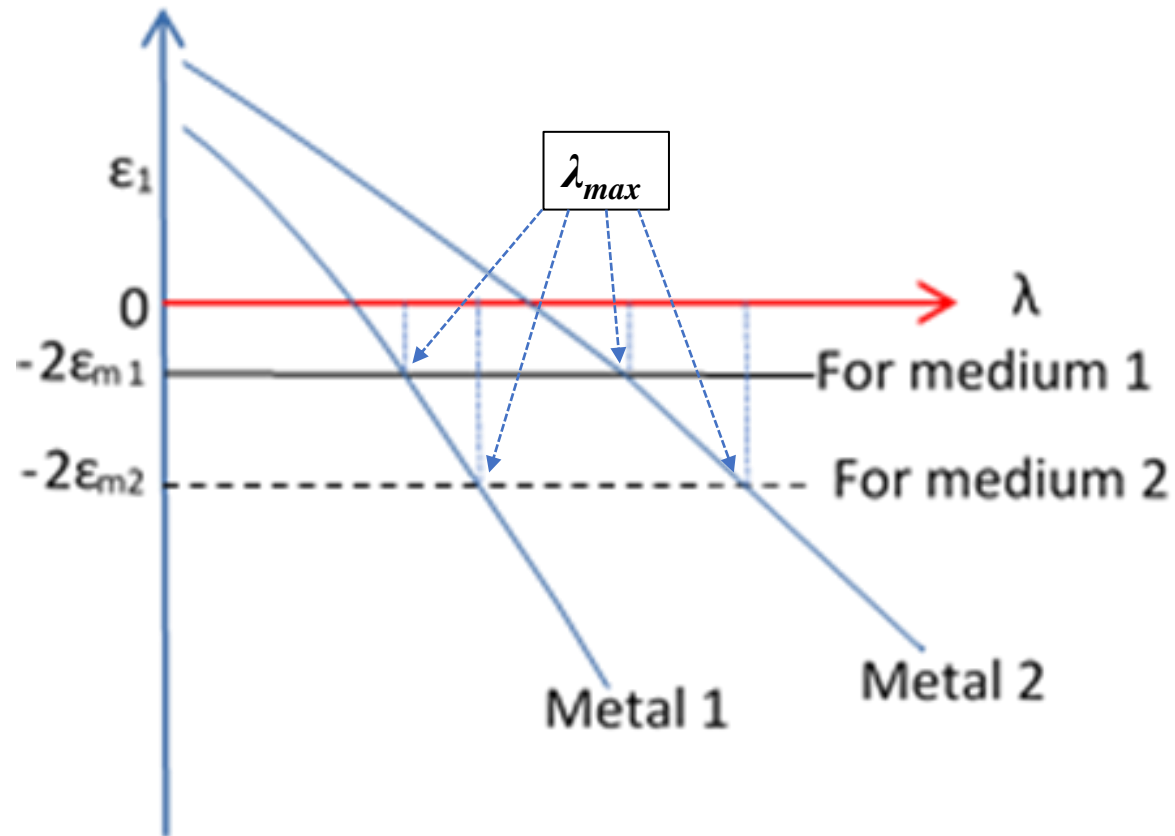**Figure 5.7** A schematic diagram showing the variations in the real in part (ε_1) of the dielectric constants of two different metals with wavelength (λ). Note the resonance conditions (λ_{max}, ***shown by vertical dotted lines***) for the corresponding metal nanospheres in two arbitrary surrounding media with dielectric constants ε_{m1} and ε_{m2}.

➢ C_{ext} depends on ε_m, the ***dielectric constant of the surrounding environment (note: $\varepsilon_m = n_m{}^2$ where n_m is the medium refractive index*)**.

➢ Since, the refractive index of the surrounding media depends on the **nature of the solvents** *and the presence of various ligands or adsorbed (bio)macromolecules on their surfaces*, the LSPR peak positions are functions of these factors.

➢ The ***peak wavelength shift*** thus ***can be used as a transducer of sensors***, such as ***refractive index, chemical and biological molecules***.

➢ Like the *aggregation of (noble) metal nanoparticles (disregarding whether they are ligand-stabilized or not), which leads to more pronounced changes of their absorption spectra due to plasmonic interaction,* **this shift** is also ideal for the **design of optical biosensors**.

❑ *Surrounding environment dependence of LSPR*

➢ Generally, NPs are dispersed in a medium, and *interactions* with such a medium can be *classified into two main categories*:

▪ (i) media that *alter the refractive index* *around metal NPs* and

▪ (ii) media formed of *molecules that complex* the metal surface.

➢ Media *not* *possessing any* *active functional groups* *do not directly interact with metal surface*; therefore, *any modification of plasmon band can be safely ascribed only to change in the* *refractive index* of the surrounding medium. *In these systems, the surface plasmon band of metal NPs gradually* **shifts toward longer wavelengths** *with increasing refractive index* of the solvent.

➢ Conversely, *media chemically interacting with the surface of metal NPs* could alter the position of the plasmon band *due to a different distribution of free electrons*. *In these systems,* **there can blue-shift or red-shift of the plasmon wavelength.**

➢ We have seen above that the *extinction coefficient* is a function of the *dielectric constant (or refractive index)* of the surrounding media, the extinction being maximum when $\varepsilon' = -2\varepsilon_{diel}$ where ε' is the real part of the dielectric constant of the metal and ε_{diel} is the dielectric constant of the surrounding medium *(again $\varepsilon_{diel} = (n_{diel})^2$ where n_{diel} is the refractive index of the (nonabsorbing) medium).*

➢ A change of the refractive index of the surrounding medium therefore leads to a change in the position of the SPR peak. The *dependence of the wavelength of the LSPR peak on the refractive index of the surrounding* environment is given by the expression,

$$\lambda_{max}^2 = \lambda_p^2(\varepsilon_\infty + 2\varepsilon_{diel})$$

or $\quad \lambda_{max}^2 = \lambda_p^2(\varepsilon_\infty + 2n_{diel}^2) \quad\quad\quad$ (11)

where $\lambda_p = 2\pi c/\omega_p \quad\quad\quad$ (12)

where λ_{max} is plasmon wavelength, λ_p is the bulk plasmon wavelength, ω_p is the bulk plasmon angular frequency, c is the speed of light in free space.

➢ Equation 11 suggests **a redshift** in the **LSPR band with** *the increase in the n_{diel}, refractive index,* **of the environment (where** $n^2{}_{diel} = \varepsilon_{diel}$).

➢ For bulk metals, the plasmon frequency (ω_p) can be shown to be:

$$\omega_p = \sqrt{\frac{ne^2}{m_e \varepsilon_0}} \qquad\qquad (13)$$

➢ The volume plasma frequency is a property of the metal.

➢ Here **n is the number density of electronic charge**, e is the electronic charge and m_e is the effective mass of the electron.

Combining equations 11, 12 and 13, one obtains

$$\lambda_{max}^2 = \frac{4\pi^2 c^2 m_e \varepsilon_0}{ne^2}(\varepsilon_\infty + 2n_{diel}^2)$$

which shows that **if electron density (n) on the nanoparticle increases, then there will be blue-shift of the plasmon wavelength and *vice versa*.**

*(note: Volume plasmon energy for **bulk** gold is 9.0 eV and for silver it is 8.9 eV, and it lies in the UV range. However, for nanoparticles the **surface** plasmon energy is small and lies in the UV-Vis-NIR range.)*
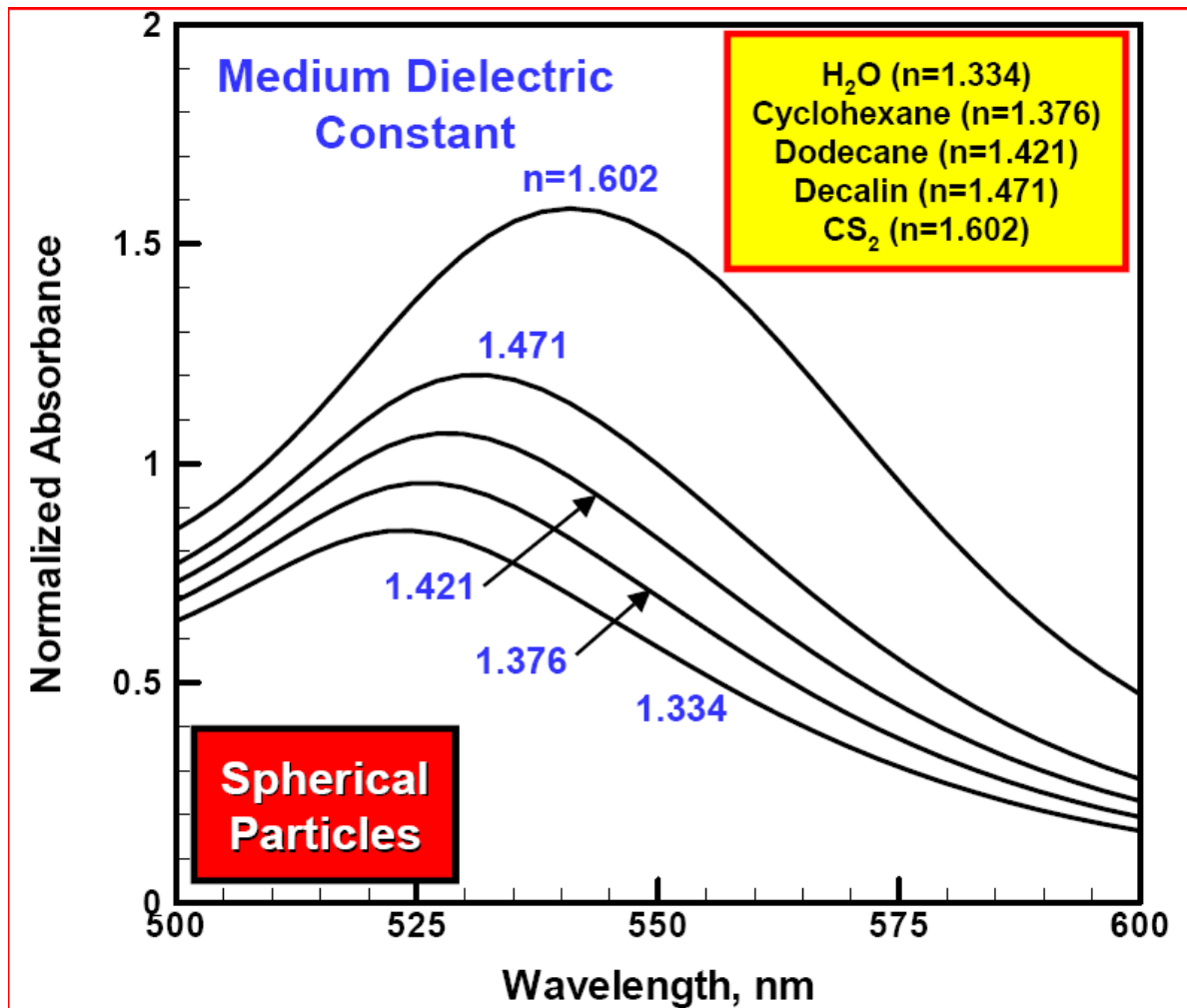
Calculated absorption spectra of gold nanoparticles in different solvents.

Figure 5.8 illustrates the media refractive index effect on LSPR of gold nanorods.

(*Collect the refractive indices of all these solvents and interpret the observations. Plot the longitudinal plasmon band position with refractive index of the solvent and carry out linear regression of the data. What is the longitudinal plasmon band position for zero refractive index?*)
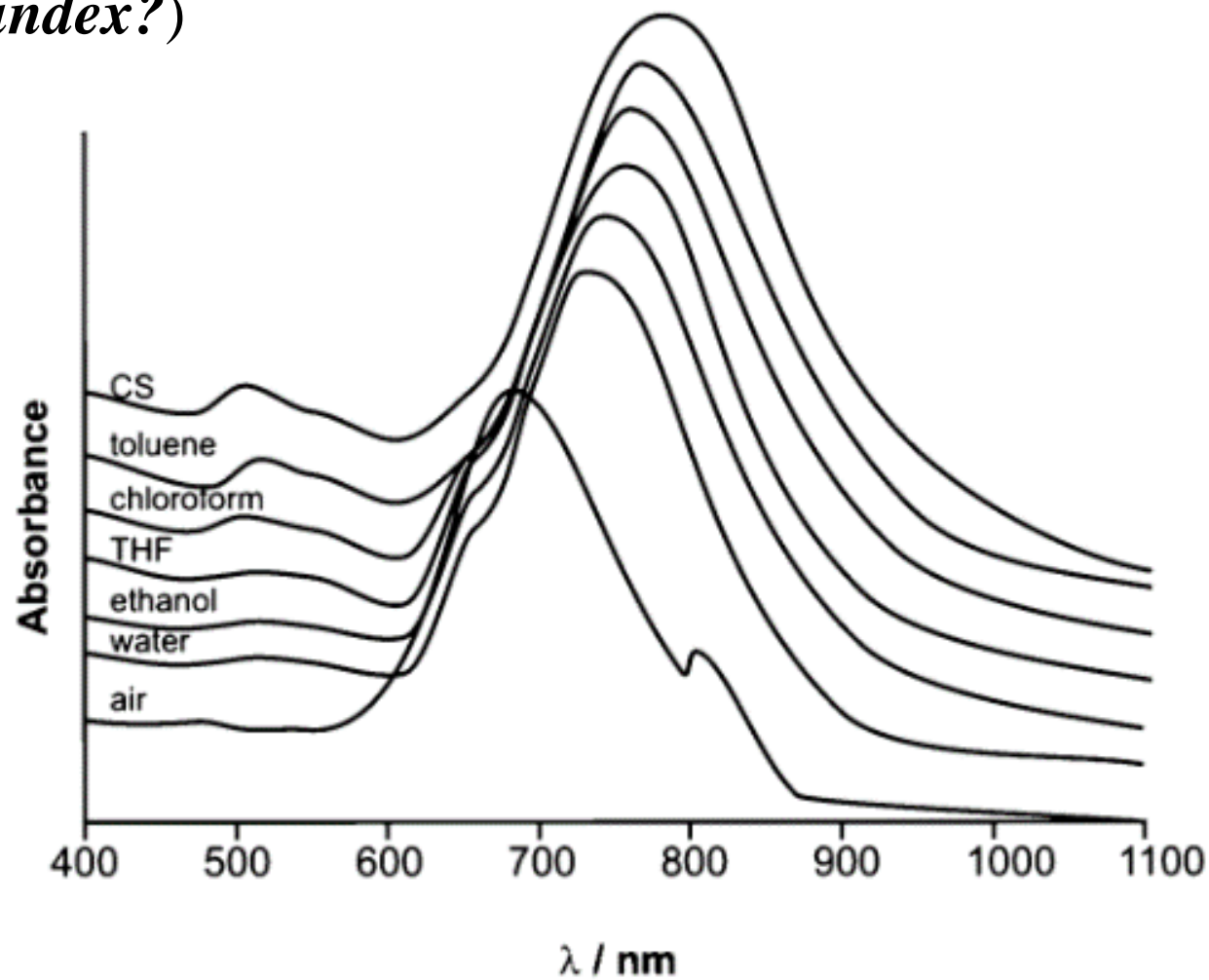

Fig. 5.8. Experimental spectra of gold nanorods in different solvents. (Reprinted with permission from Elsevier. Copyright (2005)).

❑ The **color of the semiconductor particles** is **NOT influenced** by the **surface plasmon resonance.**

➤ In the case of *semiconductor crystallites*, the *free electron concentration (density, N) is orders of magnitude smaller than in metals*, even in degenerately doped materials (i.e., $\omega_p = \sqrt{\frac{ne^2}{m\varepsilon_0}}$ *is smaller*), and as a result *surface plasmon absorption occurs in the infrared (IR) rather than in the visible part* of the spectrum. **The color of the semiconductor particles is therefore not influenced by the surface plasmon resonance.**

➤ *Semiconductor crystallites therefore do not change color significantly when the particle size is decreased below the wavelength of visible light*, although the IR spectrum may be affected.

➤ However, *when the size of the semiconductor particles decreases further, the quantum effects appear leading to a change in the electronic band structure of the crystal*, which *causes the dielectric function of the material itself to change.*

➤ The *strong color changes observed when semiconductor crystallites* are in the *quantum size* regime *due to the absorption in the visible region leading to electronic transition across the band gap*, which *emits photons* while returning to the ground state.

❖ The foundation for many biosensing applications

➢ One of the ***key complementary properties of noble metal nanoparticles that is important to their use in biomedicine*** is the ease with which they can be ***covalently conjugated*** with polymers or small molecules, typically via thiol or amine bonds at their surface.

➢ This imparts biological recognition properties to the particles that enables them to bind to specific biomolecular targets. The figure on the right illustrates some of the functionality that can be imparted to nanoparticles through surface functionalization.
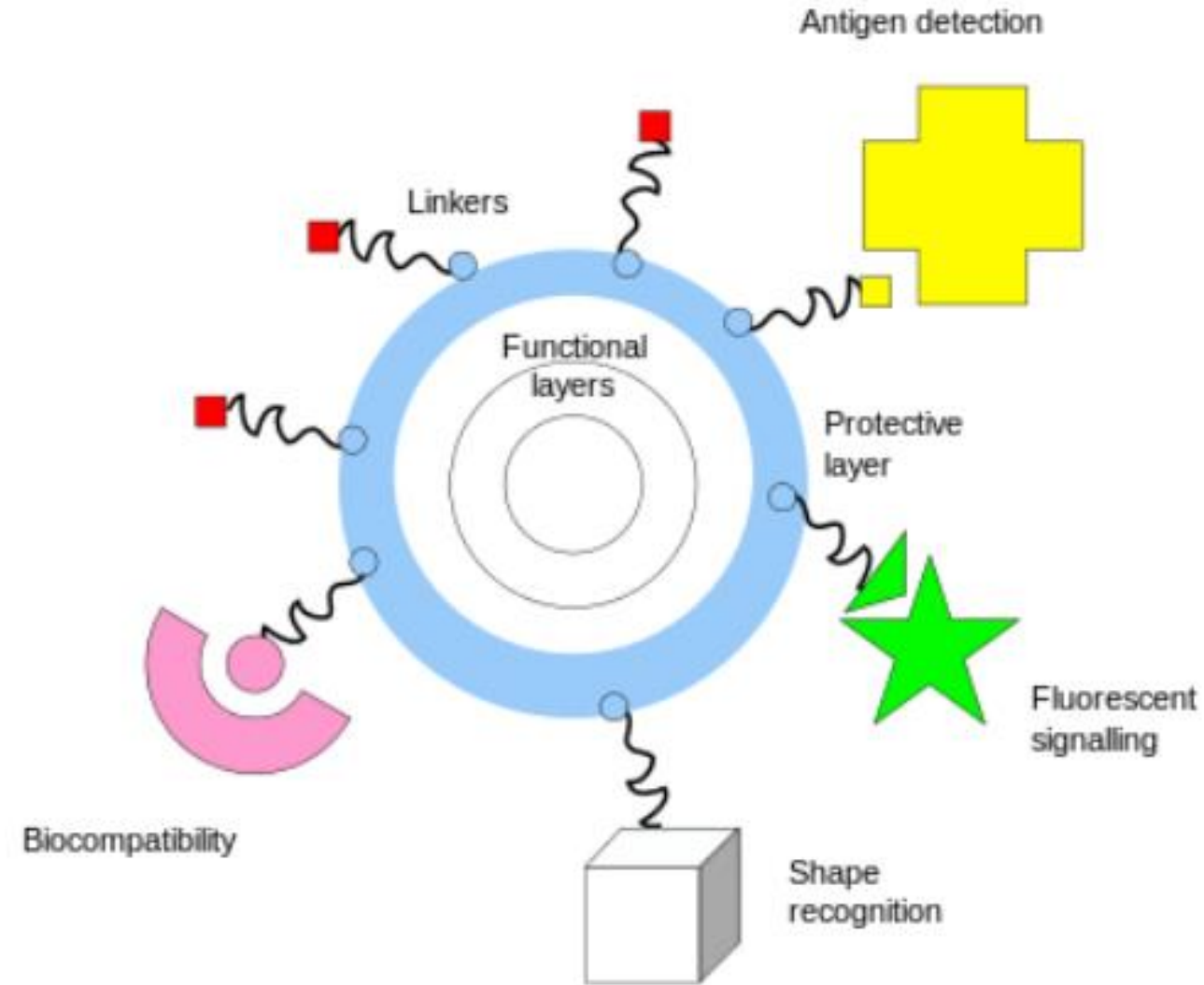
❖ **The foundation for many biosensing applications** (contd.)

➢ *Surface plasmons* should be distinguished from *bulk plasmons* (bulk plasma) which have a longitudinal nature and cannot be excited by visible light.

➢ **LSPR** differs from **SPR** as the induced plasmons oscillate locally to the nanostructure, rather than propagating on the surface.

✓ One can also have surface propagating plasmons (along the metal-dielectric interface) or *surface plasmon polaritons* in thin films as distinct from the LSPR (plasmons oscillate locally to the nanostructure) which occur at the nanoparticle's surface.

✓ It is of great mechanistic importance that surface plasmons are surface electromagnetic waves that propagate in parallel along a metal/dielectric interface.

✓ Since the ***wave is located on the boundary of the metal and the external medium (or vacuum), these oscillations are*** *very sensitive to any change in the chemical composition of this boundary*, such as the **adsorption** and **exchange of ligands** and **macromolecules** (e.g. (bio)polymers) to the metal surface.

❖ **The foundation for many biosensing applications** (contd.)

➢ The ***decay length*** of the electromagnetic field observed in *surface plasmon* ***polariton****s* is in the order of 200 nm, whereas the decay length of the electromagnetic field in ***LSPR is in the order of 10 nm*** (both decaying exponentially).

➢ **The shorter field decay length for LSPR reduces the sensitivity to interference from solution refractive index fluctuations (bulk effect)** *whilst providing increased sensitivity to refractive index changes on the surface*. *This property acts as the foundation for many biosensing applications*.

➢ **These powerful localized sources of light are useful in different areas of science and technology which include** *scanning near-field optical microscopy***,** *biosensor applications***,** **surface-enhanced Raman scattering (SERS),** *nanophotonics***, optical data storage,** etc.

➢ *Chemists and Biologists* are more interested in the following Equation (16.8) what is known as Lambert–Beer's law. *A(λ)* is the absorbance or optical density of the sample, ε_{abs} (M^{-1} cm^{-1}) is the molar absorption coefficient, c (M) is the molar concentration of the light absorbing species, and x (cm) is the optical path length.

➢ $A(\lambda) = \varepsilon_{abs(\lambda)}cx$ (16:8)

➢ Note that *the molar absorption coefficient is directly related to the absorption and scattering cross-section* by means of Equation (16.10).

➢ Conventionally, chemists measure the extinction coefficient of a solution in units of M^{-1} cm^{-1}, where the colloid concentration is the molar metal atom concentration. For particles of radius R (**cm**), this quantity is related to σ_{ext} by

➢ $\varepsilon(M^{-1}cm^{-1}) = 3 \times 10^{-3} \dfrac{V_m \sigma_{ext}}{4\pi R^3 \times 2.303}$ Equation (16.10)

where V_m (**cm**^{3} mol^{-1}) is the molar volume of the metal.

➢ **For small particles** where the absorption strongly dominates the scattering, the absorption cross section is $\sigma_{abs} = \sigma_{ext} - \sigma_{sca}, \approx \sigma_{ext}.$

➢ *Metal nanoparticles show **remarkably larger absorption cross-sections** compared to organic dyes and metal complexes.* A typical example are the nanospheres that have been used by El-Sayed et al. for the laser-induced photothermal hyperthermia treatment of cancer cells, which feature *an absorption cross-section of 2.93×10^{-15} m² ($\varepsilon = 7.66 \times 10^9$ M⁻¹ cm⁻¹) at their plasmon resonance maximum of $\lambda = 528$ nm*. This is five orders of magnitude larger than that of the commonly used NIR dye indocyanine green ($\varepsilon = 1.08 \times 10^4$ **M⁻¹ cm⁻¹** at $\lambda = 778$ nm) or the sensitizer ruthenium(II)-*tris*-bipyridine ($\varepsilon = 1.54 \times 10^4$ **M⁻¹ cm⁻¹** at $\lambda = 452$ nm) and four orders of magnitude larger than rhodamine-6G ($\varepsilon = 1.16 \times 10^5$ **M⁻¹ cm⁻¹** at $\lambda = 530$ nm) or malachite green ($\varepsilon = 1.49 \times 10^5$ **M⁻¹ cm⁻¹** at $\lambda = 617$ nm).

➢ Metal nanoparticles possess ***remarkable light-scattering properties*** as well. Gold nano-spheres of **80 nm** in diameter have approximately ***the same Mie-scattering characteristics*** as **polystyrene beads of 300 nm** *(both feature $C_{sca} = 1.23 \times 10^{14}$ m² at $\lambda = 560$ nm, corresponding to a molar scattering coefficient of 3.22×10^{10} M⁻¹ cm⁻¹).* It is noteworthy that this ***strong scattering is five orders of magnitude higher than the light emission (fluorescence) from fluorescein*** ($\varepsilon = 9.23 \times 10^4$ M⁻¹ cm⁻¹ at $\lambda = 521$ nm, emission quantum yield $\Phi = 0.98$ at $\lambda = 483$ nm).

➢ Some studies have suggested that multiple-photon absorption of gold nanostructures can be advantageous, for instance in SERS-microscopy and plasmonic heating (photo-induced hyperthermia).

➢ It should be noted that noble metal nanostructures (e.g. gold nanorods) can be easily tuned for monophotonic applications in the wavelength range from 600 to 1000 nm. Monophotonic excitation is advantageous, because its absorption cross-section is several orders of magnitude higher!

➢ Functionalization of gold nanoparticles with ***thiol-terminated single-stranded DNA*** was the basis of one of the first nanoparticle sensors, developed by the Mirkin group at Northwestern University. ***DNA-coated nanoparticles*** have the characterstic wine-red plasmonic color of spherical nano-gold. However, when these particles are linked together by ***a complementary DNA strand***, the resonance frequency shifs, resulting in a blue color. This color change, illustrated in the figure at the right, provides a "litmus test" for the ***presence of the target DNA sequence***.
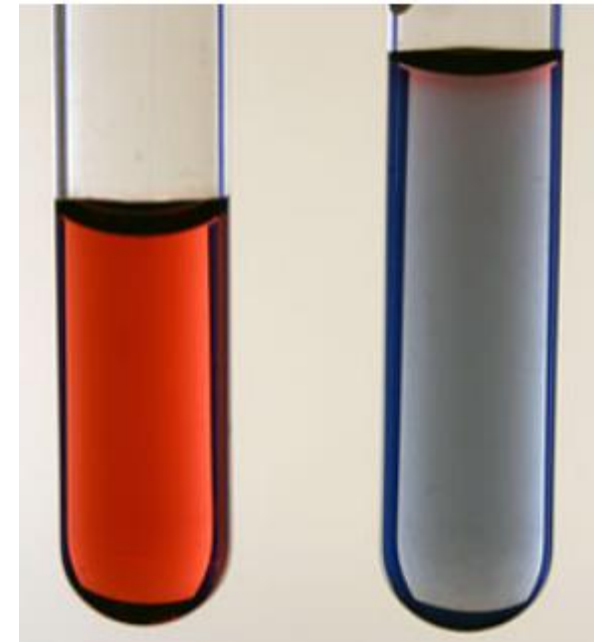
Aggregation of Au nanoparticles (in this case by adding salt to a colloidal solution) causes a color change from wine red (left) to blue (right). Photo credit: George Lisensky, Beloit College.

➢ **"*Melting*" *of the DNA*** - heating it to the temperature at which double stranded DNA dissociates to make single strands - reverses the color change. The DNA hybridization/melting transition is highly cooperative because of the aggregation of many gold particles, so the transition temperature is very sharp. With proper temperature control, the color change can be **sensitive to a single base mismatch in the target DNA** that is detected by this method.

- The ***melting process can be monitored by measuring the intensity of the surface plasmon*** as a function of temperature.

- The melting transition exhibited by DNA-AuNP assemblies is remarkably different from unmodified DNA duplex melting transitions in two distinct ways: (1) ***the melting transition of the AuNP assembly is significantly sharper***, where *the first derivative displays a full width at half maximum (FWHM) of about 2°C to 4°C compared* to an FWHM of about 12°C for DNA duplex, and (2) the melting temperature (T_m) is significantly higher than the T_m of an analogous DNA duplex under identical conditions.

- Both of these properties are a function of the DNA-AuNP conjugate and are important for the types of applications that will be described later.

- Despite these two notable differences in the melting properties, DNA-AuNPs exhibit other behaviors similar to duplex DNA. For example, *increasing the DNA length*, *DNA concentration*, or *salt concentration in the system increases* the stability of the DNA-AuNP assemblies and the T_m.

➢ *A mixture of gold nanoparticles with surface-immobilized non-complementary DNA sequences (a, b) appears red in color (absorbance at 520 nm). When a complementary DNA sequence (a'b') is added to the solution, the particles are reversibly aggregated causing a red shift in the surface plasmon absorbance to 574 nm, thus, appearing purple in color.*

➢ A representative example is shown in the lower left (Fig. 12.1) where monodisperse particles (red) are aggregated using a complementary DNA linking sequence (purple).

➢ Heating the aggregates above the melting temperature of the DNA strands mediating aggregation results in a return to the red color.

➢ This melting transition is strikingly sharp as demonstrated in the lower right where gold nanoparticle-linked DNA is compared to unmodified DNA.

➢ At any given temperature, a small aliquot of the reaction mixture can be spotted on the surface of a reverse-phase TLC plate to monitor the degree of hybridization as determined by the temperature, as shown in the bottom right.
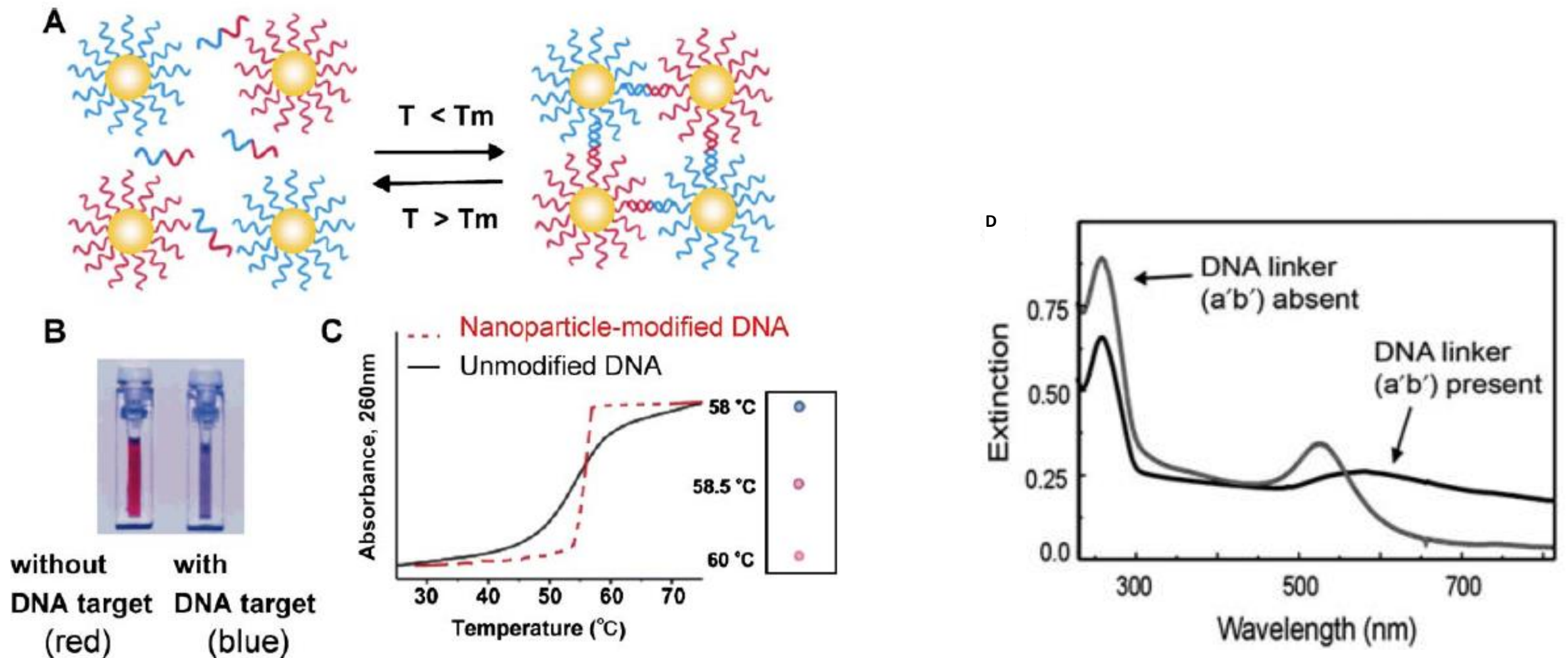
Fig. 12.1 (A) DNA-AuNPs assembled using a complementary DNA linker. (B) 13 nm DNA-AuNPs appear red in color without linker DNA and turn blue when linker DNA induces nanoparticle assembly. (C) Melting transition of unmodified duplex DNA (black) and DNA linked DNA-AuNPs (red). (D) Extinction spectrum of dispersed and assembled DNA-AuNPs.

(Reproduced with permission from C. A. Mirkin et al., Nature 1996, 382, 607–609.) (Adapted from N. L. Rosi and C. A. Mirkin, Chem. Rev. 2005, 105, 1547–1562.) *C.S. Thaxton et al., Clinica Chimica Acta 363 (2006) 120– 126.*

❑ ***Molecular plasmonic ruler***. (Alivisatos' group (UC Berkeley) demonstrated the use of plasmonic ruler.)

❖ Color effect on directed assembly of DNA-functionalized gold and silver nanoparticles.

➢ (a) First, nanoparticles functionalized with streptavidin are attached to the glass surface coated with BSA-biotin (left).

➢ Then, a second particle is attached to the first particle (center), again via biotin-streptavidin binding (right). The biotin on the second particle is covalently linked to the 3' end of a 3-3 base pair long ssDNA strand bound to the particle via a thiol group at the 5' end. Inset: principle of transmission darkfield microscopy.

➢ (b) Single silver particles appear blue (left) and particle pairs blue-green (right). The orange dot in the bottom comes from an aggregate of more than two particles.

➢ (c) Single gold particles appear green (left), gold particle pairs, orange (right). Inset: representative transmission electron microscopy image of a particle pair to show that each colored dot comes from light scatted from two closely lying particles, which cannot be separated optically.

➢ (d) Representative scattering spectra of single particles and particle pairs for silver (top) and gold (bottom).

➢ Silver particles show a larger spectral shift (102 nm) than gold particles (23 nm), stronger light scattering, and a smaller plasmon line width.

➢ Gold, however, is chemically more stable and is more easily conjugated to biomolecules via –SH, $–NH_2$ or –CN functional groups.

➢ When **DNA *hybridization* takes place** *the inter-particle* **bond becomes *rigid/stronger*** and the ***inter-particle distance increases*** compared to the flexible single DNA strand connecting the two particles.

➢ As *the interparticle distance increases* **only a few nm**, there is *a clear blue shift* of the SPR band.

➢ *By measuring this SPR band shift, one could measure small (a few nm) changes in the distance during an interaction process or between two species.*
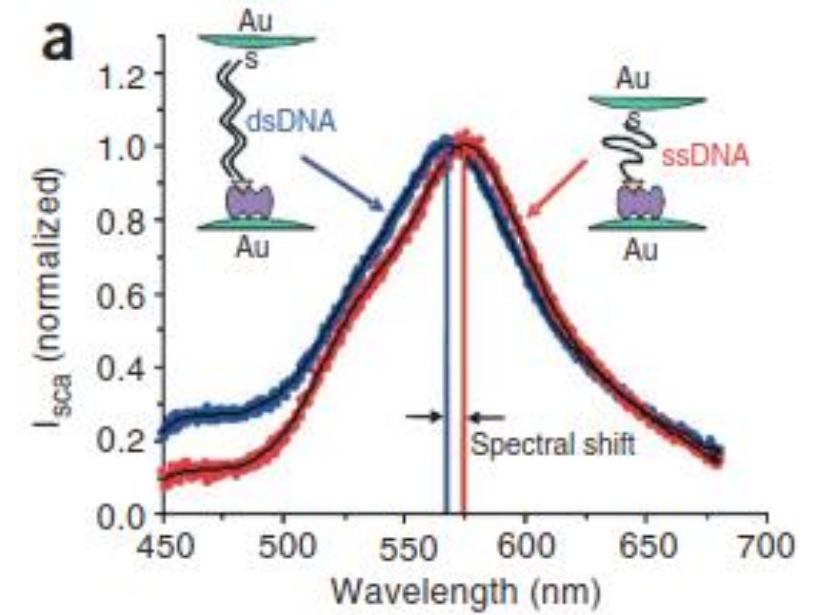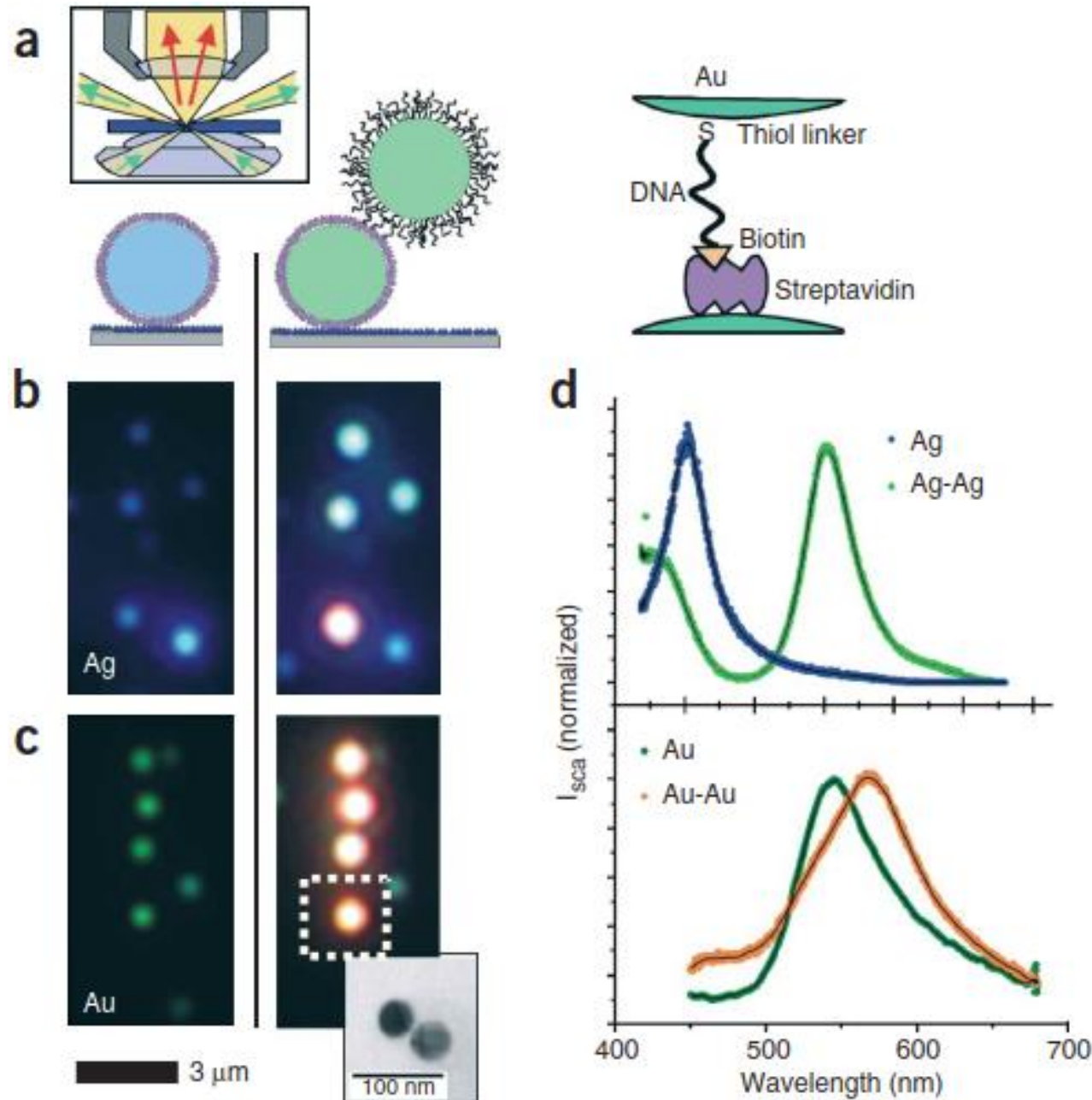
Figure 3. Spectral shift upon DNA hybridization.

(a) Example of a spectral shift between a gold particle pair connected with ssDNA (red) and dsDNA (blue). The shift is clearly visible.

➢ Subsequent research has developed sophisticated diagnostic and therapeutic ("theranostic") applications for these spherical nucleic acid particles. These particles easily penetrate cell membranes and can report on the chemistry happening inside living cells.

➢ An important property of gold nanoparticles in these applications is their ability to quench the fluorescence of reporter molecules that are near their surface. Nucleic acid strands that contain a hairpin loop can position fluorescent molecules near the gold surface, where their ***fluorescence is turned off*** by ***nanoparticle quenching***.

➢ Hybridization of these sequences to target RNA or DNA causes the ***fluorescence to turn on by moving the fluorescent molecule away from the nanoparticle surface***. These so called "nanoflares" can thus signal the up- or down-regulation of specific genes inside cells.

➢ Nanoflares are the basis of the Verigene System, developed and commercialized by Nanosphere, Inc. to detect markers for infectious diseases and cancers.
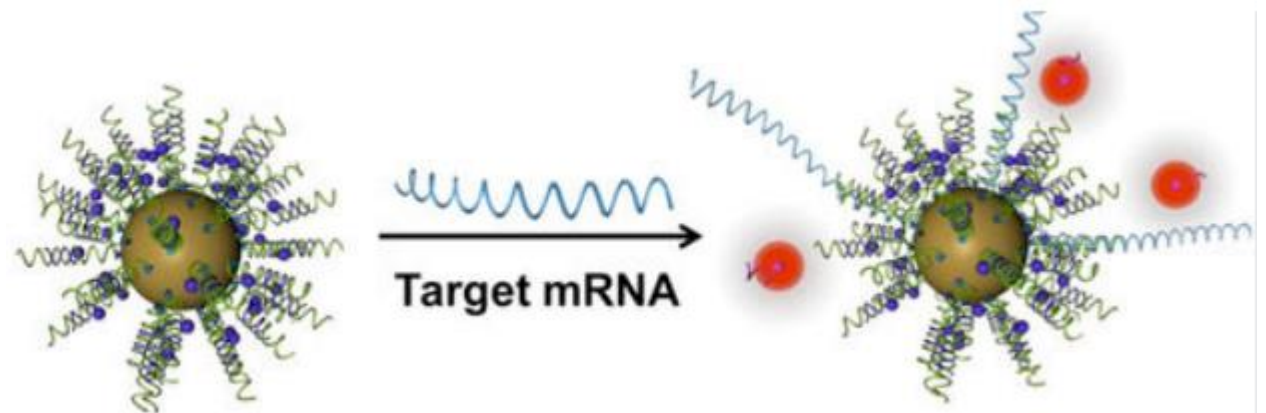
General schematic of nanoflare-based detection.

Target mRNA

❑ Enhanced Local Field and Surface-enhanced Spectroscopies

➤ In the dipole approximation, the Mie theory also predicts that the incident radiation induces a constant electric dipole moment inside the sphere, proportional to the amplitude of the light electromagnetic field (E_0). As a consequence, the local electric field on the sphere surface (i.e., located within a few nanometers from the sphere) becomes equal to:

$$E_{loc} = \frac{3\varepsilon}{\varepsilon + 2\varepsilon_m} E_0$$

where ε is the complex dielectric constant of the metal and ε_m is the dielectric constant of the surrounding medium ($\varepsilon_m = n_m^2$ where n_m is the refractive index of the (nonabsorbing) medium).

➤ *Under the resonance condition*, when $\varepsilon = -2\varepsilon_m$, where ε is the real part of the dielectric constant of the metal, E_{loc} *is strongly enhanced* with respect to the far field.

➤ This huge increase in the local field around metal nanoparticles (or metal nanostructures, in a more general point of view) is the basis of the surface-enhanced sensing applications, such as surface-enhanced Raman scattering (SERS) and surface-enhanced fluorescence (SEF) spectroscopy, which will be described later.

Local Field Effect on Raman Scattering and fluorescence

➢ In the surface-enhanced Raman spectroscopy, the *scattering of incoming light by an analyte molecule is significantly increased by the plasmon resonance*.

➢ SEF involves the *increase of fluorescence emission of suitable chromophores in the presence of a plasmonic structure*. This is also called *metal-enhanced fluorescence (MEF)*, and devices based on such phenomenon are called MEF sensors.
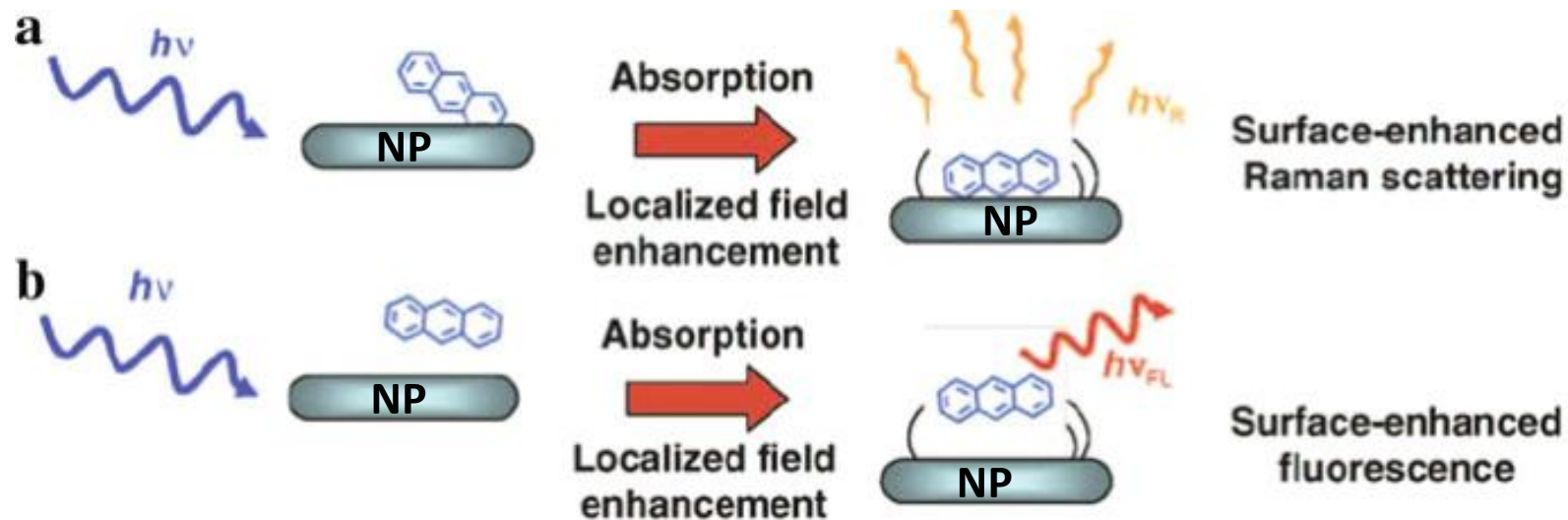

Fig. 7.27 Schematic showing surface-enhanced Raman scattering hv_R and surface-enhanced fluorescence hv_{FL}. Photons are indicated by hv. (Reprinted with permission. © 2005 Elsevier)

❑ Surface-Enhanced Raman Scattering (SERS)

❑ WHY SERS?

➢ In infrared spectroscopy, it can be shown that the intensity of a mode is proportional to the square of the scalar product of the **electric field (E)** vector of the incident wave with the derivative of the **dipole moment (μ)** vector:

$$I \propto \left(\frac{\partial \mu}{\partial q} \cdot E \right)^2 = \left(\frac{\partial \mu}{\partial q} \right)^2 E^2 \left(\cos \theta \right)^2 , \qquad (9.51)$$

where θ is the angle between the exciting electric field and the direction of the vector $\partial \mu / \partial q$.

➢ *A mode will be **more intense** as the term $\partial \mu / \partial q$ increases*, but **also as the electric field becomes more closely aligned with the direction of the derivative of the dipole moment**.

➢ Owing to the sensitivity of vibrational spectroscopy to the force constants between atoms, these *methods are often used to characterize molecules*, but also to *observe the changes they undergo when they interact with their surroundings*.

➢ Moreover, in ordered systems, these methods can be used to *determine the orientations* of molecular groups.

❑ **WHY SERS?** (contd.)

➢ Because *Raman scattering refers directly to typical vibrational frequencies of the molecule*, each **Raman spectrum determines in a univocal way a specific molecule**.

➢ For this reason, the *employment of Raman spectroscopy is very interesting in sensing*.

➢ Unfortunately, the *Raman scattering intensity is very low with respect to the incident light*.

➢ *Raman scattering intensity depends on* the incident **laser intensity** and the **number of the probed molecule (N)**, on the **analyte Raman cross section (σ_R)**:

$$I_R(v_s) \propto N I(v_0)\sigma_R \qquad (7.12)$$

where v_s is the Stokes (or anti-Stokes) line frequency.

➢ Raman scattering is a two-photon process occurring at a time scale of ca. 10^{-12} s; and σ_R is usually very low, ranging between 10^{-25} and 10^{-30} cm^{-2}.

➢ The σ_R (Raman cross-section) of a molecule for such a process is about 10^8 and 10^{10} times smaller than those of **infrared (IR)** and **fluorescence** *processes*, respectively.

➢ When compared to a *fluorescence cross-section*, whose typical value is between 10^{-17} and 10^{-16} cm^2, Raman scattering is rather weak.

❏ WHY SERS? (contd.)

➢ This optical quality is not enough for lower detection limits in analytical applications.

➢ Since Raman scattering is inherently weak, therefore, *a large number of molecules* in Raman experiments are necessary to achieve the *same signal level in fluorescence.*

➢ As *Raman technique presents low sensitivity*, the *measurement of Raman scattering requires a huge quantity of analyte*, *a powerful light source* and *very sensitive detectors*.

➢ Although the *classical theory of Raman* scattering explains the *origin of the Stokes and anti-Stokes line*, they do *not account for their differences in intensities*.

➢ The quantum mechanical theory will provide this information and forms the basis for a complete treatment of all aspects of Raman scattering.

➢ In electrodynamics, the quantum theory of radiation can be perfectly used to explain any kind of effects and phenomena related to the interaction of radiation field with matter in both qualitative and quantitative ways.

❑ **WHY SERS?** (contd.)

➢ The most important feature of quantum theory of radiation is that a concept of virtual energy can be introduced, which represents *an intermediate quantum state occupied by the combined system of the photon field and the medium.*

➢ ***According to quantum mechanics***, *a vibration is Raman active* *if the polarizability is changed during the vibration*.

➢ The *Raman scattering intensity* is proportional to ***the number of molecules illuminated***, the ***intensity of incident light*** and to ***$(v_0 - v)^4$.***

➢ *The Raman intensity can therefore be increased by increasing the incident light intensity or by using incident light of higher frequency, ω_0 (shorter wavelength).*

➢ It is indeed the development of more sensitive and cost-effective Raman instruments that was delayed until the advancements in laser and detector technology.

➢ This detection sensitivity was significantly improved in the early 1960s, when the laser was invented and then used as an ultra-intense light source for Raman spectroscopy.

➢ With the recent advances in laser and detector technology and optics, the cost and size of Raman spectrometers have significantly reduced without the sacrifice of sensitivity.

❑ *Surface-enhanced Raman scattering (SERS)*

➢ The *major breakthrough with using Raman scattering* as a characterization and detection technique came with the discovery of **the enhancement in scattering on roughened noble metal surfaces**.

➢ A discovery was made that the *Raman cross-section of a material may be increased by a factor of 10^7 or more* by the presence of *metal colloid* or *roughened metal surface*. This effect is called *surface-enhanced Raman scattering (SERS)*.

➢ In 1974, Fleischman observed the enhancement in Raman scattering of pyridine molecules on silver electrode surfaces. However, this enhancement was first explained with the increased pyridine concentration on a roughed electrode surface that resulted with an increased surface area. In 1977, Jeanmarie and Van Duyne and Albrecht and Creighton proposed two separate mechanisms, electromagnetic (EM) and charge transfer, respectively, to explain the increased Raman scattering. In 1978, Moskovits proposed a relationship between enhancement in Raman scattering and surface plasmons.

➢ In the following years, it was demonstrated that enhancement in Raman scattering did not occur only on the surface of silver, gold, and copper but also on other conductors, such as aluminum, indium, platinum, and transition metals.

➢ It is **now commonly accepted** that the **enhancement mechanism has two components** — *electromagnetic* (EM), which is related to the surface plasmons, and *chemical*, which is related to the charge transfer between the metal surface and adsorbed molecule.

➢ The contribution of the *EM enhancement is much larger than the charge transfer that depends on the chemical structure of the molecule adsorbed onto the nanostructured noble metal surface.*

Surface Plasmon-enhanced Raman Scattering: *Enhancement Mechanisms*

➢ *The intensity of normal Raman scattering from free molecules is determined by the first-order transition electric dipole, which depends on the* **transition polarizability** *of the molecule and* **the electric field strength** *of the exciting radiation.*

➢ The origin of surface enhanced Raman scattering (SERS) must therefore be sought in enhancement either of the transition polarizability or of the electric field strength experienced by the molecules when adsorbed on certain types of surface.

➢ Classical electromagnetic theory indicates that the *molecule at the metal surfaces will experience a local electromagnetic field that is larger than that of the incident radiation.*

➢ The extent of **the enhancement depends** on a number of factors, including the **dielectric properties of the metal**, **the distance of the molecule from the surface**, the **orientation of the molecule**, the **wavelength of the exciting radiation**, the **morphology of the surface** and **the size and geometry of the nanostructure**.

➢ The **polarizability can also be changed as a result of electronic interaction between the molecule and the metal**.

➢ In some cases, **charge transfer may be observed**, leading to resonances different from that of the target molecule.

➢ The **optical response of a chemisorbed molecule may differ from that of a free molecule**, which may result in wavenumber shifts of those modes involving atoms bound to the metal surface. **The maximum enhancement will be expected with SERRS, when the wavenumber of exciting radiation approaches both an electronic transition of the molecule and the plasmon absorption wavenumber of the metal for LSPR to be excited**.

➢ Surface-enhanced Raman scattering (SERS) is based on the localized surface plasmon resonance phenomenon, which can greatly increase the Raman scattering cross-section of molecules located in the vicinity of a metallic nanostructure. This enormous signal amplification can be explained by an electromagnetic (EM) mechanism of SERS that is the defining feature of the effect and can provide enhancement of several orders of magnitude.

In the dipole approximation, the Mie theory also predicts that the incident radiation induces a constant electric dipole moment inside the sphere, proportional to the amplitude of the light electromagnetic field (E_0). As a consequence, the local electric field on the sphere surface (i.e., located within a few nanometers from the sphere) becomes equal to:

$$E_{loc} = \frac{3\varepsilon}{\varepsilon + 2\varepsilon_m} E_0$$

Under the resonance condition, E_{loc} is strongly enhanced with respect to the far field. This huge increase in the local field around metal nanoparticles (or metal nanostructures, in a more general point of view) **is the basis for the sensing applications, which will be described in later Sections**.

The SERS phenomenon is a direct correspondence with the localized surface plasmon resonance (LSPR) producing an intense local electromagnetic (EM) field on the SERS-active nanostructures. SERS is primarily a phenomenon associated with the enhancement of the electromagnetic field surrounding a small metal objects optically excited near an intense and sharp dipole resonance. The enhanced re-radiated dipolar fields excite the adsorbate, and if the resulting molecular radiation remains at or near resonance with the enhancing object, the scattered radiation will again be enhanced. So, under appropriate circumstances, accumulated two-fold of electromagnetic enhancement will scale as E^4.

The total SERS enhancement, E_{SERS} is then given by:

$$E_{SERS} = N \cdot \sigma^R_{ads} \mid A(v_L) \mid^2 \cdot \mid A(v_S) \mid^2 \cdot I(v_L)$$

where, σ^R_{ads} is the Raman cross-section of the molecule in contact with the nanostructure, and N is the number of molecules involved in the SERS process, $A(v_L)$ and $A(v_S)$ represent the *enhancement factors* for an excited source of intensity $I(v_L)$ and Raman scattered fields, respectively.

We can therefore identify two separate origins for the modification of the Raman signal: a change in Raman polarizability α, which we will refer to as a "**chemical Enhancement**", and/or a change in local field $\boldsymbol{E}_{loc}$, which corresponds to the '**electromagnetic (EM) enhancement**'.

In the case of surface-enhanced resonance Raman scattering, where both of these resonance (plasmon and molecular) conditions are fulfilled, the two enhancement mechanisms are multiplicative and can lead to large enhancement factors that often make a easier way to detect a single molecule.

Such enhanced field can be exploited for any field dependent property study…… Particularly in the field of Raman spectroscopy this can result in enormous sensitivity enhancements. The enhancement factor (EF) (i.e., by how much the Raman signal can be amplified) can be large enough to allow, in many cases, the observation of single molecules — an interesting subfield of SERS in its own right.

The enhancement factor (*EF*) may be defined determined experimentally by the following relationship:

$$EF = \frac{I_{SERS}/C_{SERS}}{I_{RS}/C_{RS}}$$

where, I_{SERS}/C_{SERS} is the Raman scattering intensity per unit concentration due to SERS results and I_{RS}/C_{RS} is the normal Raman scattering intensity per unit concentration.

Because LSPR critically depends not only on the nature of the metal but also on architectures of metal nanostructures; and the preparation of substrates is central to gain a higher SERS activity. Different types of nanoparticles give rise to different Raman enhancement characteristics, as the amplification of Raman signals depends on the molecular coupling with localized electromagnetic excitation on the surface of metal nanostructures. Hence, optimizing and tuning of the SERS characteristics require an appropriate control of SERS substrates: size, shape, spacing between nanoparticles, functionalization of nanoparticles and the dielectric environment.

Nanoparticle optical properties are also sensitive to the *proximity* of other plasmonic materials. When two or more plasmonic nanoparticles are near each other (with edge-to-edge separations of one particle diameter or less) their surface plasmons couple as the conduction electrons on each particle surface collectively oscillate. This effect is similar to molecular orbital theory in that plasmon coupling results in the oscillating electrons assuming the lowest energy state, causing the plasmon resonance wavelength of the coupled particles to red-shift to longer wavelengths (lower energies). This coupling effect is responsible for the dramatic changes in the visible color of plasmonic nanoparticle solution when nanoparticles aggregate and also the basis of many different types of plasmonic nanoparticle sensors.

The Raman enhancement can be considerable, arising essentially from the creation of very strong electric fields at the interface of metal particles due to the *coupling of the fields between neighboring particles*. For this reason, surfaces must be prepared in a perfectly controlled way with regard to particle size and interparticle distances.

Figure 7 shows the near field coupling between NPs. Here, the restoring force acting on the oscillating electrons of each NP in the chain is either increased or decreased by the charge distribution of neighboring particles. Depending on the polarization direction of the exciting light, this leads to a blue-shift of the plasmon resonance for the excitation of transverse modes, Figure 7 (a), and a red-shift for longitudinal modes, Figure 7 (b).

Figure 7. Schematic of near-field coupling between metallic NPs for two different polarizations.

It is believed that the greatest enhancements ($\sim 10^{10}$) that enabled single-molecule detection only occurred at specific sites (junctions or gaps between two or more closely spaced nanoparticles) termed hot spots.

The finding that individual nanoshells can vastly enhance the Raman effect opens the door for biosensor designs that use a single nanoshell, something that could prove useful for engineers who are trying to probe the chemical processes within small structures such as individual cells, or for the detection of very small amounts of a material, like a few molecules of a deadly biological or chemical agent. Nanoshells are already being developed for applications including cancer diagnosis, cancer therapy, testing for proteins associated with AD, drug delivery, and rapid whole-blood immunoassays.

Although LSPR sensors can be used to monitor the binding of molecules to functionalized nanoparticle surfaces, extinction spectroscopy does not allow for specific identification of the chemical entity.

Vibrational spectroscopy, on the other hand, is capable of revealing molecular characteristics of the analyte. SERS shows a 10^6-10^{14} enhancement in effective Raman cross-section when the analyte is bound or close to the surface of plasmonic nanoparticles. SERS, similar to Raman scattering, is an inelastic scattering process in which photons incident on a sample transfer energy to or from the sample's vibrational or rotational modes. Individual bands in a SERS spectrum are characteristic of a specific molecular motion. As a result, each chemical entity has its own unique Raman signature.

SERS is an important technique that can display intrinsic interfacial sensitivity and selectivity.

There is an enormous interest to utilize surface-enhanced Raman scattering (SERS) in a variety of applications. This is mostly due to its sensitivity and power to provide very specific chemical information about the molecule or molecular structure of interest in a short time without significant sample preparation steps. Due to the fact that this information can be used for detection and identification besides characterization, it has become an important analytical technique in recent years and it is considered one of the most sensitive diagnostic tools available to the scientist.

Silver and gold are usually used because they yield the largest enhancement. SERS has also been demonstrated using copper and several other metals like indium and the alkali metals. Both visible and near-infrared excitation can be used for SERS on silver. Red or near-infrared excitation is required for SERS on gold or copper. By combining SERS enhancement with resonance enhancement (surface enhanced resonance Raman scattering - SERRS), Raman cross section has been increased by a factor of 10^{11}, making single molecule Raman scattering possible. In 1997, by using SERS, single molecules on nanoparticles were successfully detected.

SERS has been used to study quantitative and qualitative study in biological systems. Recent years have seen an explosion in the use of Raman spectroscopy for biological purposes such as blood analyte detection and cellular examination, pharmaceutical product design and production processes. In addition, in forensic sciences for the unambiguous identification of unknown substances, it has also biomedical applications to demonstrate the sensitivity to distinguish between cancerous, pre-cancerous and normal tissues; and its sensitivity to changes in cell metabolites and protein structures etc., which elevate it above competing spectroscopic techniques.

By combining SERS and LSPR spectroscopy, the binding of molecules can be confirmed on the nanosensors.

In the mid-1970s, SERS was discovered which impacted surface science and spectroscopy because of its extremely high surface sensitivity. Most chemical sensors rely on properties such as mass, fluorescence, or a refractive index, which are often not specific for the substance in question. In contrast, Raman spectroscopy offers rich molecular information, and thus provides unequivocal identification of chemical and biological materials of interest. The discovery of SERS has triggered many highly sensitive detection technology development in analytical chemistry, biomedical engineering, and life sciences.

Another important source of Raman signal enhancement is the molecular resonance effect, which is employed by laser excitation that falls within the envelope of an electronic transition of the molecular system, called resonance Raman scattering (RRS). In SERS experiments, enhancements typically up to 10^6 in the Raman signal can be obtained for molecules adsorbed on nanostructures of copper, silver, and gold.

A Few Special Classes of Nanomaterials

Nanomaterials particles are often classified according to their nature as *inorganic, organic, or hybrid*.

1. **Inorganic Nanomaterials:** *Inorganic nanoparticles* are engineered nanoparticles *made from inorganic sources*. Inorganic nanoparticles cover a broad range of substances: *semiconductor nanocrystals, elemental metals, metal oxides,* metal salts, and so on……

   A) **Semiconductor nanocrystals** or **Quantum dots** (Group II–VI (e.g., CdSe, CdTe, CdS, and ZnSe), III–V (e.g., InP and InAs), or IV–VI (e.g., PbSe), etc.)
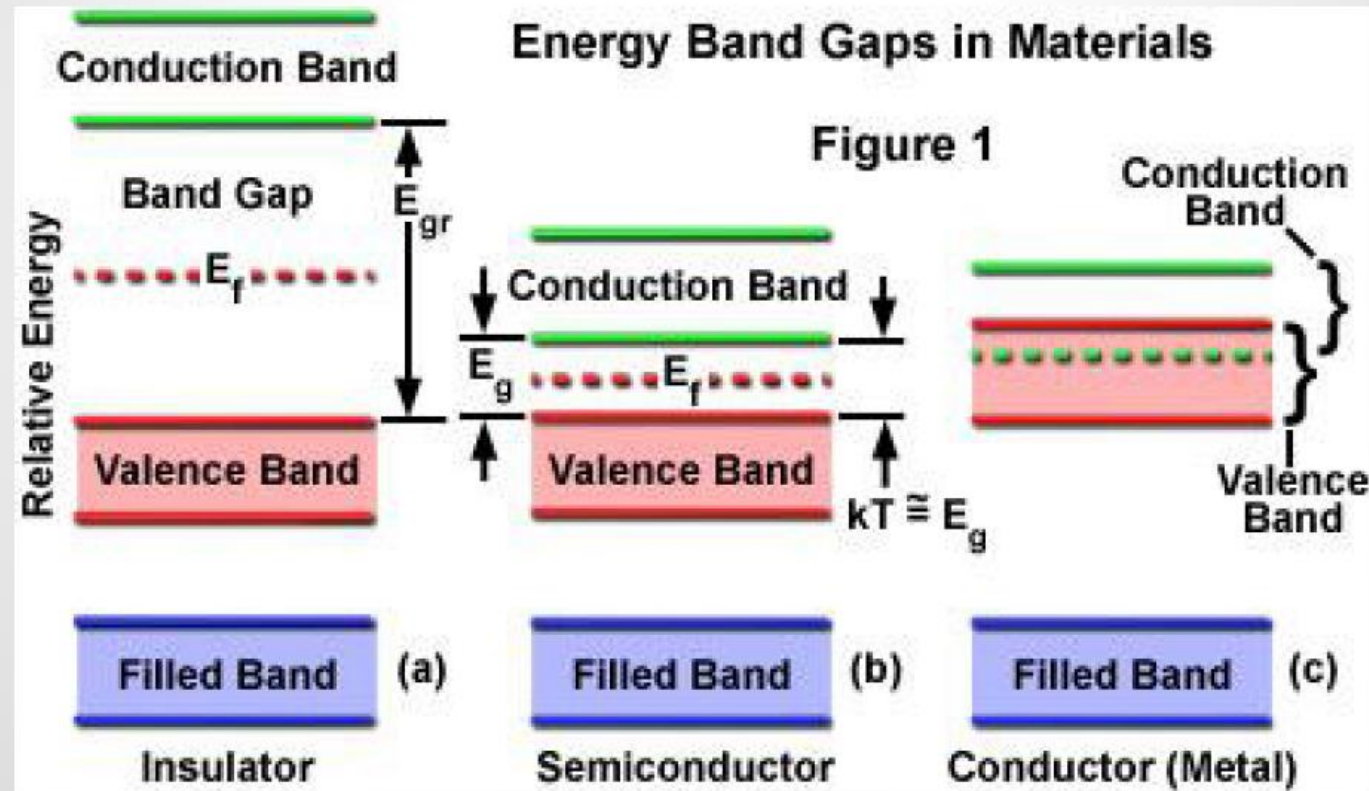
Band theory of Metal, Semiconductor and Insulator
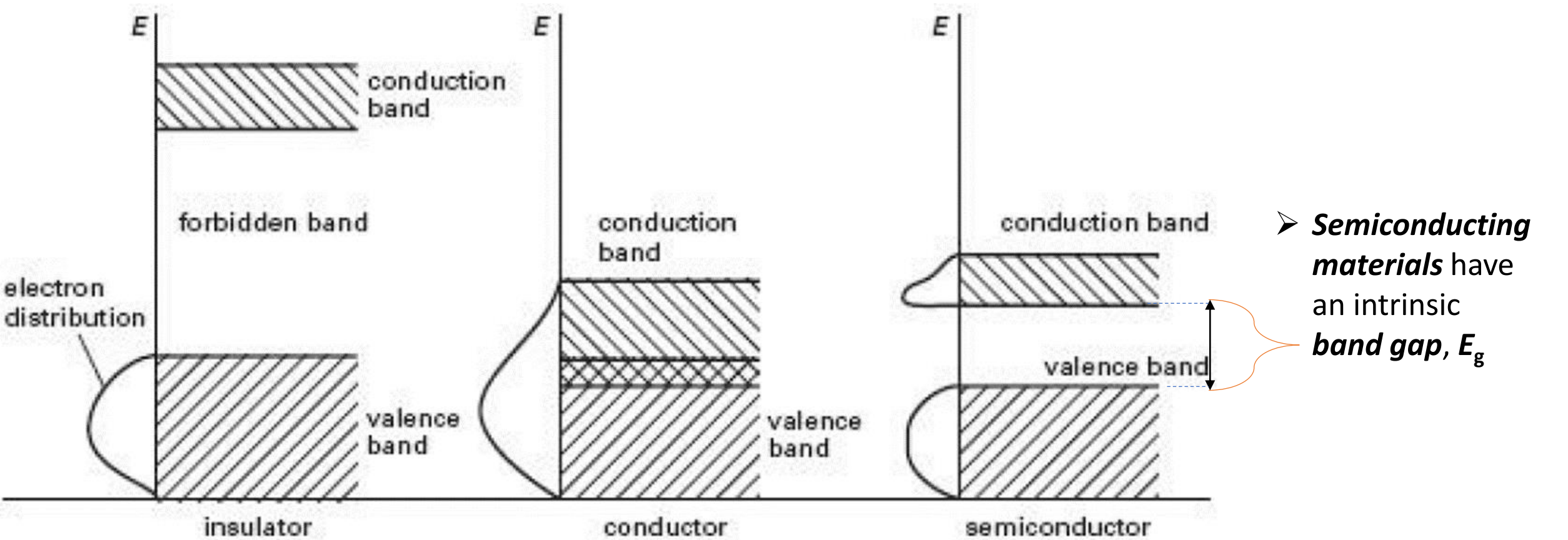
> ➤ *Semiconducting materials* have an intrinsic *band gap, E_g*

Band Gap Theory and Conduction

- Band Gap (or lack thereof) responsible for conductors, semiconductors, and insulators.

- Fermi Level: naturally half-way between conduction and valence bands

Energy Band Gaps in Materials

Figure 1

- Semiconducting materials, they have an intrinsic band gap, E_g

Semiconductor nanocrystals or Quantum dots (QDots or QDs)

❑ Semiconducting nanoparticles have been investigated intensively for their optical properties.

❑ These particles are often called **quantum dots (QD)** because quantum effects become important in *these three-dimensionally confined particles (dots).*

➤ We know that in atoms and small molecules, electrons occupy discrete atomic/molecular orbitals, whereas in macroscale solids the electrons occupy delocalized bands.

❑ Semiconductors have valence and conduction band separated by a band gap, E_g.

❑ For semiconductors, both theory and experiment tell us that when the semiconductor particle size is *roughly* at 1 to 10 nm (about 10–100 atoms across) or below, the semiconductors show discrete energy states likes molecules or atoms. The exact number depends on the specific semiconductor material.

➤ The equations of quantum mechanics that were used for electrons in atoms can be applied to electrons (and holes) in semiconductors to estimate the size where materials undergo a crossover from molecular orbitals to bands.

❑ Because *these effects become important at ~1 to 10 nm, semiconductor particles with diameters in this size range are called* **quantum dots (or artificial atoms).**

FIGURE 10.1 Diagrams illustrating the fundamental principles of quantum confinement and size-dependent properties of semiconductor quantum dots.

➤ As the dimensionality decreases, the energy levels become less continuous and more discrete. In zero-dimensional structures such as quantum dots, the energy levels appear as sharp, quantized lines.

➤ The QD bandgap energy is the function of particle size, which allows continuous tuning of the emission wavelength.
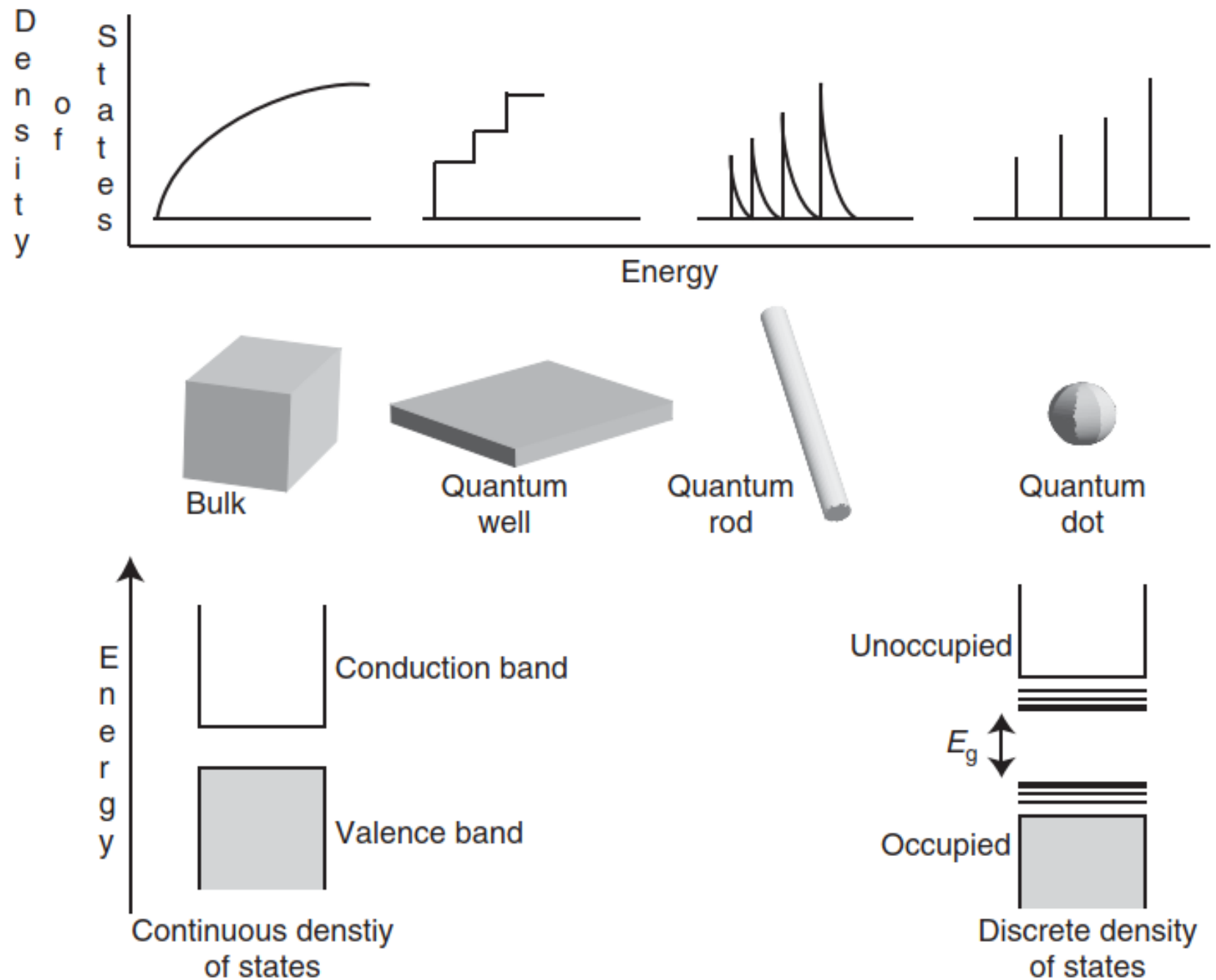
A) Semiconductor nanocrystals or Quantum dots (QDots or QDs)

➢ As semiconducting materials, they have an intrinsic band gap (E_g) through which electrons can be excited by incident light of appropriate energy (wavelength).

➢ However, *unlike bulk semiconducting materials*, quantum dot's energy states are too sparse to create the continuous valence and conduction bands typical of macroscopic semiconductors.

➢ Instead, **quantum dots produce a rarefied electronic structure** *that is more reminiscent of the discrete electronic states found in single atoms. Therefore, sometimes quantum dots are called* **"artificial atoms".**

➢ *Unlike bulk semiconducting materials,* **the band gap (E_g) depends on the size of the QDs**. The *larger* the quantum dot, the *smaller* its *band gap (E_g)*.

➢ The larger a quantum dot becomes, the more continuous its electronic structure and the closer its band gap becomes to that of the bulk material (see Figure 5).

➢ Unlike a single atom, however, **this size dependence allows the band gap energy to be modulated by varying the size of the quantum dot**, *essentially allowing for the synthesis of materials with arbitrary band gap energies*.

➢ The size-dependence of the emission color comes primarily from a particle-in-a-box effect. The electron and hole that are created when the quantum dot absorbs light are bound together as an exciton by the confines of the "box". Louis Brus used first-order perturbation theory to determine that the bandgap of a semiconductor quantum dot is given approximately by:

$$E_{gap} = E_{gap,bulk} + \frac{h^2}{8\mu R^2} - \frac{1.8e^2}{4R\pi\varepsilon\varepsilon_0} + \ldots$$

➢ where R is the particle radius, μ is the electron-hole reduced mass ($1/\mu = 1/m_e^* + 1/m_h^*$), m_e^* and m_h^* are the electron and hole effective masses, and ε is the dielectric constant of the semiconductor.

➢ In this equation, the first term after the bulk bandgap is the kinetic energy due to confinement of the exciton, and the second term represents the electrostatic attractive energy between the confined electron and hole.

➢ **Because the energy is a function of R ,** *it can be* **widely tuned across the visible spectrum by changing the size of the quantum dot.**
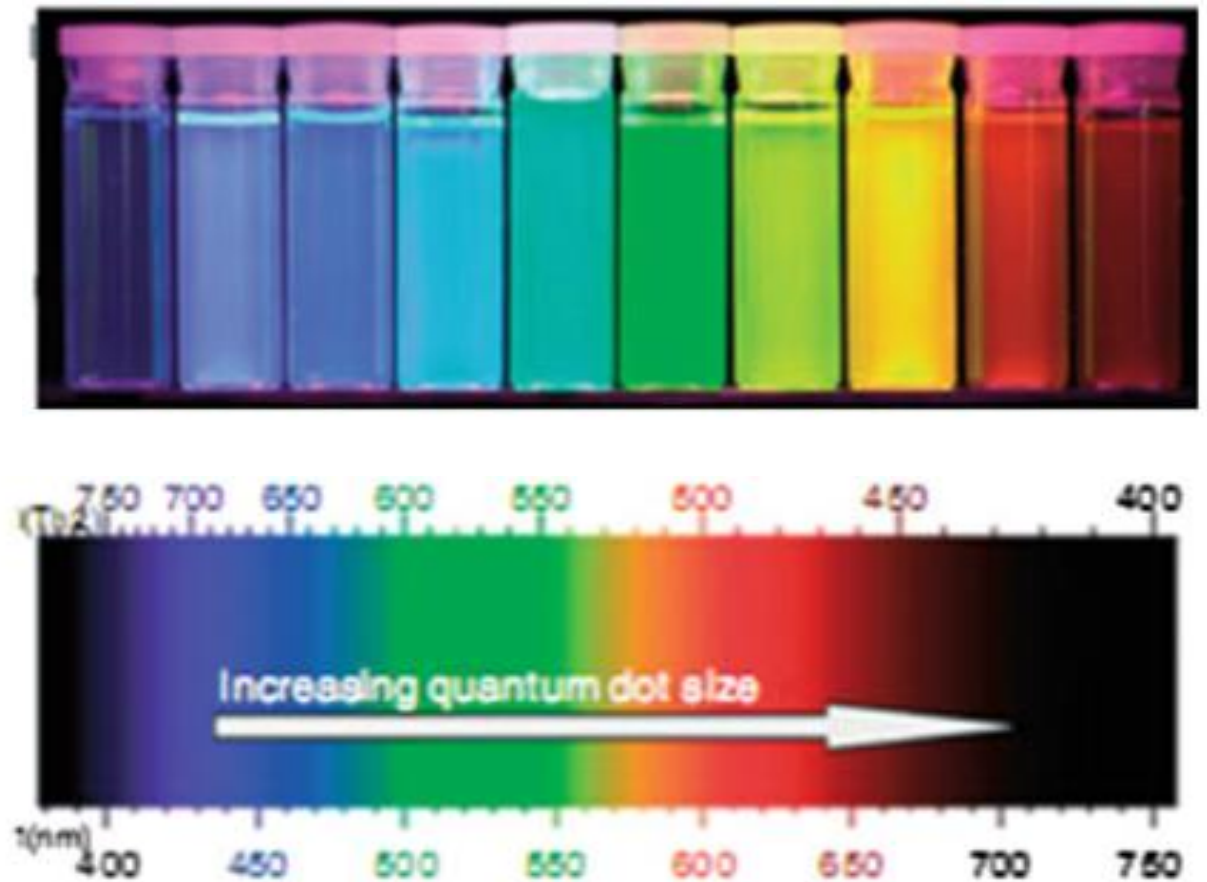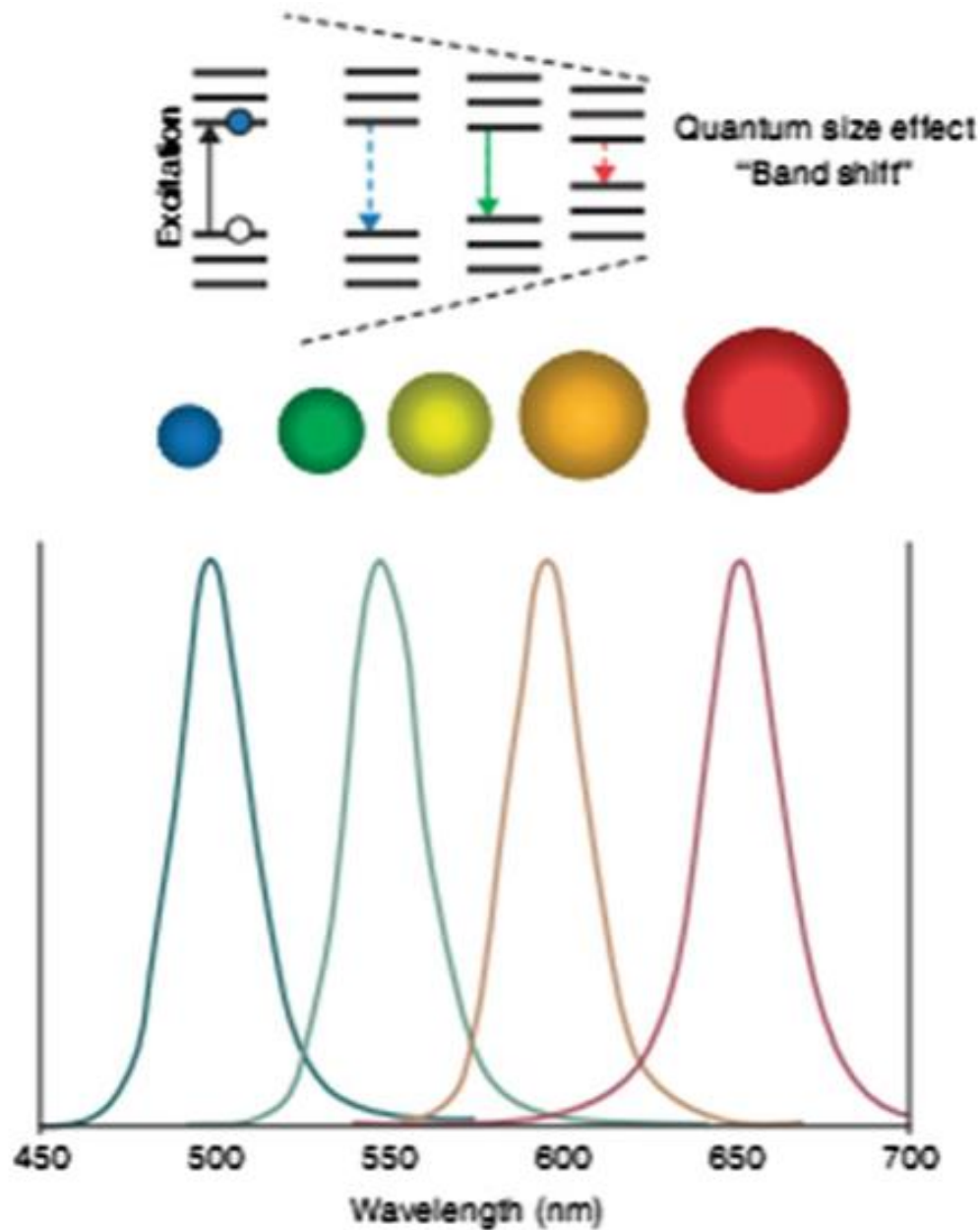
Fig. 5 Size-dependent PL colors of semiconductor QDs. Electronic structure of QDs correlated with the QD radius and resulting 'blue shift' due to quantum confinement as the QD size decreases.

The wavelengths of interband transitions depend on the size of the dots and it is possible to tailor their luminescence simply by changing their size. A key example of these QD materials is CdSe.

By varying the size of the CdSe nanoparticle it is possible to tune emission over the entire visible spectrum, making them ideal for *LED and fluorescent display technologies*.

| $r_{CdSe\ core}$ (Å) | 13.5 | 14.5 | 17.5 | 19.0 | 21.5 | 24.0 |
| $\lambda_{max\ em.}$ (nm) | 510 | 530 | 555 | 570 | 590 | 610 |

Fig. (Top) Photo demonstrating the size-tunable fluorescence properties and spectral range of the six QD dispersions versus CdSe core size. All samples were excited at 365 nm with a UV source. *r* = core radius.

(Bottom) Absorption and emission of six different CdSe QD dispersions. The black line shows the absorption of the 510-nmemitting QDs.
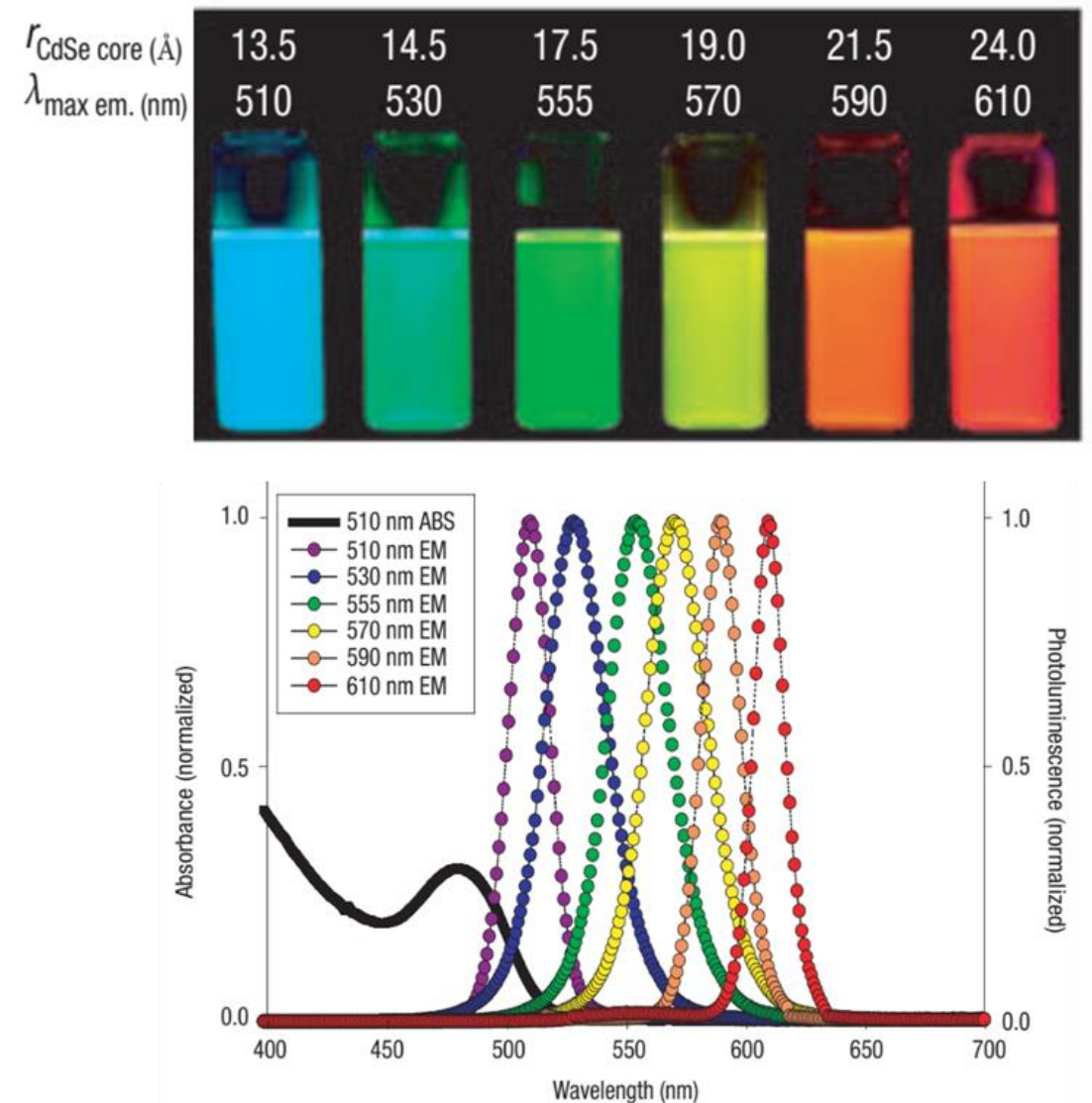
➢ Quantum dots are nearly spherical, luminescent nanosized crystals made of semiconductor materials, of the order of 2–10 nm comprising 200–10 000 atoms.

➢ Their optical properties are size-dependent. A decrease in the crystal size causes an increase in energy shift between the absorbing and the emitting state.

➢ Optical excitation across the band gap in a semiconductor depends on the size of the crystal even for larger crystals, as large as those comprising 10 000 atoms. A similar trend can be expected with the quantum dots which are often far too small with a minimum of 200 atoms extending to a maximum of 10 000 atoms.

➢ The band gaps of such nanocrystals are often tunable to the interest of the user, for instance a CdS crystal can be tuned between 2.5 and 4 eV.

Figure 5: The electronic structure of quantum dots varies with the size of the dot.

$$E_g = h\nu = hc/\lambda$$
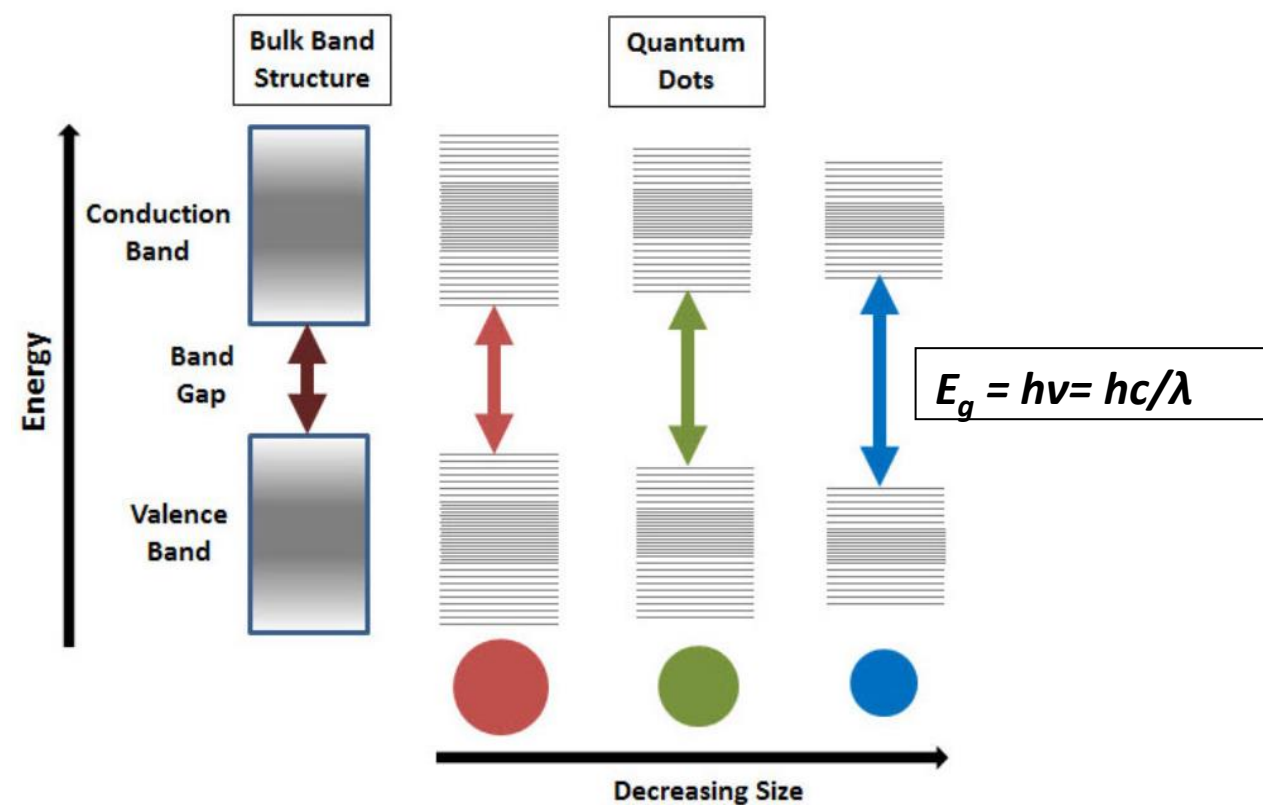
As we learned earlier that some semiconductor devices can emit light when a voltage is applied. Another way to make semiconductors emit light is to illuminate them with light whose photons have energies larger than the energy of the band gap of the semiconductor. A photon with a certain energy E_P can be absorbed if its energy is exceeding the band gap energy of the QD, i.e., $E_P > E_g$. Hence, larger QDs are allowed to absorb photons with lower energy than smaller QDs. An electron that was elevated from the valence band to the conduction band upon absorption of a photon can relax radiatively to the ground state by emitting another photon, a process called **photoluminescence (fluorescence)**.

❑ One of the *most spectacular effects of reducing the size of a semiconductor crystal is that the band gap changes substantially with size in the 1–10-nm range*. **As the particle gets smaller, the band gap gets larger**, an effect observable by the naked eye, as shown in Figure 12.44.

➢ Could you explain the origin of the color change?

Semiconductor particles ~1–10 nm diameter are "quantum dots."

Bulk

Molecular limit

Decreasing size

Increasing band gap energy

Figure 12.44 *Cd$_3$P$_2$ powders with different particle sizes*. The arrow indicates decreasing particle size and a corresponding increase in the band gap energy, resulting in different colors.

- One of the *most spectacular effects of reducing the size of a semiconductor crystal is that the band gap changes substantially with size in the 1–10-nm range*. **As the particle gets smaller, the band gap gets larger**, an effect observable by the naked eye, as shown in Figure 12.44.

➢ On the macro level, the semiconductor cadmium phosphide looks black because its band gap is small (E_g = 0.5 eV), and it absorbs all wavelengths of visible light.

➢ As the crystals are made smaller, ***the material progressively changes color until it looks white!*** *It looks white because* now *no visible light is absorbed*. The band gap is so large that only high-energy ultraviolet light can excite electrons into the conduction band (E_g = 3.0 eV).
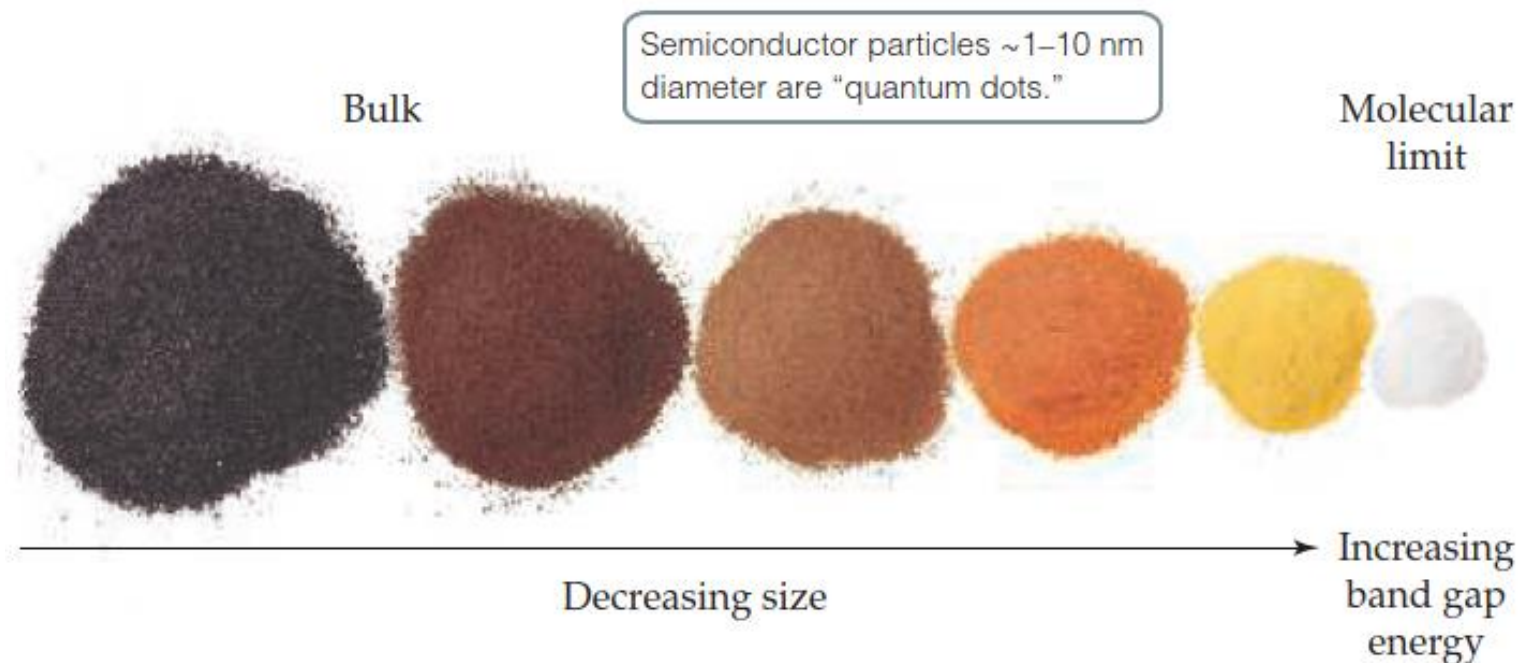
Figure 12.44 *Cd_3P_2 powders with different particle sizes*. The arrow indicates decreasing particle size and a corresponding increase in the band gap energy, resulting in different colors.

Semiconductor particles ~1–10 nm diameter are "quantum dots."

Bulk

Molecular limit

Decreasing size

Increasing band gap energy

❑ *Use in LED and fluorescent display technologies:*

As an example, Fig. 4.1 shows the dependence of the fluorescence wavelength on the *dimensions* **and** *material composition* **of the nanocrystals.** The large wavelength differences between the blue, green, and red (BGR) emissions result here from using materials having different band gaps: CdSe (blue), InP (green), and InAs (red). The fine-tuning of the fluorescence emission within each color is controlled by the size of the QDs.

Figure 4.1 Nanocrystal quantum dots (NCQD) illuminated by UV-light emit light at a wavelength that depends both on the material composition and the size of the NCQDS. *Large differences in the fluorescence wavelength result from different band gaps of the materials*. **Within each color (blue, green, and red) the wavelength is defined by the different sizes of the NCQD**s.
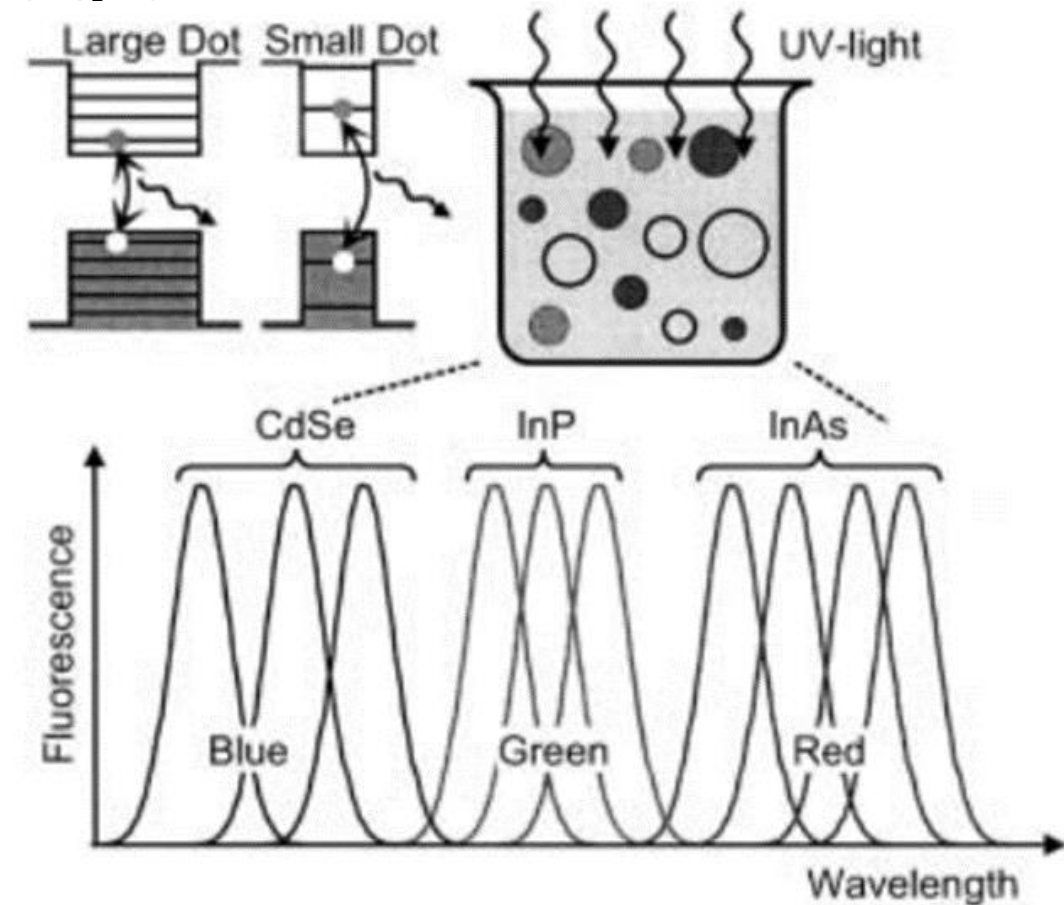
❏ Novel Properties of QDs: Summary

➢ In addition to the *LED and fluorescent display technologies*, another exciting use of QDs is as chromophores for '**biotags**', where dots of different sizes are functionalized to detect different biological analytes.

➢ The QDs have **novel optical properties** that are not available from organic dyes and fluorescent proteins.

✓ **First**, QDs have **very large molar extinction coefficients** in the order of $0.5–5×10^6$ M^{-1} cm^{-1}, which makes them **brighter probes** under photon-limited in-vivo conditions (where light intensities are severely attenuated by scattering and absorption).

✓ The **second** manifestation of quantum confinement is that the available quantized energy levels inside a QD have *no net linear momentum and therefore transitions between them do not require any momentum transfer*. As a result, ***the transition probabilities between any two states are high***. This lack of momentum dependence also explains the ***broadband absorption nature of QDs because probabilities are high for most transitions from the occupied valence band states to unoccupied conduction band states***.

Probabilities are also high for intraband transitions, transitions of electrons between states in the LUMO band or of holes in the HOMO band. *These relatively intense intraband transitions are typically in the infrared region of the spectrum and are currently being exploited to make devices such as infrared photodetectors, sensors, and lasers.*

✓ **Third**, in theory, the *lifetime-limited emission rates for single QDs are 5–10 times lower than those of single organic dyes because of their longer excited state lifetimes (20–50 ns).* In practice, however, fluorescence imaging usually operates under absorption-limited conditions, in which the rate of absorption is the main limiting factor of fluorescence emission. *Since the molar extinction coefficients of QDs are about 10–50 times larger than that (5–10×10^4 M^{-1}cm^{-1}) of organic dyes,* **the QD absorption rates will be 10–50 times faster than that of organic dyes** *at the same excitation photon flux* (number of incident photons per unit area). Due to this increased rate of light emission, individual QDs have been found to be 10–20 times brighter than organic dyes.
Furthermore, the *longer excited state lifetimes of QDs provide a means for separating the QD fluorescence from background fluorescence* through a technique known as *time-domain imaging*.

✓ **Fourth**, QDs have ***size- and composition-tunable fluorescence emission*** from visible to infrared wavelengths, and *one light source can be used to excite multiple colors of fluorescence emission*. This leads to very large ***Stokes spectral shifts*** (measured by the distance between the excitation and emission peaks) that ***can be used to further improve detection sensitivity***. This factor becomes especially important for in-vivo molecular imaging due to the high *autofluorescence background* often seen in complex biomedical specimens. Indeed, the Stokes shifts of semiconductor QDs can be as large as 300–400 nm, depending on the wavelength of the excitation light.

Organic dye signals with a small Stokes shift are often buried by strong tissue autofluorescence, whereas ***QD signals with a large Stokes shift*** are clearly recognizable above the background. This ''*color contrast*'' is only available to QD probes because the signals and the background can be separated by wavelength-resolved or spectral imaging.

A further advantage is that ***multicolor QD probes*** can be used to ***image and track multiple*** molecular ***targets simultaneously***. It turns out that, although they emit at specific tunable wavelengths, QDs exhibit broadband absorption for energies above the band gap. The intriguing point for bio-applications is that it is possible to excite an array of distinct QD chromophores with a single broadband excitation and to simultaneously detect multiple analytes by their distinct optical emissions. This is a very important feature because tracking a panel of molecular markers at the same time will allow scientists to understand, classify, and differentiate complex human diseases. Most complex human diseases such as cancer and atherosclerosis involve a large number of genes and proteins. These materials have been used to image breast cancer cells and live nerve cells to track small molecule transport to specific organelles.

Multiple parameter imaging, however, represents a significant challenge for magnetic resonance imaging (MRI), positron emission tomography (PET), computed x-ray tomography (CT), and related imaging modalities. **On the other hand, fluorescence optical imaging provides both signal intensity and wavelength information, and multiple wavelengths or colors can be resolved and imaged simultaneously (color imaging).** Therefore, different molecular or cellular targets can be tagged with different colors. *In this regard, QD probes are particularly attractive because their broad absorption profiles allow simultaneous excitation of multiple colors*, and *their emission wavelengths can be continuously tuned by varying the particle size and chemical composition*.

For organ and vascular imaging , in which micrometer-sized particles could be used, optically encoded beads (polymer beads embedded with multicolor QDs at controlled ratios) could allow multiplexed molecular profiling in vivo at high sensitivities.

➢ **In addition**, QDs are several thousand times **more stable** against *photobleaching* than dye molecules and are thus well suited for continuous tracking studies over a long period of time.

- **Optical tunability, multicolor light emission, and better photostability position QDs as the preferred fluorescent probes for dynamic live cell imaging tools and in vivo animal models.**

- They have unparalleled *sensitivity and spatial resolution*, compared to the organic fluorophores currently available.

- QDs with organic capping perform even better; these QDs usually have a core crystal with an inorganic capping with an outer organic group which helps during QD conjugation for functionalization. For instance, a ZnS capped CdS QD is 20 times brighter than rhodamine (a popular organic dye) and at the same time 100 times more stable to photobleaching.

- QDs can be used for the *study of live cell single-molecule dynamics, monitoring of intracellular protein–protein interactions, disease detection in deeper tissues, detection of cancer/tumor cells* based on *selective binding of bioconjugated QDs to known cancer biomarkers,* and much more.

Fig. 3.3 shows green QDs conjugated to streptavidin, emitting green fluorescence. The image shows F-actins of fixed fibroblasts.
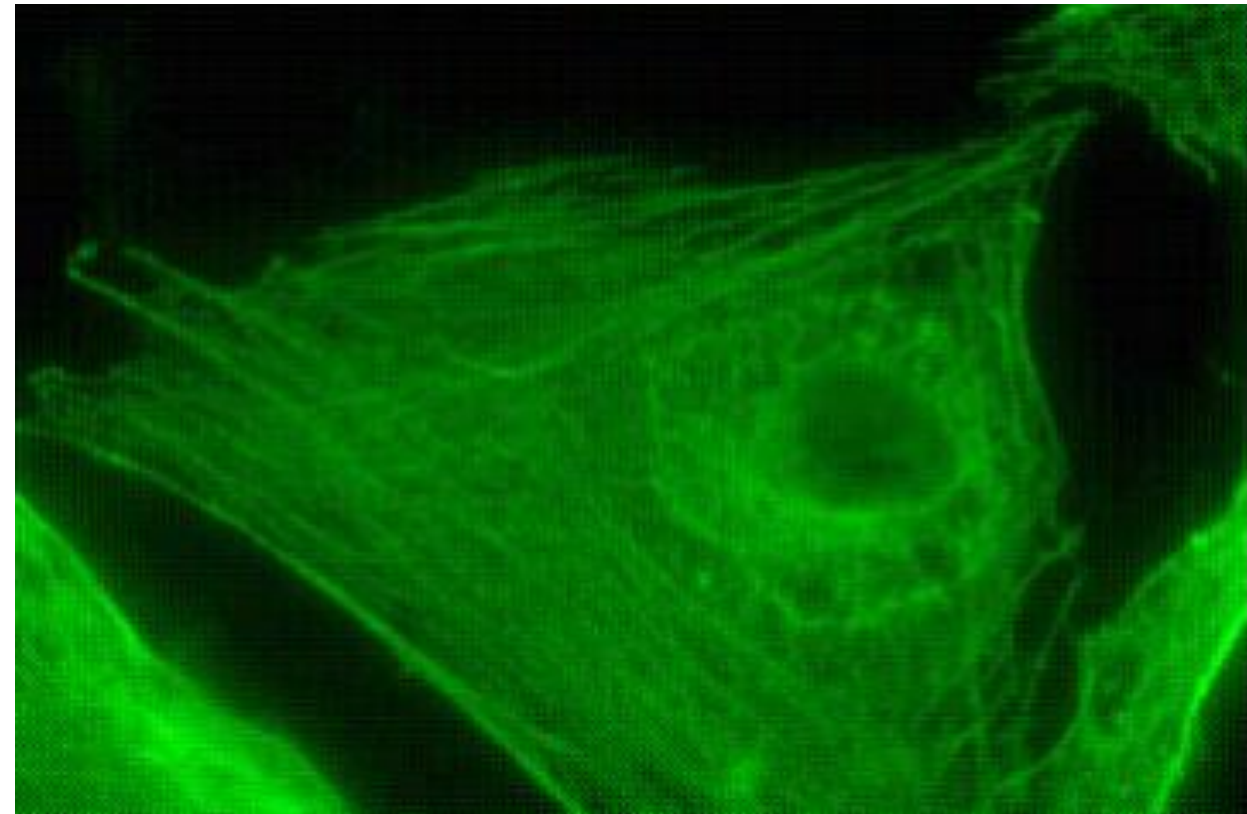

FIGURE 3.3: Immunocytochemical stain of F-actin in fixed fibroblast cells using green quantum dots.

Fig. 3.4 shows the image of cellular uptake of QD-cationic peptide conjugates. The red-fluorescent (CdSe)ZnS QDs were incubated with a monolayer of living human cancer cells. The QDs were previously conjugated with TAT peptides. The image further suggests, from the aggregation of QDs in internal cellular structures, that they are present in endocytotic vesicles.
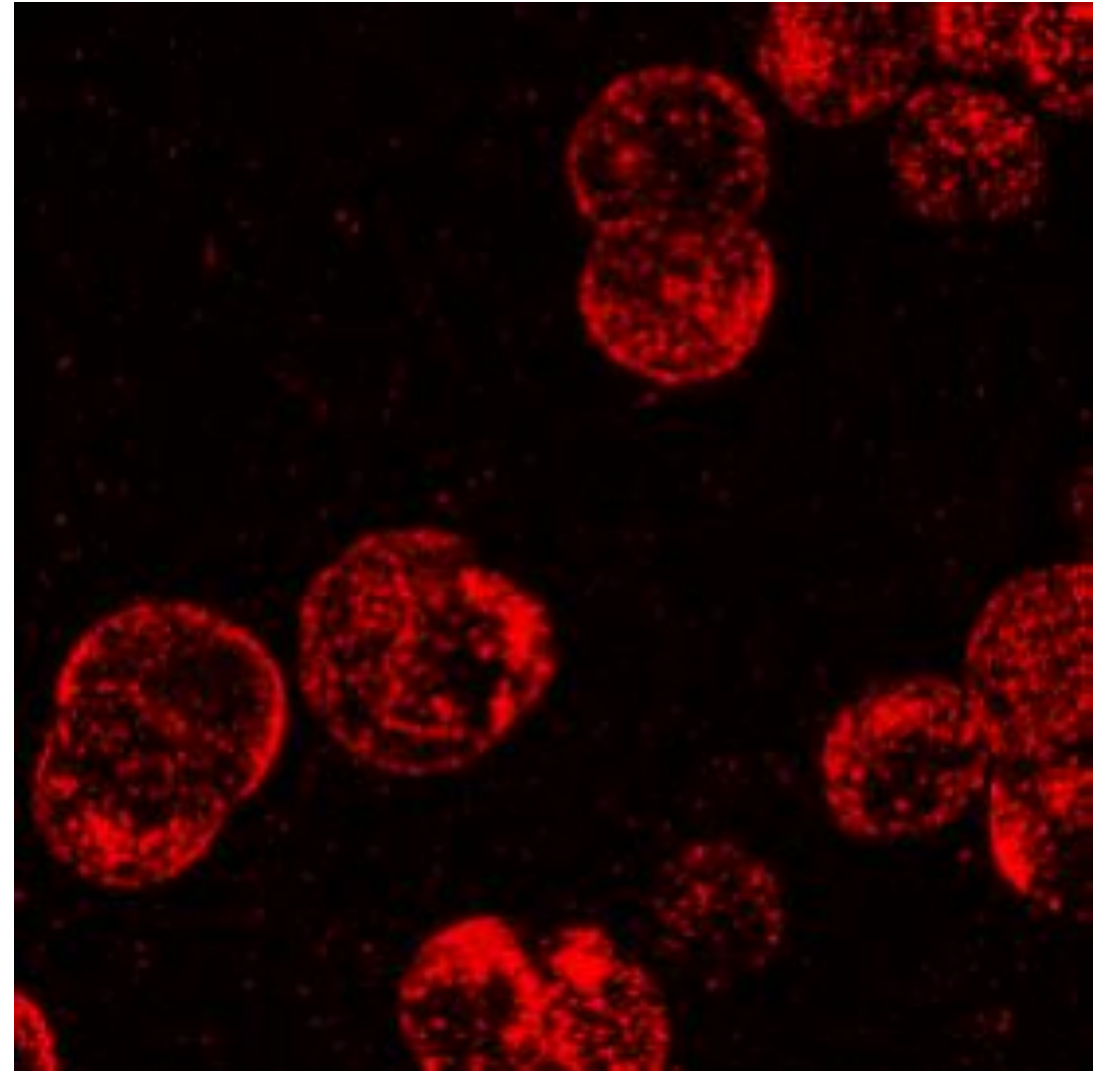

FIGURE 3.4: Cellular uptake of QD-cationic peptide conjugates. Monolayers of living human cancer
cells were incubated with red fluorescent (CdSe)ZnS QDs conjugated to TAT peptides. The aggregation
of QDs in internal cellular structures is indicative of their presence in endocytotic vesicles

FIGURE 3.8: Versatile applications of QDs in biomedical and biotechnology.